COPPER-CATALYZED SYNTHESIS OF BENZO-BIMANE DERIVATIVES

A Thesis Submitted to
the Graduate School of Engineering and Sciences of
İzmir Institute of Technology
in Partial Fulfillment of the Requirements for the Degree of

MASTER OF SCIENCE
in Chemistry

by

Hüseyin Zeybek

July 2016

İZMİR

We approve the thesis of **Hüseyin ZEYBEK**

Examining Committee Members:

Assoc. Prof. Dr. Mustafa EMRULLAHOĞLU
Deparment of Chemistry, İzmir Institute of Technology

Assist. Prof. Dr. Yaşar AKDOĞAN
Deparment of Material Science and Engineering, İzmir Institute of Technology

Assist. Prof. Dr. Tuna Subaşı

Deparment of Food Engineering, Ahi Evran University

21 July 2016

Assoc. Prof. Dr. Mustafa EMRULLAHOĞLU
Supervisor, Deparment of Chemistry,
İzmir Institute of Technology

Prof. Dr. Ahmet Emin EROĞLU
Head of the Deparment of Chemistry

Prof. Dr. Bilge KARAÇALI
Dean of the Graduate School of
Engineering and Science

ACKNOWLEDGEMENTS

The work presented in this thesis has been performed at the Department of Chemistry, Izmir Institute of Technology, in the time period from September 2014 to November 2015. At that time, someone has contribution to this study.

In the beginning, I am glad to thank my supervisor, Mustafa EMRULLAHOĞLU, for presenting me to a motivating and very interesting projects, helpful insights, helpful discussions and always patiently answering my questions.

To Muhammed ÜÇÜNCÜ, Erman KARAKUŞ and Ceyla ÇETİNTAŞ that cordially helped me with the operation of thesis study. To my labmates; thank you for the good atmosphere and spirit. Among my labmates, I would like to extend my special thanks to Muhammed ÜÇÜNCÜ and Erman KARAKUŞ for their support, help, friendship and especially for their patience during two years. They were like a brother to me and I am more than grateful for all of the things they have done for me.

Also, special thanks to Assist. Prof. Dr. Yaşar AKDOĞAN and Assist. Prof. Dr. Tuna Subaşı for participating as a committee member and reviewing my work and as well as Dr. Hüseyin ÖZGENER for instrumental analysis, Fırat ZİYANAK for NMR analysis and all technical stuff for their endless support.

I would like to thank to the TÜBİTAK (113Z157) and İZTECH for support during this project.

Last but not least, my endless appreciation also goes to my family and friends who have supported me and listened to my triumphs and complaints as the chemistry work evolved. To mom and dad, who always inspire me to do my best. A special thanks to my brother Tevfik Can ZEYBEK, for his support.

ABSTRACT

COPPER-CATALYZED SYNTHESIS OF BENZO-BIMANE DERIVATIVES

1,5-Diazabicyclo[3.3.0]octadienediones (shortly 9,10-dioxabimanes or "bimanes") are small heterocyclic structures which have important chemical, photochemical and photophysical properties. There are two existing structural isomers for bimane compounds ("syn" and "anti"). The syn-isomers have strong UV absorption properties and high quantum yields and are highly fluorescent. Bimane compounds are widely used for fluorescent labelling in biological systems because of their high photo-stability and bio-compatibility. Despite their unique properties, there is very few examples of study in literature. Because of synthetic difficulties of literature examples and their requirements such as hazardous chemicals, new methodologies are in high demand.

In this study, new methods utilising metal catalysis for the effective synthesis of bimane compounds have been developed. Bimanes, which in the literature are synthesised with extreme difficulties and low yields, were synthesised in this work through simple and efficient protocols that employ metal, ligand and base. We further investigated the photophysical properties for all newly synthesized bimane derivatives.

In the course of thesis study, a new and efficient method have been developed and optimised for the facile synthesis of benzo-bimane compound via the copper(I) catalyzed intramolecular C-N bond formation reaction. Moreover, with the aid of this new methodology, various analogues of benzo-bimane compound were synthesized in moderate to good yields under mild reaction conditions . Also, photophysical properties of benzo-bimanes were investigated carefully.

Keywords : BIMANE, Copper, Ullmann reactions

ÖZET

BAKIR KATALİZLİ BENZO-BİMAN TÜREVLERİNİN SENTEZİ

1,5-Diazabisiklo[3.3.0]oktadiendion (kısa adıyla 9,10-diokzabiman ya da "biman") yapıları önemli kimyasal, foto-kimyasal ve foto-fiziksel özelliklere sahip küçük heterosiklik yapıdaki bileşiklerdir. Biman bileşiklerinin iki yapısal izomeri ("sin" ve "anti") bulunmaktadır. "Sin" yapısındaki biman bileşikleri yüksek kuantum verimlerine sahiptir ve güçlü floresan ışıması yapmaktadırlar. Biman bileşikleri oldukça foto-kararlı ve biyo-uyumlu olmaları sebebiyle biyolojik sistemlerde floresan işaretleyici olarak sıklıkla kullanılmaktadır. Oldukça üstün özellikleri bulunmasına rağmen biman sentez yöntemleri üzerine oldukça az çalışma bulunmaktadır. Mevcut yöntemlerin zorluğu ve tehlikeli kimyasal gerektirmeleri yeni yöntemlere duyulan ihtiyacı artırmıştır.

Bu projede farklı kimyasal yapılarda biman bileşiklerinin sentezlenebilmesi için metal katalizörlerinin kullanılacağı yeni ve özgün yöntemler tasarlanmıştır. Literatürde son derece güç yöntemlerle ve çok düşük verimlerle sentezlenebilen biman bileşikleri bu çalışmada metal ve organik/anorganik bazlar kullanılarak çok daha basit yöntemlerle yüksek verimlerle sentezlenmiştir. Sentezlenen her yeni biman bileşiğinin foto-fiziksel özellikleri dikkatli bir şekilde incelenmiştir.

Proje kapsamında benzo yapısındaki biman bileşikleri bakır katalizörleri ve çeşitli ligantlar varlığında başarılı bir şekilde sentezlenmiş ve ürün çeşitliliği sağlanmıştır. Ayrıca elde edilen bileşiklerin foto-fiziksel özellikleri de dikkatli bir şekilde incelenmiştir.

Anahtar Kelimeler : BİMAN, Bakır, Ullmann reaksiyonları

TABLE OF CONTENTS

LIST OF FIGURES

Figure **Page**

LIST OF TABLES

Table **Page**

LIST OF ABBREVIATIONS

Bimane	1,5-Diazabicyclo[3.3.0]octadienediones
i-Pr_2NEt	*N*,*N*-Diisopropylethylamine
THF	Tetrahydrofuran
PNO	Amino(methyl)phosphinate
RT	Room Temperature
MeCN	Acetonitrile
DEPC	Diethylphosphoryl Cyanide
DMF	Dimethylformamide
MeOH	Methanol
TLC	Thin Layer Chromatography
n-BuLi	*n*-Butyllithium
EtOH	Ethanol
DCE	Dichloroethane
DCC	*N*,*N'*-Dicyclohexylcarbodiimide
DMAP	4-Dimethylaminopyridine
DCM	Dichloromethane
DMSO	Dimethyl Sulfoxide

CHAPTER 1

INTRODUCTION

In 1958, at first 1,5-Diazabicyclo[3.3.0]octadienedione (shortly ‘’9,10-dioxabimane’’ or "bimane") compounds had been serendipitiously synthesized by Carpino and co-workers in synthesis of 2-alkynoic acid derivatives via the treatment of 4,4-dichloro-3-pyrazolin-5-one compound with base (Figure 1.1). However, Carpino did not spend any effort to understand the structure of this side product. The structure of bimane compound was fully clarified by Kosower and co-workers in 1977. With this invention, synthetic and photophysical studies of bimane compounds and its derivatives were fulfilled through Carpino procedure in 1978. It has been an important milestone for the synthesis of highly stable and fluorescent molecule in literature (Carpino et al., 1958).

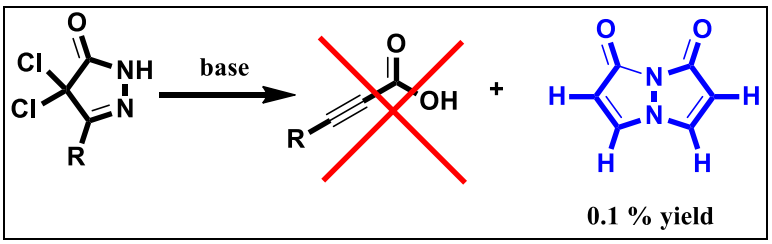

Figure 1.1. Synthesis of Bimane compounds

(Source: Carpino et al., 1958)

1,5-Diazabicyclo[3.3.0]octadienediones (shortly ‘’9,10-dioxabimanes’’ or "bimanes") are small heterocyclic structures having important chemical, photochemical and photophysical properties. There are two types of structural isomers of bimane compounds as "syn" and "anti" (Figure 1.2). The syn isomers are strongly fluorescent by reason of having strong UV absorption properties and high quantum yields. Bimane compounds are often used for fluorescent labelling procedures in biological systems because of their high photo-stability and bio-compatibility (Pazhenchevsky et al., 1978).

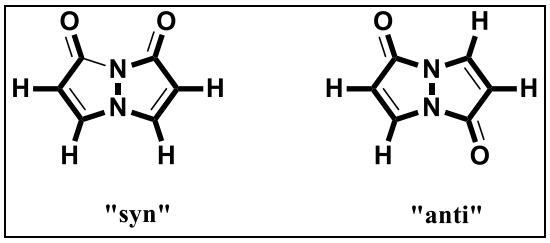

Figure 1.2. “Syn” ve “anti” bimane compounds

(Source: Pazhenchevsky et al., 1978)

Although bimanes have extraordinary photophysical properties, there are only two synthesis methods in hand to get bimane compounds. These methods requires the usage of highly expensive and hazardous chemicals. In addition, the high prices of commercially available bimane derivatives, that are because of diffuculties of synthetic methodology, limits the usage of these compunds in many applications. Because of these limitations, development of new and effective methods are in high demand.

In this study , a new and efficient method have been developed for the synthesis of benzo-bimane compounds via the copper(I) catalyzed intramolecular C-N bond formation reaction. With the aid of this new methodology, substituted benzo-bimane compounds were synthesised in moderate to good yields under mild reaction conditions.

CHAPTER 2

BACKGROUND INFORMATION

2.1 Studies over Bimane Compounds in Literature

Bimane compounds are small fluorescent molecule bearing exceptional photophysical and chemical properties. They are used in several areas such as labelling agents, and sensors. Although bimane compounds are very useful for various applications, there are only two methods to obtain them. The first method was developed by Kosower and co-workers in 1977 (Figure 2.1). As shown in ‘’Figure 2.1’’, this approach requires highly reactive alkoxide compounds and extremely hazardous chlorine gas. Therefore, new reaction pathways excluding these reactive and toxic substances are required for facile synthesis (Kosower et al., 1980).

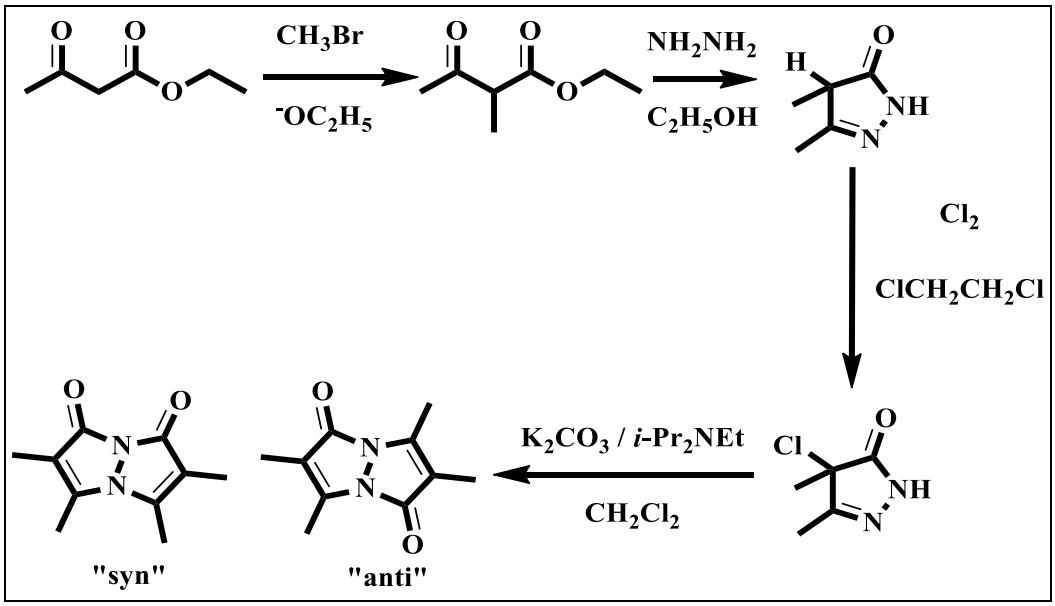

Figure 2.1. Synthesis of Bimane compounds fulfilling Kosower’s method

(Source: Kosower et al., 1980)

In another approach, Fischer carbenes are exploited to synthesise bimane compounds (Figure 2.2). However, as shown below, ‘’Figure 2.2’’ various pyrazol

derivatives are afforded in this reaction as side products. In addition to the non-selectivity of this method, utilisation of a stoichiometric amount of chromium and tungsten metal compounds is a prerequisite. Moreover, carbene compounds are very air sensitive and difficult to handle which renders this method useless and vulnerable (Zheng et al., 2006).

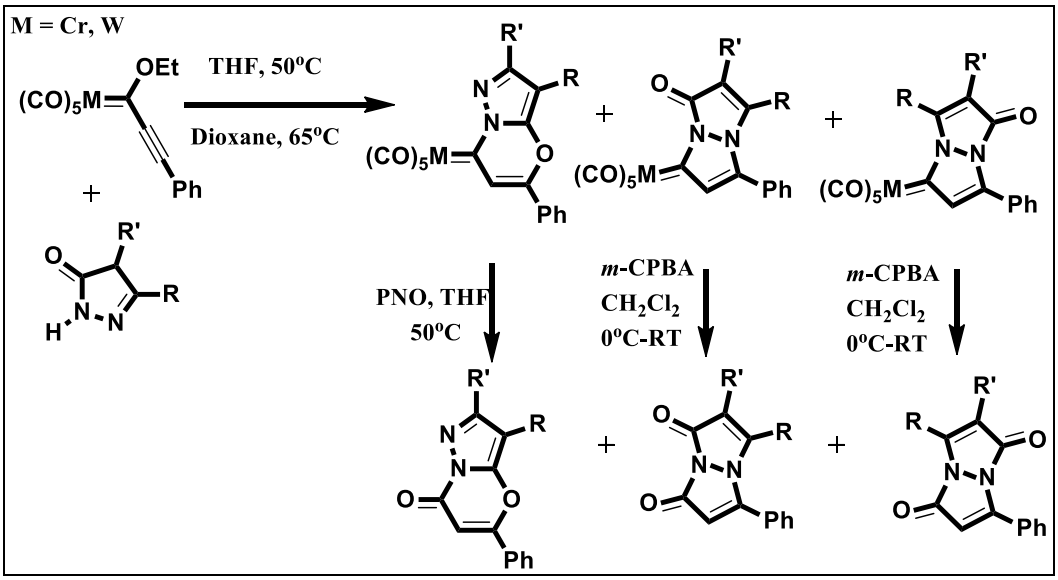

Figure 2.2. Synthesis of Bimane compounds with Fischer carbene complexes (Source: Zheng et al., 2006)

The bimane compounds synthesised by the methods mentioned above have widespread applications in numerous fields in the literature. In 1979, Kosower and co-workers used bimane compounds as fluorescent labelling agents. With the aid of this study, reactive thiol species of haemoglobin and, glutathione compounds inside membrane proteins and red blood cells are labelled along with both mono/dibromo bimanes and monobromo trimethyl ammonium bimane under physiological conditions (Figure 2.3) (Ranney et al., 1979).

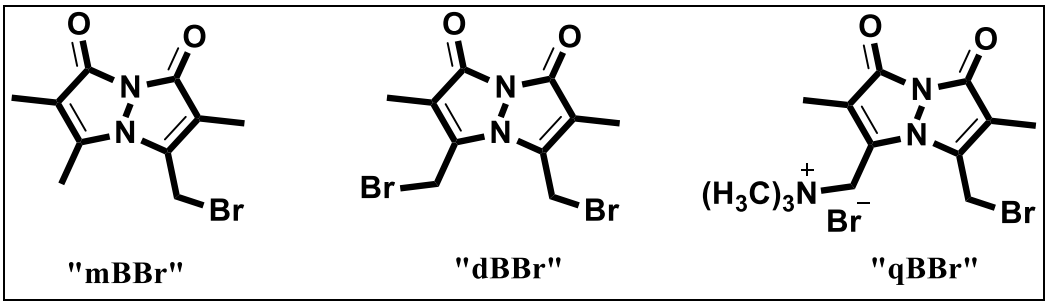

Figure 2.3. Bimane fluorescent labels

(Source: Ranney et al., 1979)

In this study, Kosower and co-workers not only synthesised different bimane compounds but also elucidated their structures and established all their photophysical properties (Shoshan et al., 1996). Moreover, in a further study, Kosower and co-workers elaborated kinetic studies of reactions between halogenated bimane compounds and various thiols (Radkowsky et al., 1986).

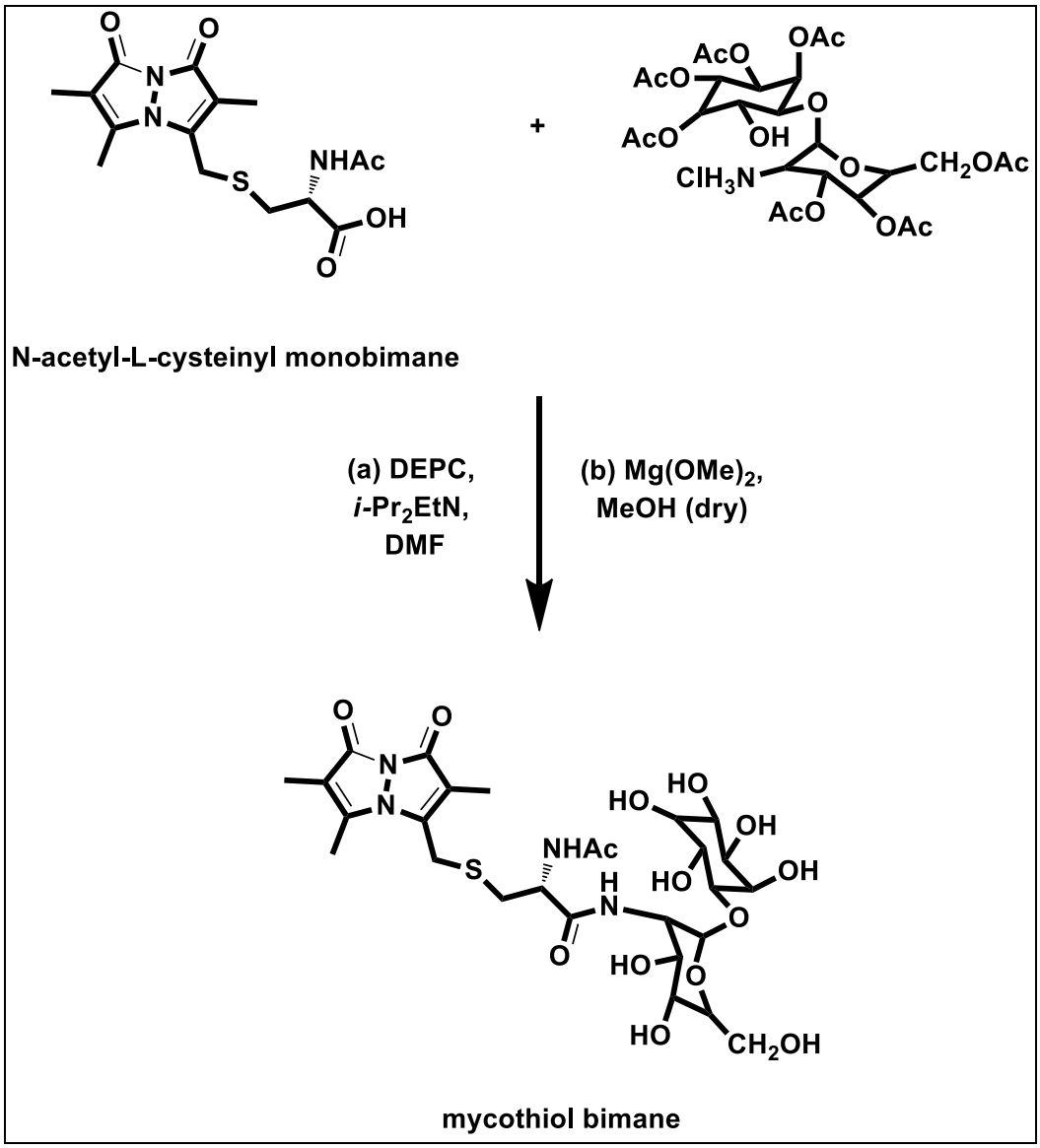

Figure 2.4. Total synthesis of mycothiol bimane
(Source: Nicholas et al.; 2002)

At the beginning of 2002, an article published by Bewley and co-workers described the total synthesis of mycothiol bimane. Acetyl-glucopyranoside amine hydrochloride initially reacts with N-acetyl-L-cysteinyl monobimane in the presence of diethylphosphoryl cyanide and, diisopropylethylamine reagents in dimethylformamide, followed by the addition of $Mg(OMe)_2$ in methanol to form mycothiol bimane (Nicholas et al.; 2002).

After a detailed literature investigation, it can be observed that bimane compounds have been particularly used as fluorescent labelling agents. In 2004, a study performed by Mansoor and Farrens effectively illustrated that the secondary structures of 25 different T4 lysozyme proteins could be readily determined by labelling with a (2-pyridyl)dithiobimane fluorophore (Figure 2.5) (Mansoor et al., 2004).

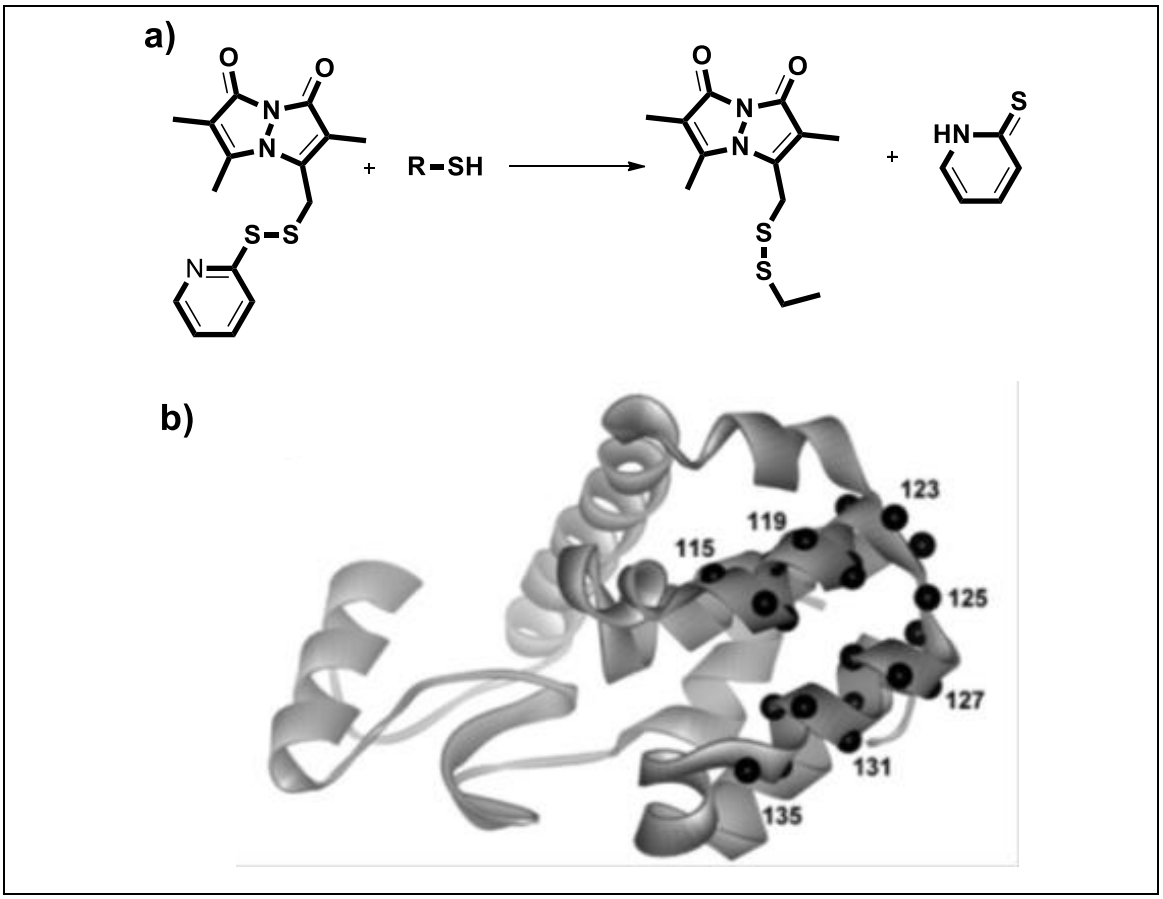

Figure 2.5. a) Reaction of (2-pyridyl)dithiobimane fluorophore with thiols. b) Seconder structure model of T4 lyzozyme protein after the reaction with (2-pyridyl)dithiobimane fluorophore

(Source: Mansoor et al., 2004)

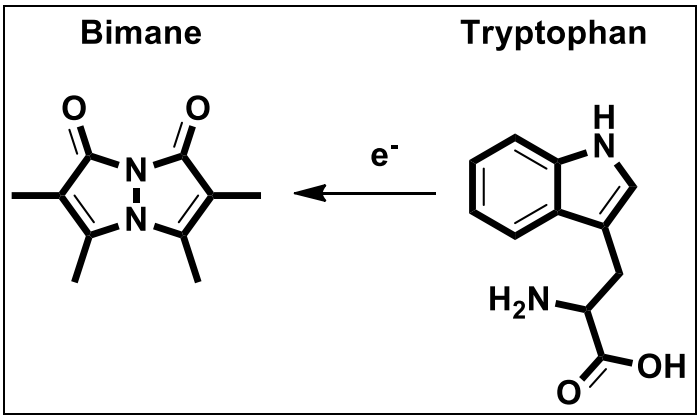

Figure 2.6. Quenching mechanism of fluorescent bimane molecule by electron transfer from tryptophan

(Source: Islas and Zagotta, 2006)

Research conducted by Islas and Zagotta in 2006 employed fluorescent bimane molecules to observe short-range molecular rearrangements in ion channels. Utilising a quenching mechanism of bimane fluorescence by electron transfer from tryptophan, the structure and dynamics of short-range interactions in the channel can be measured. Moreover, it is stated that this approach is applicable to a variety of gating rearrangements and suggests promising results to determine the gating rearrangements in the channels of well-known structures (Islas and Zagotta, 2006).

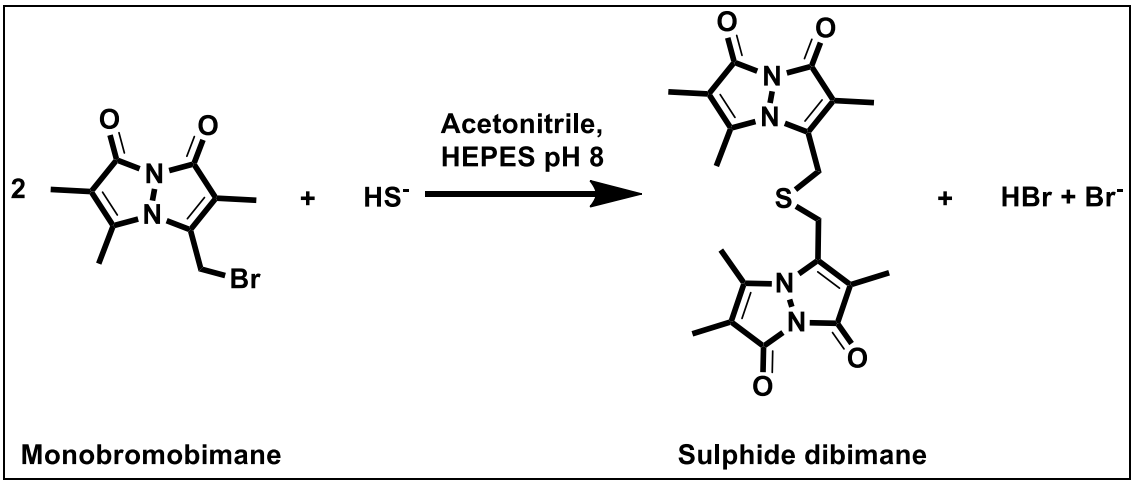

Figure 2.7. Reaction of monobromobimane with sulphide to form sulphide dibimane

(Source: Wintner et al., 2010)

The article published by Wintner and co-workers in 2010, describes the development of a novel type of pharmacological method covering non-fluorescent monobromobimane. By exploiting the formation of highly fluorescent sulphide dibimane after the reaction of monobromobimane and sulphide, the pharmacokinetic profile of reactive sulphide species in blood can be measured. The method employed in this study could potentially be used to determine the cysteine residues of one or more proteins (Wintner et al., 2010).

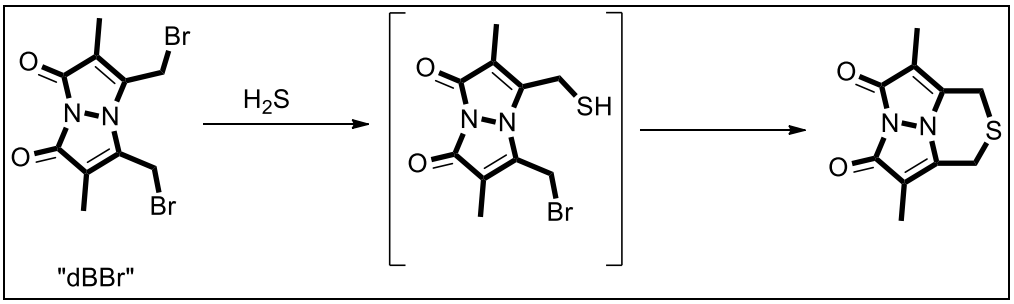

Figure 2.8. Fluorescent sensor application of Bimane compounds for H_2S (Source: Montoya et al., 2014)

In addition to their usage as labelling agents, it is also possible to use bimane compounds as fluorescent sensors (Figure 2.8). In 2014, Pluth and Kevil published an article that describes a method to detect H_2S by using monobimane and dibromo bimane derivatives. In their study, H_2S was selectively detected with a low detection limit (Montoya et al., 2014).

Bimane compounds, having widespread applications by virtue of their unique photophysical and chemical properties, cannot be efficiently synthesised using current method. Therefore, new methods to synthesise bimanes are of vital importance for new developments. In addition to the unique properties of these compounds, the principal factor for a compound to be commonly used is the ease of its production or synthesis. However, the harsh reaction conditions for the synthesis of bimane compounds, as discussed above, result in high prices and inadequate scope of reactions for these compounds. The prices of bimane compounds used as commercial labelling agents are tabulated in ‘’Table 2.1’’. These high prices affect the supply and effective use of bimane compunds (www.sigmaaldrich.com).

Table 2.1. Commercial bimane derivatives (Source: www.sigmaaldrich.com)

	Commercial Names	Bimane	Price; Aldrich
1	3-Aminomethyl-2,5,6-trimethyl-1*H*,7*H*-pyrazolo[1,2-a]pyrazole-1,7-dione, Aminobimane	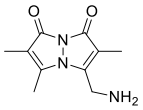	**5mg; 354 euro**
2	2,3,5,6-Tetramethyl-1*H*,7*H*-pyrazolo[1,2-a]pyrazole-1,7-dione, 3,4,6,7-Tetramethyl-1,5-diazabicyclo[3.3.0]octa-3,6-diene-2,8-dione	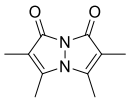	**10 mg; 54 euro**
3	3-Azidomethyl-2,5,6-trimethyl-1*H*,7*H*-pyrazolo[1,2-a]pyrazole-1,7-dione, Azidobimane	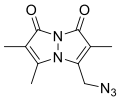	**5mg; 204 euro**
4	Monobromobimane	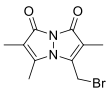	**100 mg; 386 euro**
5	Chlorobimane	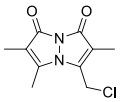	**100 mg; 791 euro**

To come up with this problem, a new synthetic method have been described for "syn" benzo-bimanes and in the course of this study, different analogues of benzo-bimanes have been synthesised.

2.2 Ullmann Reactions

For many years, there has been a high demand for catalytic synthesis of molecules, which incorporate unique structures and have a wide range of application areas in industries (such as diaryl ethers, alkylaryl ethers, diaryl amines, alkylaryl amines, diaryl thioethers, and alkylaryl thioethers). To synthesise these molecules, the typical copper-catalysed Ullmann reaction has frequently been used in methods reported in the literature (Ley et al., 2003).

Ullmann reactions initially employed extremely harsh reaction conditions (temperatures of up to 200^{o}C or 300^{o}C, strong bases, stoichiometric amounts of copper or copper salts, activated aryl halides and, long reaction times) which generally affected the scope and yields of the reactions. Because of these handicaps, Ullmann reactions could not be employed effectively until the 2000s (Ley et al., 2003; Ullmann, 1904).

The first example of this type of reactions was demonstrated by Ullman and co-workers in 1901. This reaction was the pioneering example in the area of copper catalyst. In addition, copper catalyzed C-X or C-C coupling reactions are called Ullman reactions after the report of Ullman in 1901. In the subject of study, Ullman demonstrated the copper catalyzed synthesis of biaryls from aryl halides via C-C coupling mechanism. Among various transition metal catalysts, copper catalysts were the most effective for this reaction (Ullmann, 1901).

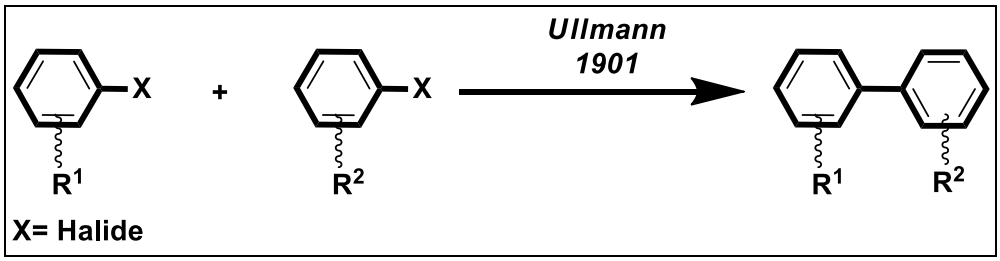

Figure 2.9. Synthesis of biaryls by Ullmann in 1901

(Source: Ley et al., 2003)

Ullmann condensation reaction is a good tool for the synthesis of diaryl ethers, diaryl amines, or diaryl thioethers. Via copper catalyst, the reaction in between an aryl halide and a phenol, an aniline, or a thiophenol forms a C(aryl)-O, a C(aryl)-N, or a C(aryl)-S bond, respectively (Ullmann, 1903).

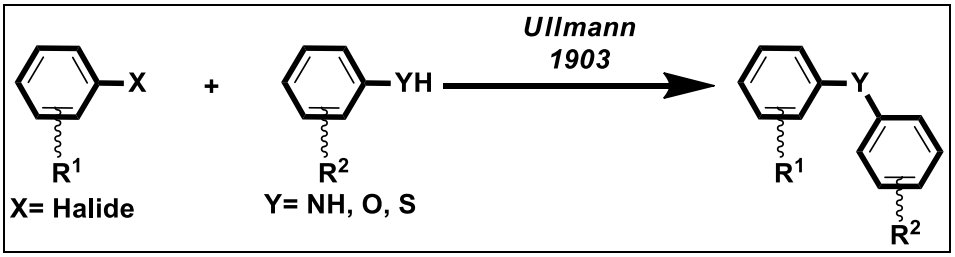

Figure 2.10. Synthesis of diaryl ethers, diaryl amines, or diaryl thioethers by Ullmann (Source: Ley et al., 2003)

In the 2000s, there have been three major breakthroughs which facilitates Ullmann reactions to be employed under mild reaction conditions. These developments have generally been facile methods for products which have importance in the pharmaceutical and industrial-scale applications and are synthesised via C-N coupling mechanism (Ley et al., 2003).

Initial of these methods have been proposed in 2001 by Buchwald and co-workers. Coupling reactions of lactams, primary amides, and formamides derived from primary amines and acetanilide with a variety of aryl iodides have been succesfully demonstrated in this study. Generally, the required reagents for an effective synthesis are 1 mol % of air stable CuI along with 10 mol % of economic racemic *trans*-cyclohexanediamine (1a) in the presence of K_3PO_4. The products are synthesized in 23 h at 110°C in moderate to excellent yields under comparatively milder reaction conditions than previously reported methods in the literature (Klapars et al., 2001).

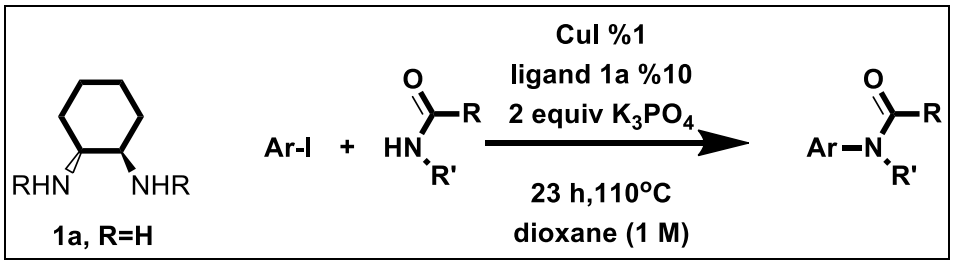

Figure 2.11. Copper-Catalyzed Amidation of Aryl Iodides
(Source: Klapars et al., 2001)

Another method has been offered in 2003 by Ma and co-workers. In the course of this study, mild method for Ullmann coupling reaction of amines and aryl halides have been developed. By employing CuI as catalyst and either *N*-methylglycine or L-proline as the ligand in the presence of K_2CO_3, Ullmann-type aryl amination of aryl iodides and aryl bromides afforded the corresponding *N*-arylamines or *N*,*N*-diarylamines which have yields ranging from good to excellent in DMSO at 40-90°C (Ma et al., 2003).

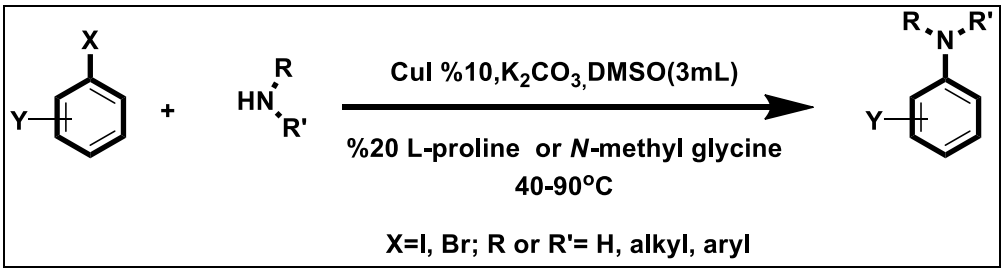

Figure 2.12. Coupling Reaction of Aryl Halides with Amines under the Catalysis of CuI and L-Proline
(Source: Ma et al., 2003)

The last of these methods have been suggested in 2004 by Taillefer and co-workers. In this study, highly efficient and mild method has been developed for nitrogen heterocycles, amides and carbamates with copper catalyzed N- and C-arylation process. Via economic, air stable copper salts or oxides as catalyst in combination with structurally unpretentious chelating ligands in the presence of Cs_2CO_3 in acetonitrile,

the N-arylation of imidazole with aryl iodides or bromides is discovered to be thoroughly sped up in 24-100 h at 50-82^{o}C (Cristau et al., 2004).

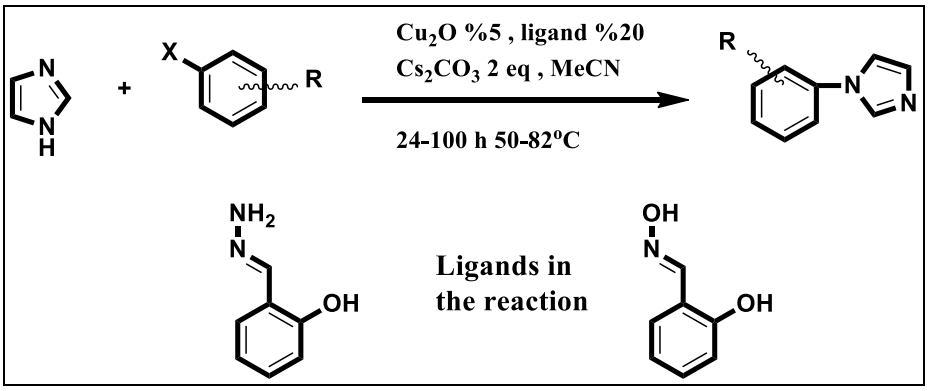

Figure 2.13. Copper-catalyzed N-arylation of imidazole with functionalized aryl bromides or iodides under mild conditions and ligands employed
(Source: Cristau et al., 2004)

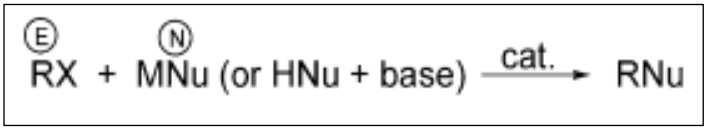

Figure 2.14. Overall equation for Ullmann reactions
(Source: Beletskaya et al., 2004)

Generally, Ullmann reactions occur in between an electrophilic aryl halide and a nucleophile. This type of reactions, which are accelarated and employed in the presence of catalyst (copper or palladium catalyst), are so-called as cross-coupling reactions and approved as nucleophilic substitution reactions in literature (Beletskaya et al., 2004).

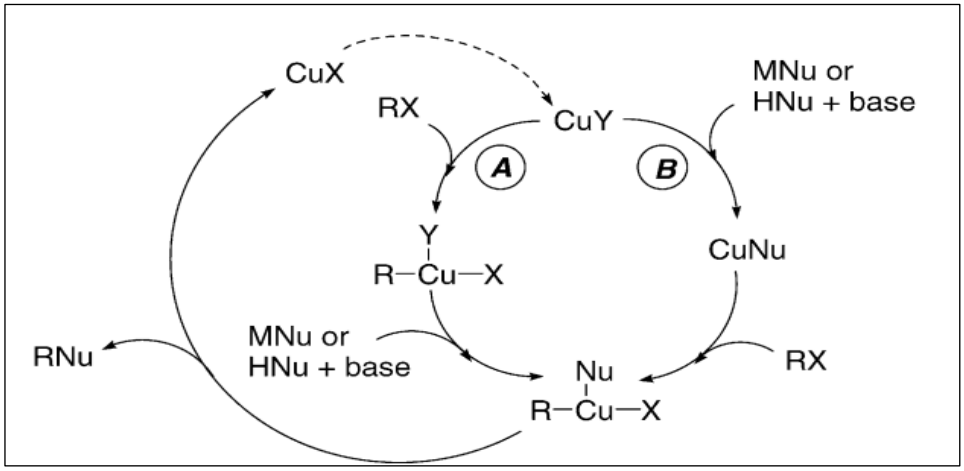

Figure 2.15. A rough picture of the possible catalytic cycle driven by Cu
(Source: Beletskaya et al., 2004)

There is no consensus on the exact mechanism of the Ullmann reaction; however, there are two possible approaches to predict the reaction pathway. One approach assumes that the copper catalyst forms a complex with the electrophilic aryl halide, forming a copper-nucleophile-electrophilic aryl halide complex in the presence of base and thereby succesfully completing the synthesis of the final product. Another approach supposes that the copper catalyst forms a complex with the nucleophile, also forming a copper-nucleophile-electrophilic aryl halide complex in the presence of base and thereby succesfully implementing the synthesis of the target product. In the literature, both pathways are considered to be acceptable and valid (pathways A or B in Figure 2.15, omitting all details such as ligands, etc). As a general consideration, the catalyst is predicted to take roles in successive oxidative addition, transmetallation, and reductive elimination reactions (Beletskaya et al., 2004).

Nowadays, there is a great variety of applications utilising Ullmann reactions. Some modern techniques of Ullmann reactions are demonstrated below.

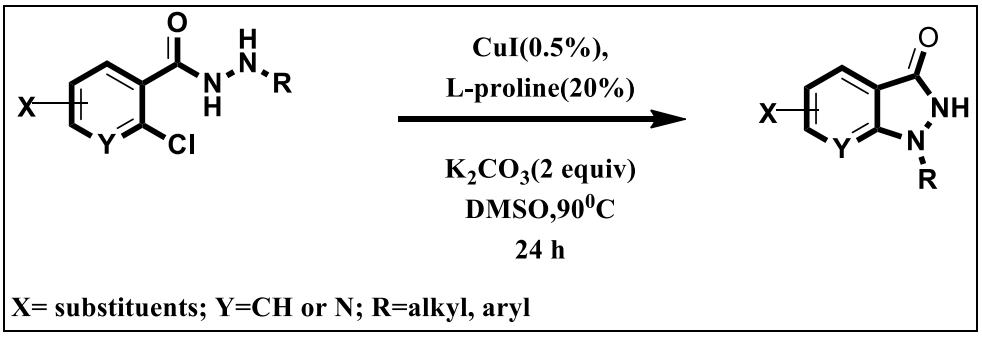

Figure 2.16. Synthesis of substituted indazolone derivatives
(Source: Tanimori et al., 2012)

Tanimori and co-workers have described an efficient and favourable method for the synthesis of derivatised indazoles, many of which display analgesic, antitumour, anticancer, anti-inflammatory, and antifertility activities, from 2-chloroarenes via an intramolecular C-N bond formation at low catalyst loading (effective even at a 0.5 mol% loading of copper (I) iodide). The products are synthesised under mild reaction conditions, employing CuI (0.5 mol%) associated with L-proline (20 mol%) in the presence of two equivalents of potassium carbonate in dimethylsulfoxide, for 24 h at 90^{o}C in moderate to excellent yields. The syntheses in our research are principally derived from this method (Tanimori et al., 2012).

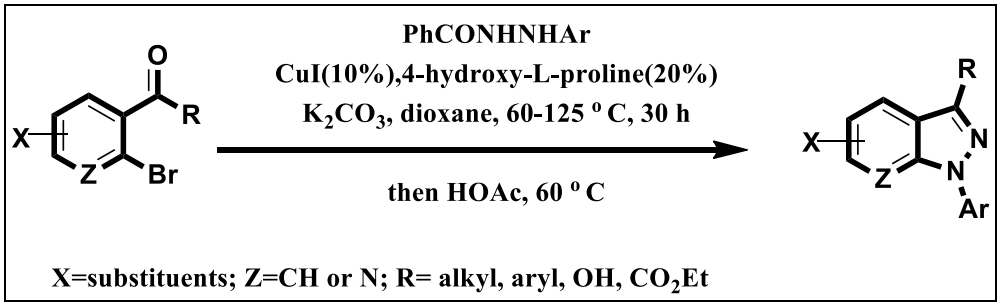

Figure 2.17. One-pot reaction process for assembly of 1-aryl-1*H*-indazoles
(Source: Xiong et al., 2012)

In this scientific study, Ma and co-workers have enhanced a facile strategy for the assembly of *N*,*N*-disubstituted hydrazines, -which are bioactive as sensory neuron

inhibitors, cell harm inhibitors, α-adrenoceptor antagonists and, potential agents for the treatment of thrombolic disease, and as well as practical intermediates for assembling azo heterocycles, such as indazoles, indoles-, and 1-aryl-1*H*-indazoles via copper-catalysed Ullmann coupling reactions. Initially, an efficient pathway is found for assembling *N*,*N*-diaryl hydrazines to synthesise *N*-acyl-*N'*,*N'*-disubstituted hydrazines by reacting *N*-acyl-*N'*-substituted hydrazines and aryl iodides at 60 ^{o}C -90 ^{o}C via copper catalysed Ullmann coupling (ligand-free media including CuI catalyst in the presence of K_2CO_3 in DMSO). Moreover, via a catalytic system of CuI/4-hydroxy-L-proline in the presence of K_2CO_3 and HOAc, respectively in dioxane, *N*-acyl-*N'*-substituted hydrazines react with 2-bromoarylcarbonylic compounds at 60 ^{o}C-125 ^{o}C to afford 1-aryl-1*H*-indazoles (Xiong et al., 2012).

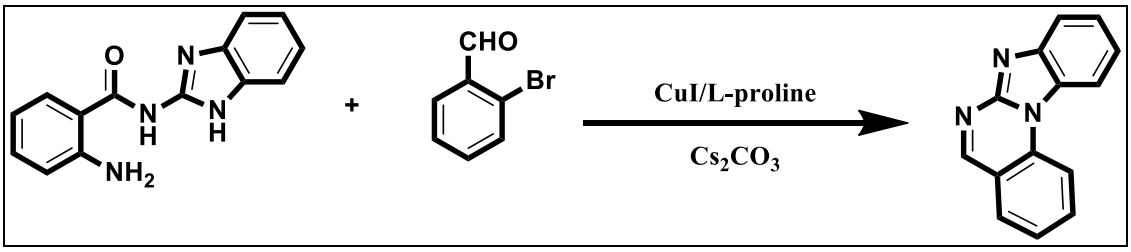

Figure 2.18. Synthesis of Benzimidazo[1,2-a]quinazoline derivatives
(Source: Li et al., 2014)

In this study, Wang and co-workers have improved a straightforward method for the synthesis of benzimidazo[1,2-*a*]quinazoline analogues, which are of considerable interest because of their assorted anticancer activities, by drawing upon a domino reaction of *N*-(2-benzimidazolyl)-2-aminobenzamide and 2-halogenated benzaldehydes using a copper catalyst. This effective method, based on a consecutive CuI-catalysed Ullmann reaction (C−N bond formation) exploits a CuI catalyst in conjunction with L-proline as a ligand in the presence of caesium carbonate and gives moderate to good yields for the target products (Li et al., 2014).

CHAPTER 3

EXPERIMENTAL METHODS

3.1. General Methods

All reagents were purchased from commercial suppliers (Aldrich and Merck). Dimethylsulfoxide was used without further purification. Tetrahydrofuran and dichloromethane were used after drying with Molecular Sieves 3Å at 400^{o}C. ^{1}H NMR and ^{13}C NMR were measured on a Varian VNMRJ 400 Nuclear Magnetic Resonance Spectrometer and chemical shifts were calibrated using residual solvents signals ($CDCl_3$: δ (H)= 7.26, δ (C)= 77, CD_3SOCD_3: δ (H)= 2.49, δ (C)= 39.7) or TMS. UV absorption spectra were measured on Shimadzu UV-2550 Spectrophotometer. Fluorescence experiments were performed by using Varian Cary Eclipse Fluorescence spectrophotometer. Infrared spectra were obtained using a Perkin–Elmer Spectrum 100 by ATR method with neat samples. The synthesized compounds were analyzed by GC-MS (HP 6890/5973N) and isolated by column chromatography using a hexane-ethyl acetate system.

3.2. Synthetic Methods

3.2.1. Synthesis of Terminal Alkynes (Sonogashira Coupling Reaction)

All reactions were conducted at 50^{o}C under argon gas. Firstly, aryl halides (5.8 mmol) were dissolved with degased triethylamine (25 ml) in two-necked glass flask. To this solution, $Pd(PPh_3)_3Cl_2$ (79 mg, 0.12 mmol) and CuI (11 mg, 0.06 mmol) in catalytic amounts were added in return under argon atmosphere and were stirred for 10 minutes. Then, 1.2 equivalent of trimethylsilylacetylene were added and stirred until completion of all reactants. The reaction monitored by TLC was quenched at the time of starting material consumption. After the solvent was removed in vacuo under reduced pressure

the crude product was extracted with dichloromethane. The organic phase was dried with anhydrous Na_2SO_4 and then concentrated in vacuo. The re-concentrated crude mixture was purified by column chromatography on silica gel (Cheng et al., 2015; Tanaka et al., 2004; O'Rourke et al., 2014).

The purified silylated product was dissolved in 25 ml methanol and stirred for two hours by adding 97 mg, 0.7 mmol K_2CO_3 to the reaction media under argon gas. When all starting material was consumed the reaction was quenched and solvent was vaporised. Terminal alkynes were afforded purely by column chromatography (Cheng et al., 2015; Tanaka et al., 2004; O'Rourke et al., 2014).

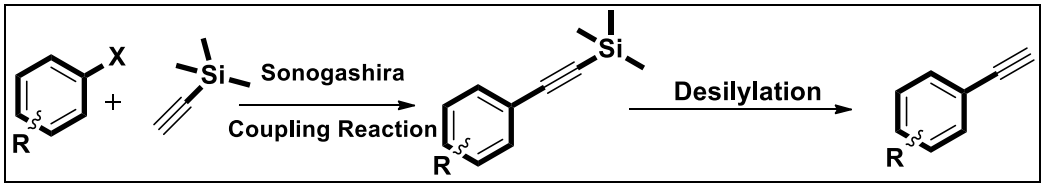

Figure 3.1. Synthesis of terminal alkynes

All synthesised terminal alkynes employing this method were tabulated below (Table 3.1).

Table 3.1. Terminal alkynes synthesized in this study

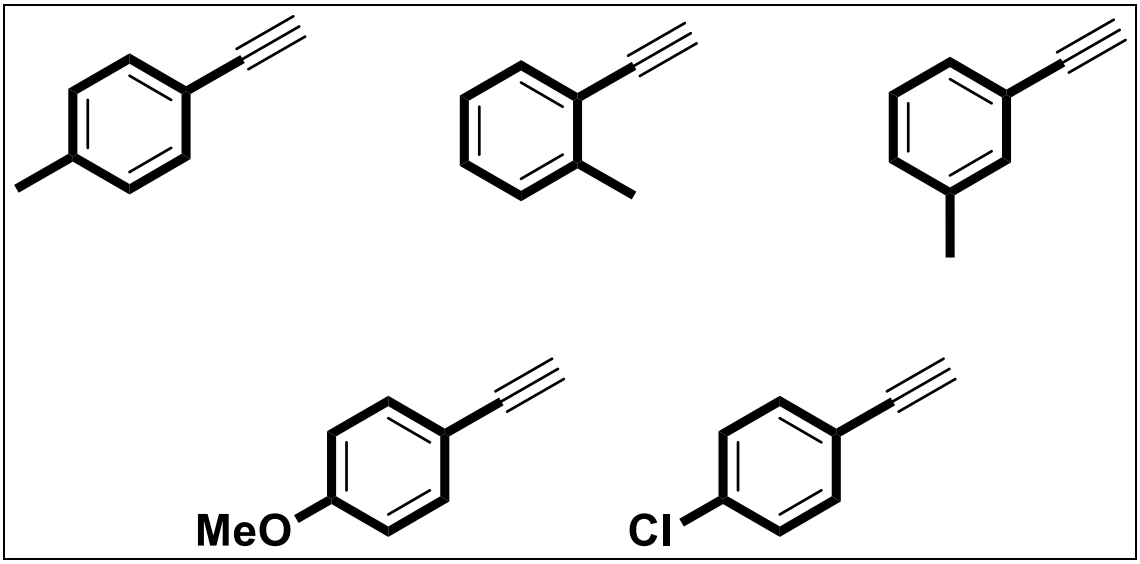

3.2.2. (1)_ Synthesis of Propiolates

Literature procedure was employed to synthesise propiolates. Terminal alkyne (7.7 mmol) was taken into two-necked glass flask by dissolving with dried tetrahydrofurane and was cooled to -78^{o}C. To reaction medium, (1.6M in hexane solution, 8.1 mmol, 5.1 mL) butyl lithium solution was added drop by drop and stirred vigorously for 1 hour at that temperature. Then, by keeping the temperature same as -78^{o}C, ethyl chloroformate was added drop by drop and reaction was stirred for 2 hours. The reaction which was quenched with distilled water was extracted with diethylether and dried with Na_2SO_4. Propiolates were afforded purely by column chromatography (Cheng et al., 2015; Tanaka et al., 2004; O'Rourke et al., 2014).

.

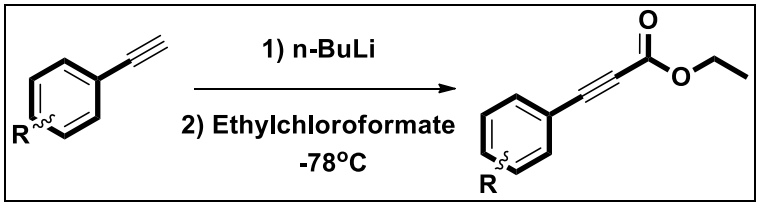

Figure 3.2. Synthetic route to propiolates

All synthesised propiolates employing this method were tabulated below (Table 3.2).

Table 3.2. Propiolates synthesized in this study

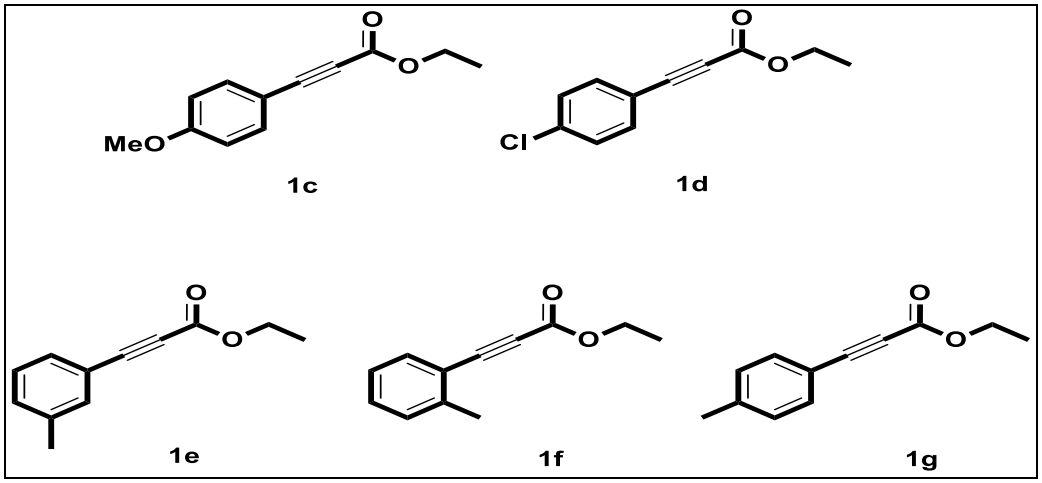

3.2.3. (2)_ Synthesis of Pyrazoles

The reaction was performed with condenser at reflux under argon atmosphere. The synthesised propiolate was dissolved in ethanol and mixture was stirred at reflux. Then, 0.4 mL hydrazine hydrate ($NH_2NH_2.H_2O$, 50-60% v/v) were added to the reaction medium and stirred vigorously overnight. The afforded precipitate in consequence of reaction was filtrated with cold ethanol and dried under vacuum. The desired pyrazoles were synthesised purely without further purification.

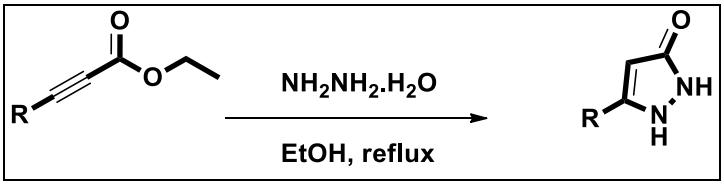

Figure 3.3. Synthesis of pyrazoles

All synthesised pyrazoles employing this method were tabulated below (Table 3.3).

Table 3.3. Pyrazoles synthesized in this study

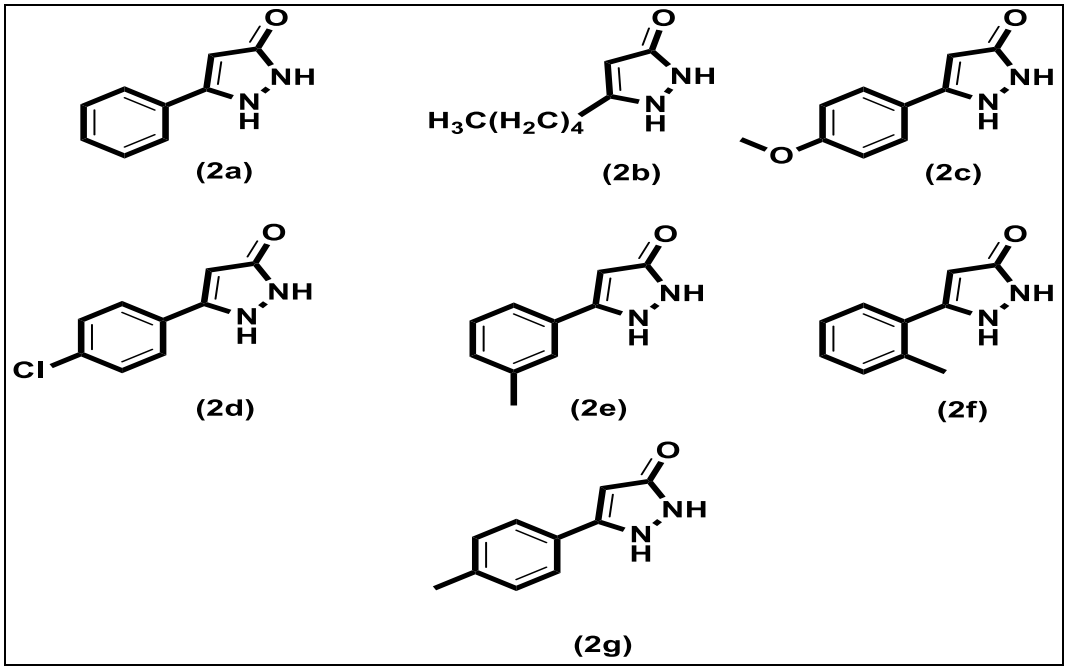

3.2.4. (3)_ Synthesis of 2-halobenzoyl chloride

The reaction was performed with condenser at reflux under argon atmosphere. 2-halobenzoic acid (1.6 g, 6.6 mmol) was dissolved in dichloroethane (5 mL) and thionylchloride was added to the reaction media. The reaction was stirred vigorously for 3 hours at reflux and then, the solvent was removed in vacuo after completion of the reaction. The afforded product was used without further purification.

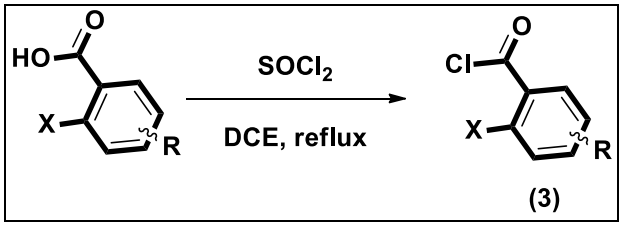

Figure 3.4. Synthesis of 2-halobenzoyl chlorides

3.2.5. (4)_ Synthesis of (2-halobenzoyl)-pyrazoles

Method A:

The reactant number (4) to be employed in cyclisation reaction was synthesised via the reaction of pyrazole (2) and 2-halobenzoic acid with ratios 1:1.1 in the presence of 0.3 equivalent of 4-dimethylaminopyridine and 1.2 equivalent of *N*,*N*'-dicyclohexylcarbodiimide reagents in dichloromethane overnight at RT (Figure 3.5). The afforded product was purified by column chromatography in dichloromethane eluent.

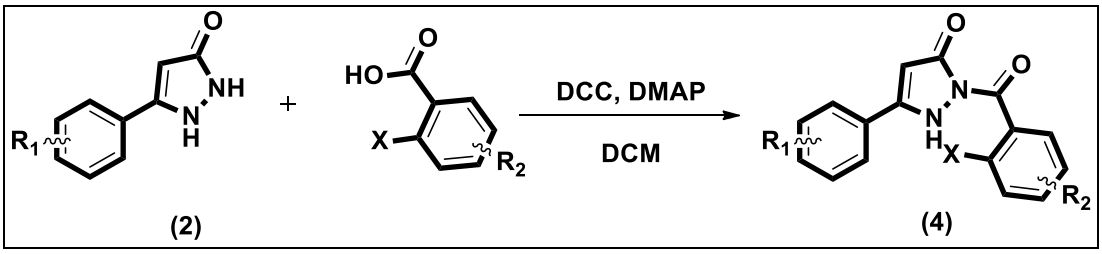

Figure 3.5. Synthesis of (2-halobenzoyl)-pyrazoles via 2-halobenzoic acid

Method B:

The reactant number (4) to be employed in cyclisation reaction was synthesised via the reaction of pyrazole (2) and 2-halobenzoyl chloride with ratios 1:1.2 in the presence of 1 equivalent of caesium carbonate reagent in dichloromethane overnight at RT (Figure 3.6). The afforded product was purified by column chromatography in dichloromethane eluent.

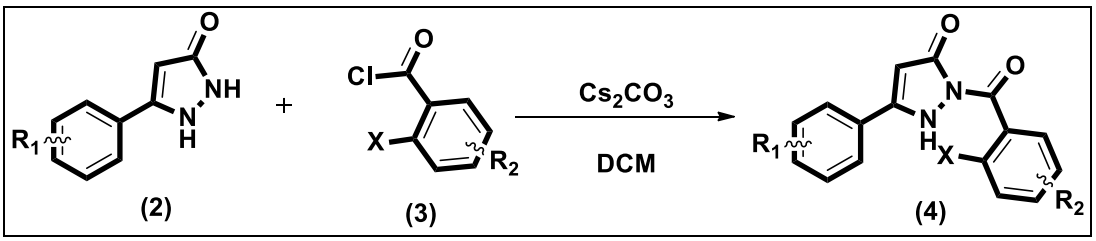

Figure 3.6. Synthesis of (2-halobenzoyl)-pyrazoles via 2-halobenzoyl chloride

All synthesised (2-halobenzoyl)-pyrazoles employing this method were tabulated below (Table 3.4).

Table 3.4. (2-halobenzoyl)-pyrazoles synthesized in this study

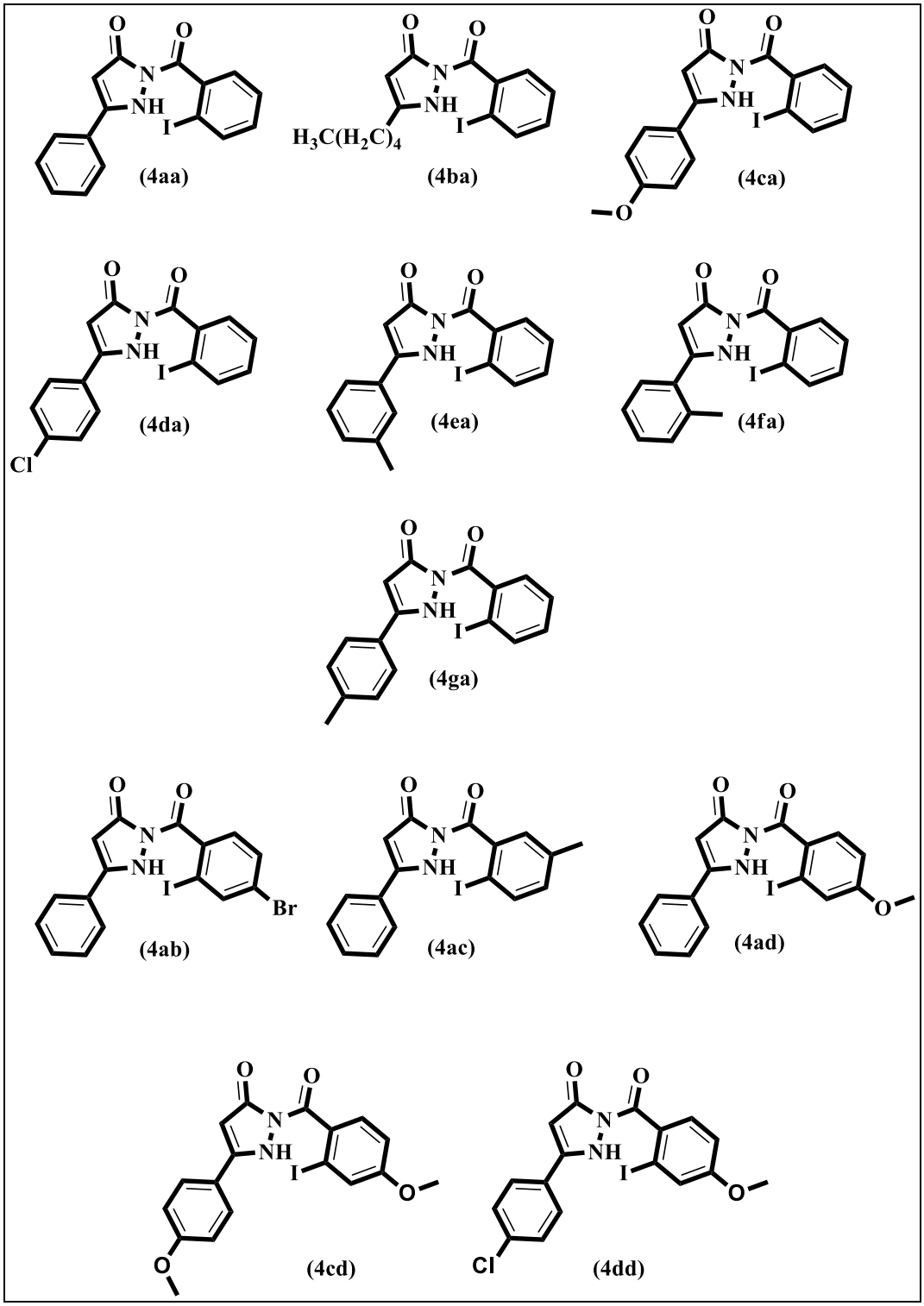

3.2.6. (5)_Synthesis of Benzo-Bimanes

Firstly, 2-iodo-benzoyl-pyrazole (0.3 mmol) was dissolved in DMSO (2 mL). To the reaction, 1 mol% copper at first, 40 mol% ligand (triphenylphosphine) 3 minutes later and K_2CO_3 (0.6 mmol) 30 minutes later were added respectively and stirred vigorously. The reaction was monitored by thin layer chromatography until the completion of the reaction. After the solvent was removed in vacuo the afforded product was isolated by column chromatograhy using hexane-ethyl acetate system.

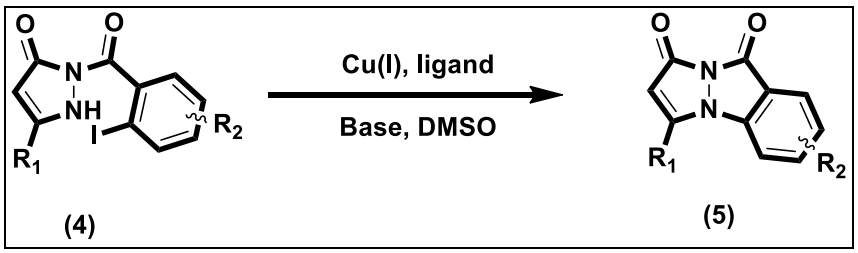

Figure 3.7. Synthetic route to Benzo-Bimanes

All synthesised benzo-bimanes employing this method were tabulated below (Table 3.5).

Table 3.5. Benzo Bimanes synthesized in this study

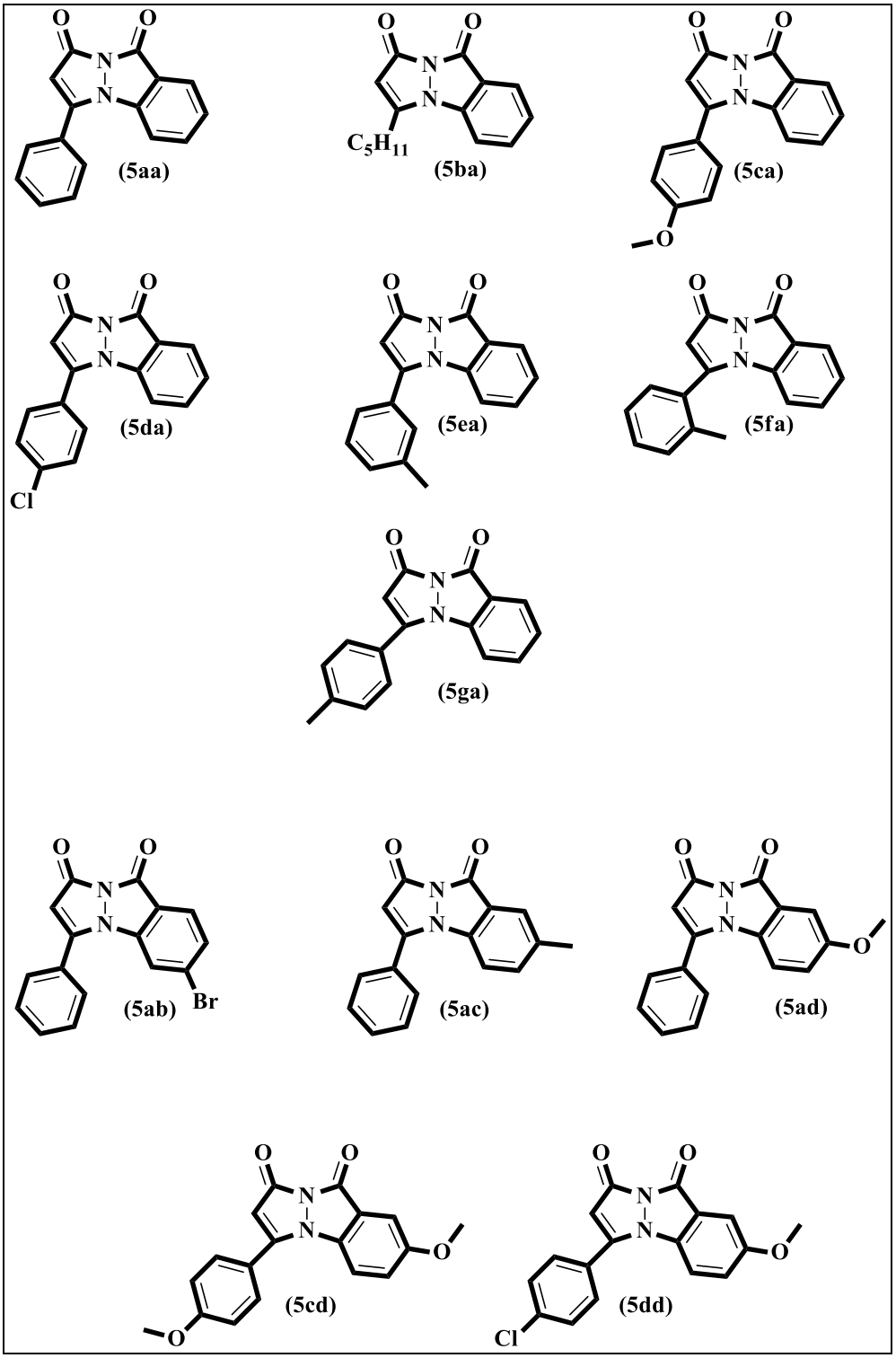

3.3. Characterization of Pyrazoles, Reactants and Products

All synthesised pyrazoles, reactants and products were characterized by ^{1}H and ^{13}C NMR spectroscopies. NMR data of all novel pyrazoles, reactants and products for literature were given below.

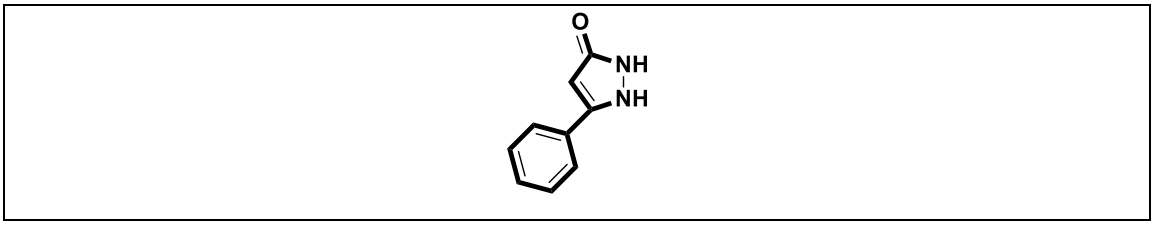

Figure 3.8. 5-phenyl-1*H*-pyrazol-3(2*H*)-one

2a: ^{1}H NMR (400 MHz, DMSO-d_6) δ: 11.16 (bs, 2H), 7.66 (d, J= 7.6 Hz, 2H), 7.38 (t, J=7.6 Hz, 2H), 7.28 (t, J= 7.6Hz, 1H), 5.89 (s, 1H). ^{13}C NMR (100 MHz, DMSO-d_6) δ: 166.2, 148.6, 135.7, 134.0, 132.52, 132.9, 129.69, 129.9, 92.0.

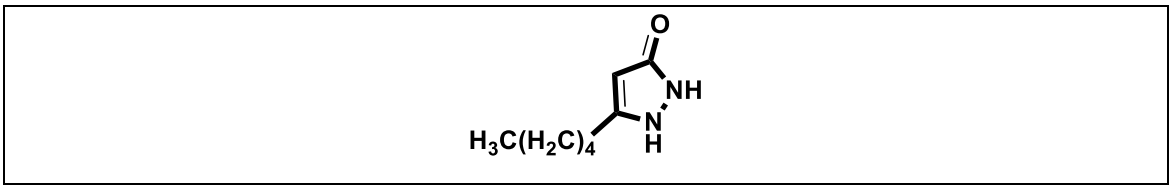

Figure 3.9. 5-pentyl-1*H*-pyrazol-3(2*H*)-one

2b: ^{1}H NMR (400 MHz, DMSO-d_6) δ: 10.37 (bs, 2H), 5.22 (s, 1H), 2.41 (t, J=7.6 Hz, 2H), 1.51 (pent, J= 7.6 Hz, 2H), 1.30-1.22 (m, 4H), 0.84 (t, J=6.8 Hz, 3H). ^{13}C NMR (100 MHz, DMSO-d_6) δ: 161.4, 144.8, 88.4, 31.2, 28.8, 26.0, 22.2, 14.3.

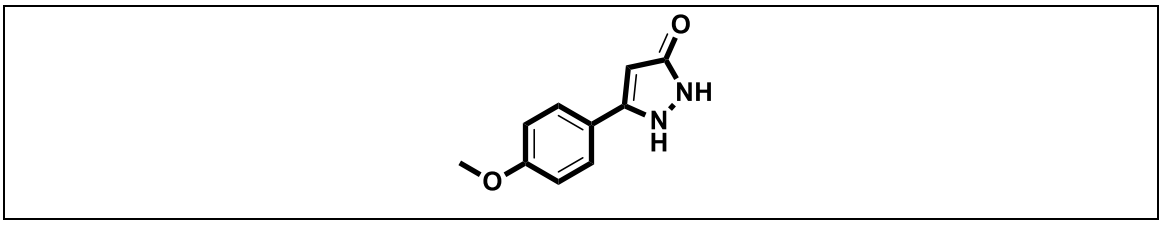

Figure 3.10. 5-(4-methoxyphenyl)-1*H*-pyrazol-3(2*H*)-one

2c: ^{1}H NMR (400 MHz, DMSO-d_6) δ: 10.83 (bs, 2H), 7.58 (d, J= 8.4 Hz, 2H), 6.95 (d, J=8.8 Hz, 2H), 5.78 (s, 1H), 3.76 (s, 3H). ^{13}C NMR (100 MHz, DMSO-d_6) δ: 161.5, 159.3, 143.5, 126.6, 123.5, 114.6, 86.7, 55.6.

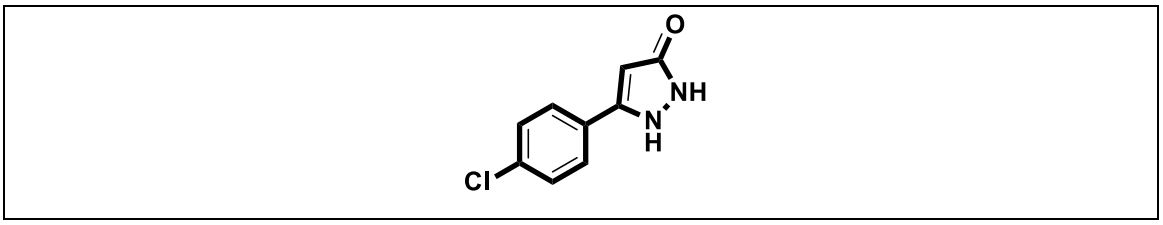

Figure 3.11. 5-(4-chlorophenyl)-1*H*-pyrazol-3(2*H*)-one

2d: ^{1}H NMR (400 MHz, DMSO-d_6) δ: 11.86 (bs, 2H), 7.68 (d, J= 8.8 Hz, 2H), 7.44 (d, J= 8.4 Hz, 2H), 5.89 (s, 1H). ^{13}C NMR (100 MHz, DMSO-d_6) δ: 161.0, 142.9, 132.5, 132.52, 130.2, 129.2, 129.2, 126.9, 87.2.

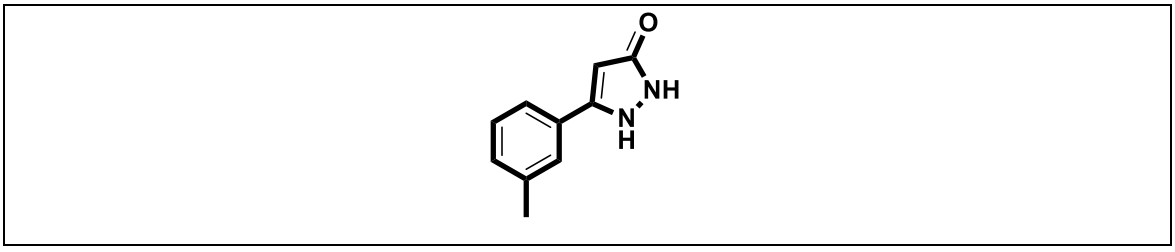

Figure 3.12. 5-(m-tolyl)-1*H*-pyrazol-3(2*H*)-one

2e: ^{1}H NMR (400 MHz, DMSO-d_6) δ: 11.73 (bs, 1H), 9.87 (bs, 1H), 7.47 (s, 1H), 7.44 (d, J= 7.6 Hz, 1H), 7.27 (t, J=7.6 Hz, 1H), 7.10 (d, J= 7.6 Hz, 1H), 5.85 (s, 1H), 2.32 (s,3H). ^{13}C NMR (100 MHz, DMSO-d_6) δ: 161.4, 143.9, 138.4, 130.8, 129.1, 128.9, 125.8, 122.3, 87.3, 21.5.

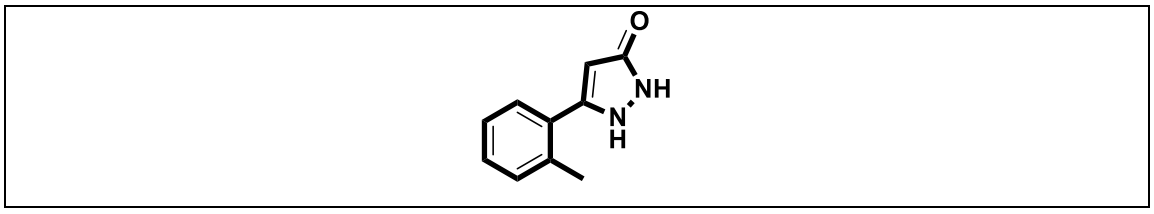

Figure 3.13. 5-(o-tolyl)-1*H*-pyrazol-3(2*H*)-one

2f: ^{1}H NMR (400 MHz, DMSO-d_6) δ: 10.52 (bs, 2H), 7.39-7.37 (m, 1H), 7.24-7.20 (m, 3H), 5.64 (s, 1H), 2.35 (s, 3H). ^{13}C NMR (100 MHz, DMSO-d_6) δ: 161.1, 143.1, 135.6, 131.2, 131.0, 128.8, 128.4, 126.3, 90.6, 21.1.

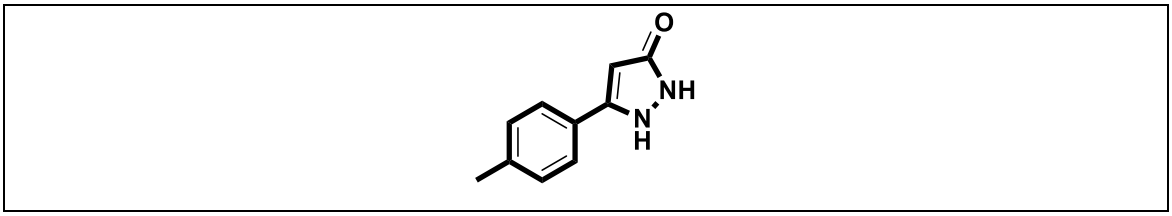

Figure 3.14. 5-(p-tolyl)-1*H*-pyrazol-3(2*H*)-one

2g: ^{1}H NMR (400 MHz, DMSO-d_6) δ: 11.71 (bs, 1H), 9.81 (bs, 1H), 7.52 (d, J= 8.4 Hz, 2H), 7.18 (d, J= 7.6 Hz, 2H), 5.81 (s, 1H), 2.28 (s, 3H). ^{13}C NMR (100 MHz, DMSO-d_6) δ: 161.5, 143.6, 137.5, 129.7, 128.1, 125.1, 87.0, 21.2.

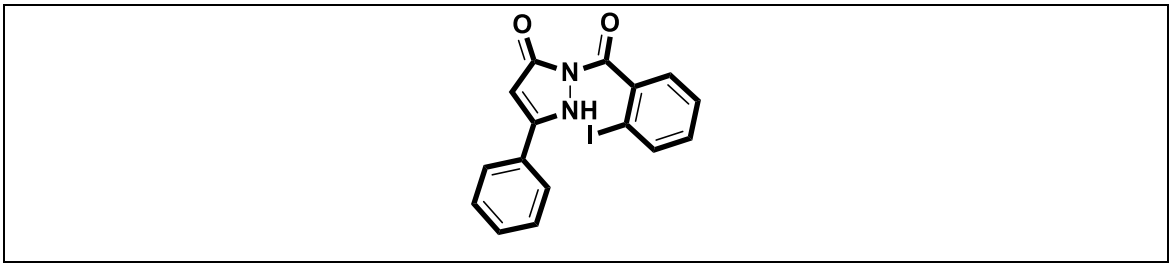

Figure 3.15. 2-(2-iodobenzoyl)-5-phenyl-1*H*-pyrazol-3(2*H*)-one

4aa: ^{1}H NMR (400 MHz, DMSO-d_6) δ: 13.23 (s, 1H), 8.14 (d, J= 7.6 Hz, 1H), 8.02 (d, J=8.0 Hz, 1H), 7.79 (d, J=7.6 Hz, 2H), 7.63 (t, J=7.2 Hz, 1H), 7.50 (t, J=7.4 Hz, 2H) , 7.40 (t, J=7.6 Hz, 2H), 6.71 (s, 1H). ^{13}C NMR (100 MHz, DMSO-d_6) δ: 164.2, 155.7, 143.7, 141.7, 134.4, 134.0, 131.6, 129.5, 129.1, 129.0, 125.5, 95.6, 93.6.

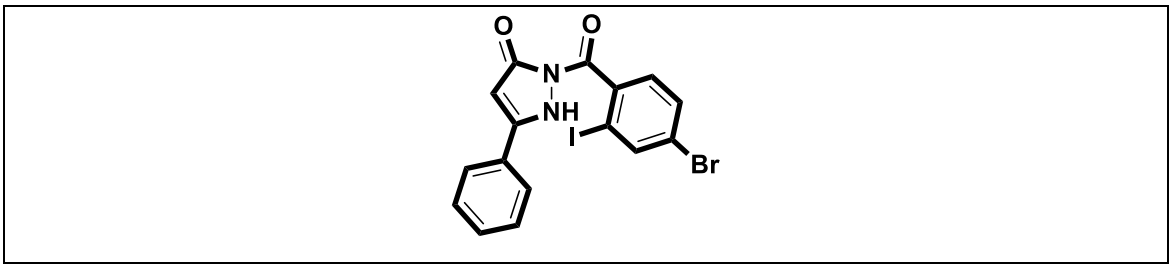

Figure 3.16. 2-(4-bromo-2-iodobenzoyl)-5-phenyl-1*H*-pyrazol-3(2*H*)-one

4ab: ^{1}H NMR (400 MHz, $CDCl_3$) δ: 12.39 (s, 1H), 7.94 (d, J=8 Hz, 1H), 7.64 (d, J=1.6 Hz, 1H), 7.62 (d, J=7.6 Hz, 2H), 7.46 (dd, J=8.8, 1.6 Hz, 1H), 7.35 (t, J=7.2 Hz, 2H), 7.26 (t, J=7.2 Hz, 1H), 6.50 (s, 1H) ^{13}C NMR (100 MHz, $CDCl_3$) δ: 161.5, 155.6, 143.9, 135.8, 134.1, 133.3, 130.1, 129.4, 128.9, 128.5, 127.5, 127.2, 125.4, 92.9.

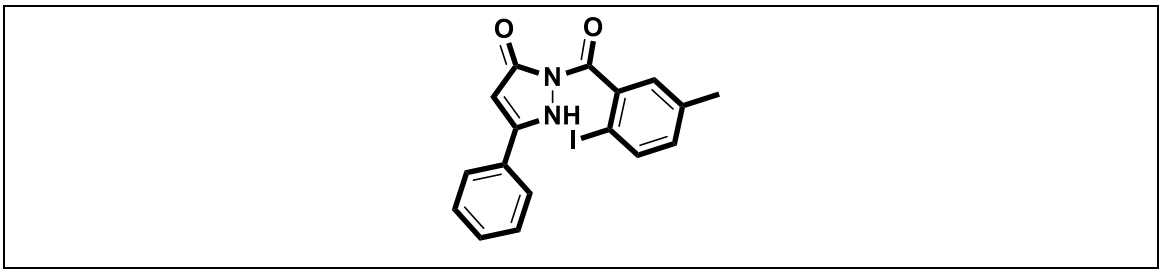

Figure 3.17. 2-(2-iodo-5-metylbenzoyl)-5-phenyl-1*H*-pyrazol-3(2*H*)-one

4ac: ^{1}H NMR (400 MHz, $CDCl_3$) δ: 10.78 (s, 1H), 7.86 (d, J=6 Hz, 1H), 7.60 (d, J=8 Hz, 3H), 7.38 (t, J=7.6 Hz, 2H), 7.34 (t, J=7.6 Hz, 1H), 7.21 (dd, J=8 Hz, 1H), 6.65 (s, 1H), 2.35 (s, 3H) ^{13}C NMR (100 MHz, $CDCl_3$) δ: 162.7, 144.4, 137.5, 134.5, 134.4, 132.8, 129.7, 129.1, 128.9, 128.6, 125.4, 119.4, 93.9, 20.7.

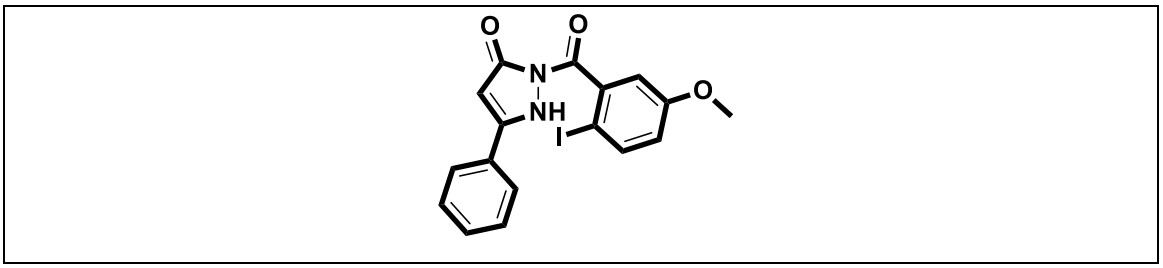

Figure 3.18. 2-(2-iodo-5-methoxybenzoyl)-5-phenyl-1*H*-pyrazol-3(2*H*)-one

4ad: ^{1}H NMR (400 MHz, $CDCl_3$) δ: 12.33 (s, 1H), 7.62 (d, J=6.8 Hz, 2H), 7.54 (s, 1H), 7.53 (d, J=5.2 Hz, 1H), 7.35 (t, J=8 Hz, 2H), 7.27 (t, J=7.2 Hz, 1H), 6.91 (dd, J=8.4, 3.2 Hz, 1H), 6.52 (s, 1H), 3.78 (s, 3H) ^{13}C NMR (100 MHz, $CDCl_3$) δ: 162.7, 158.6, 135.3, 130.9, 129.4, 128.9, 128.4, 125.4, 119.9, 116.8, 112.8, 93.0, 55.7.

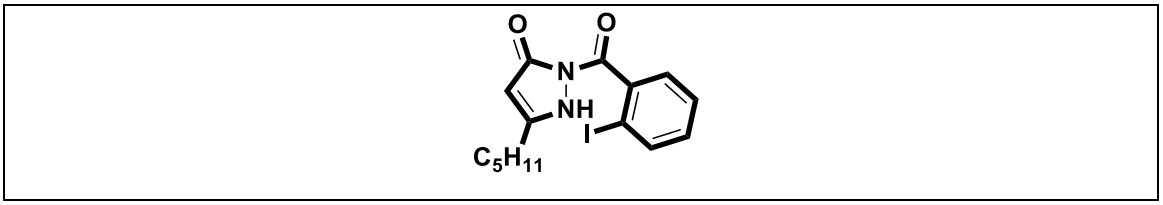

Figure 3.19. 5-pentyl-2-(2-iodobenzoyl)-1*H*-pyrazol-3(2*H*)-one

4ba: ^{1}H NMR (400 MHz, $CDCl_3$) δ: 11.01 (s, 1H) , 8.04 (t, J=7.6 Hz, 2H), 7.45 (t, J=7.6 Hz, 1H), 7.20 (t, J=7.6 Hz, 1 H), 6.11 (s, 1H), 2.58 (t, J=7.6 Hz, 2H), 1.54 (pent, J=10.8 Hz, 2H), 1.21-1.11 (m, 4H), 0.79 (t, J=7.2 Hz, 3H) ^{13}C NMR (100 MHz, $CDCl_3$) δ: 163.2, 155.2, 145.9, 141.8, 133.5, 133.26, 131.7, 128.1, 94.9, 93.8, 31.2, 28.4, 26.2, 22.3, 14.0.

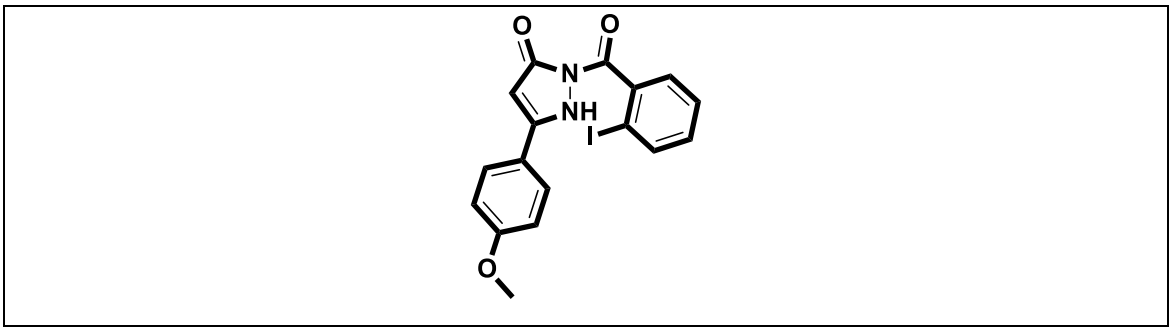

Figure 3.20. 2-(2-iodobenzoyl)-5-(4-methoxyphenyl)-1*H*-pyrazol-3(2*H*)-one

4ca: ^{1}H NMR (400 MHz, $CDCl_3$) δ: 10.85 (s, 1H), 8.08 (d, J=7.6 Hz, 1H), 7.71-7.63 (m, 1H), 7.52 (d, J=9.2 Hz, 2H), 7.46 (t, J=7.6 Hz, 1H), 7.22 (td, J=8.0, 1.6 Hz 1H), 6.94 (d, J=9.2 Hz, 2H), 6.55 (s, 1H), 3.83 (s, 3H) ^{13}C NMR (100 MHz, $CDCl_3$) δ: 163.0, 160.2, 156.1, 144.3, 141.8, 133.5, 132.9, 131.9, 128.1, 126.9, 121.7, 114.5, 95.1, 93.2, 55.4.

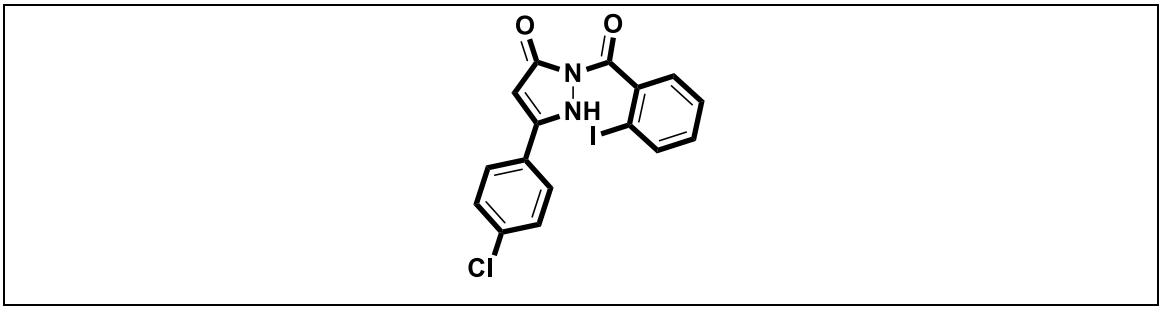

Figure 3.21. 2-(2-chlorobenzoyl)-5-(4-iodophenyl)-1*H*-pyrazol-3(2*H*)-one

4da: ^{1}H NMR (400 MHz, $CDCl_3$) δ: 10.37 (s, 1H), 8.08 (d, J=7.6 Hz, 1H), 7.97 (d, J=8 Hz, 1H), 7.54 (d, J=8 Hz, 2H), 7.44 (t, J= 7.6 Hz, 1H), 7.30 (d, J=7.6 Hz, 2H), 7.23 (t, J=7.6, 1H), 6.61 (s, 1H) ^{13}C NMR (100 MHz, $CDCl_3$) δ: 162.9, 155.9, 143.5, 141.9, 134.8, 133.6, 132.7, 131.9, 129.3, 128.1, 127.5, 126.8, 95.1, 93.9.

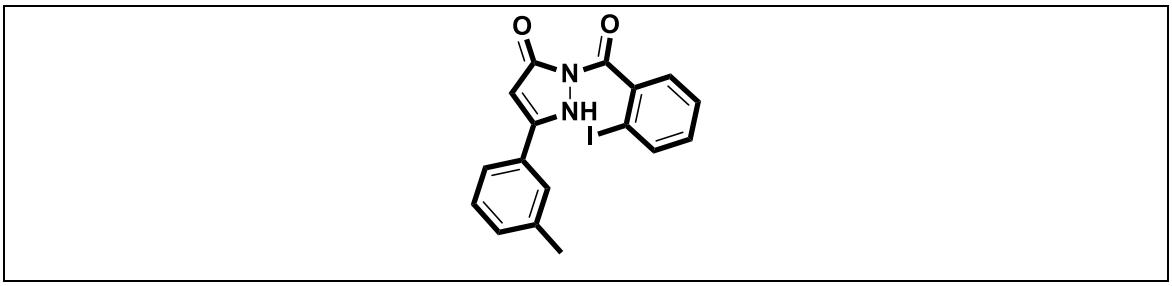

Figure 3.22. 2-(2-iodobenzoyl)-5-(m-tolyl)-1*H*-pyrazol-3(2*H*)-one

4ea: ^{1}H NMR (400 MHz, $CDCl_3$) δ: 10.63 (s, 1H), 8.07 (t, J=6.8 Hz, 2H), 7.45 (t, J=8 Hz, 1H), 7.40 (s, 1H), 7.39 (s, 1H), 7.29 (t, J=8 Hz, 1H), 7.24 (td, J=7.6, 1.6 Hz, 1H), 7.16 (d, J=8 Hz, 1H), 6.64 (s, 1H), 2.38 (s,3H) ^{13}C NMR (100 MHz, $CDCl_3$) δ: 163.0, 156.2, 144.6, 141.9, 138.9, 133.5, 132.9, 131.9, 129.8, 129.0, 128.1, 126.2, 122.5, 95.1, 93.8, 21.4.

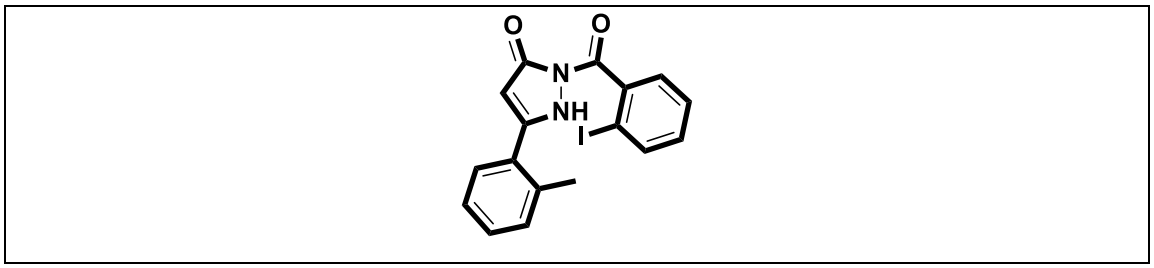

Figure 3.23. 2-(2-iodobenzoyl)-5-(o-tolyl)-1*H*-pyrazol-3(2*H*)-one

4fa: ^{1}H NMR (400 MHz, $CDCl_3$) δ: 10.11 (bs, 1H), 8.13-8.08 (m, 2H), 7.48 (t, J=8Hz, 1H), 7.41 (d, J= 6.8 Hz, 1H), 7.32-7.22 (m, 4H), 6.49 (s,1H), 2.45 (s, 3H) ^{13}C NMR (100 MHz, $CDCl_3$) δ: 163.0, 155.7, 143.6, 141.9, 136.1, 133.6, 132.9, 132.1, 131.1, 129.2, 129.0, 128.7, 128.1, 126.3, 96.8, 95.1, 20.7.

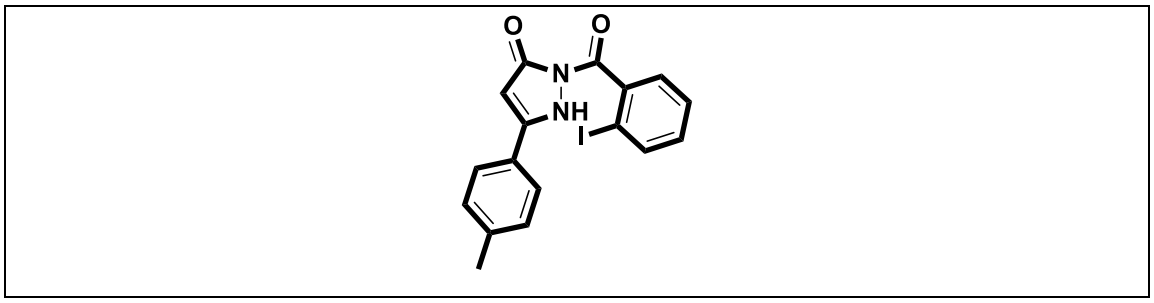

Figure 3.24. 2-(2-iodobenzoyl)-5-(p-tolyl)-1*H*-pyrazol-3(2*H*)-one

4ga: ^{1}H NMR (400 MHz, $CDCl_3$) δ: 10.68 (bs, 1H), 8.07 (t, 2H), 7.50-7.43 (m, 3H), 7.25-7.19 (m, 3H), 6.60 (s, 1H), 2.35 (s, 3H) ^{13}C NMR (100 MHz, $CDCl_3$) δ: 163.0, 156.2, 144.5, 141.9, 139.1, 133.5, 132.9, 132.0, 129.8, 128.1, 126.2, 125.3, 95.1, 93.6, 21.3.

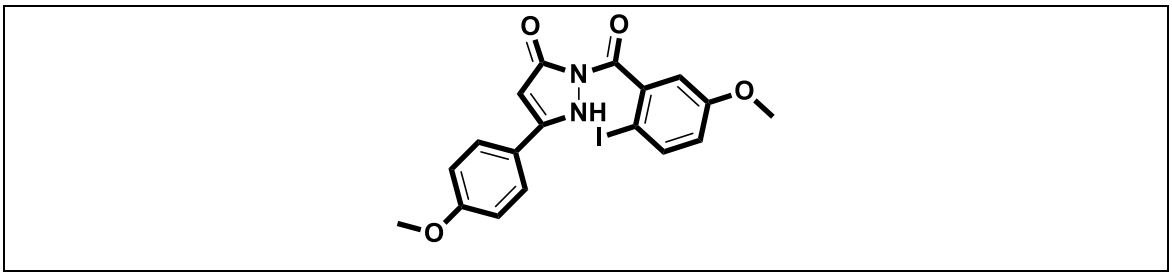

Figure 3.25. 2-(2-iodo-5-methoxybenzoyl)-5-(4-methoxyphenyl)-1*H*-pyrazol-3(2*H*)-one

4cd: ^{1}H NMR (400 MHz, $CDCl_3$) δ: 10.84 (bs, 1H), 7.59 (d, J= 8.8 Hz, 1H), 7.53-7.51 (m, 3H), 6.96 (dd, J=3.2, 2.8 Hz, 1H), 6.90 (d, J= 8.4 Hz, 2H), 6.54 (s, 1H), 3.81 (s, 3H), 3.79 (s, 3H) ^{13}C NMR (100 MHz, $CDCl_3$) δ: 162.5, 160.1, 158.6, 156.1, 144.4, 135.4, 130.6, 126.8, 121.7, 120.3, 116.7, 114.5, 113.1, 93.1, 55.7, 55.3.

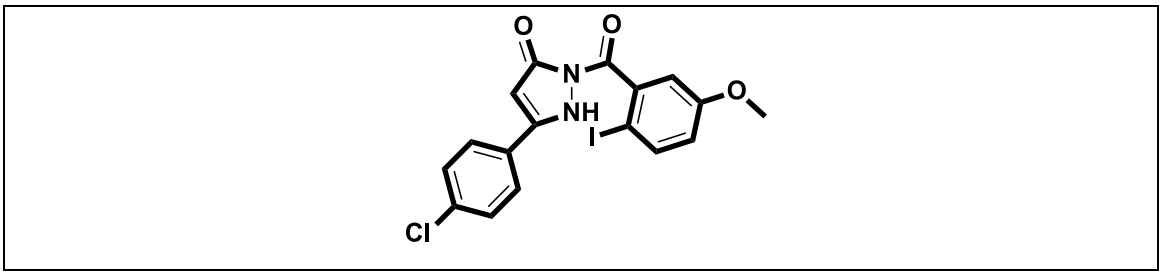

Figure 3.26. 5-(4-chlorophenyl)-2-(2-iodo-5-methoxybenzoyl)-1*H*-pyrazol-3(2*H*)-one

4dd: ^{1}H NMR (400 MHz, $CDCl_3$) δ: 10.99 (bs, 1H), 7.61 (d, J= 9.2 Hz, 1H), 7.54 (s, 1H), 7.52-7.51 (m, 2H), 7.35 (d, J= 8.4 Hz, 2H), 6.98 (dd, J= 3.2, 3.2 Hz, 1H), 6.62 (s,1H), 3.83 (s,3H) ^{13}C NMR (100 MHz, $CDCl_3$) δ: 162.5, 158.6, 156.0, 143.5, 135.5, 135.0, 130.5, 129.4 127.5, 126.7, 120.2, 116.9, 113.0, 94.2, 55.7.

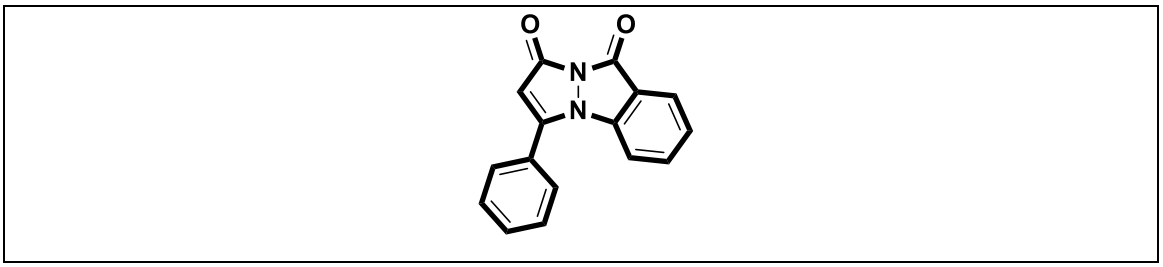

Figure 3.27. (5aa) 3-phenylpyrazolo[1,2-a]indazole-1,9-dione

5aa: ^{1}H NMR (400 MHz, $CDCl_3$) δ: 8.39 (d, J=6.8 Hz, 1H), 8.00 (d, J=6.4 Hz, 2H), 7.78 (t, J=7.2 Hz, 1H), 7.44 (d, J=7.2 Hz, 5H), 6.43 (s, 1H). ^{13}C NMR (100 MHz, $CDCl_3$) δ: 156.1, 153.8, 153.6, 152.0, 135.9, 131.5, 129.8, 128.7, 126.7, 125.1, 116.9, 114.1, 86.6.

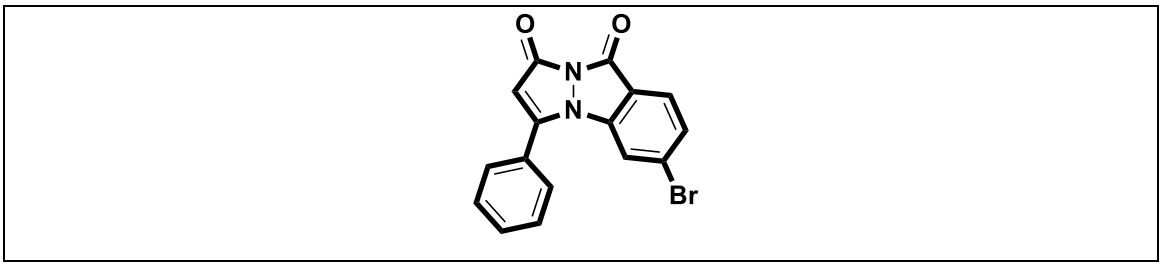

Figure 3.28. 6-bromo-3-phenylpyrazolo[1,2-a]indazole-1,9-dione

5ab: ^{1}H NMR (400 MHz, $CDCl_3$) δ: 8.22 (d, J=8.4 Hz, 1H), 7.96 (dd, J=2, 0.8 Hz, 2H), 7.61 (d, J=1.6 Hz, 1H), 7.56 (dd, J=7.2, 1.6 Hz, 1H), 7.46-7.39 (m, 3H), 6.42 (s, 1H) ^{13}C NMR (100 MHz, $CDCl_3$) δ: 156.2, 153.7, 152.9, 151.7, 131.2, 130.3, 129.9, 129.8, 128.7, 126.7, 120.2, 113.1, 87.0.

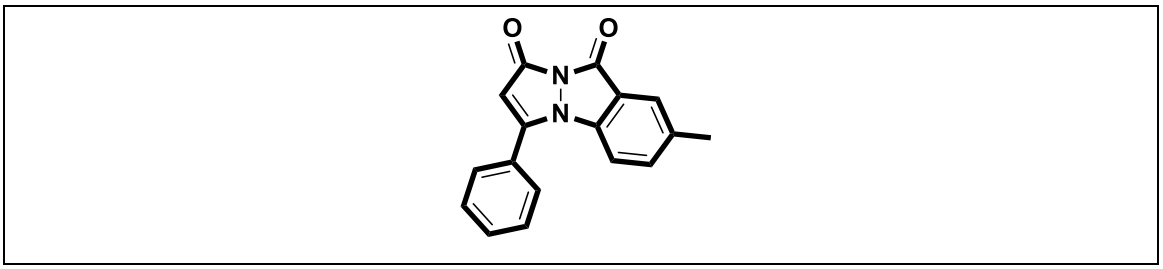

Figure 3.29. 7-methyl-3-phenylpyrazolo[1,2-a]indazole-1,9-dione

5ac: ^{1}H NMR (400 MHz, $CDCl_3$) δ: 8.18 (d, J=8 Hz, 1H), 8.00 (dd, J=8, 1.2 Hz, 2H), 7.58 (dd, J=8.4, 2 Hz, 1H), 7.48-7.42 (m, 3H), 7.34 (d, J=8.8 Hz, 1H), 6.41 (s, 1H), 2.48 (s, 3H) ^{13}C NMR (100 MHz, $CDCl_3$) δ: 156.0, 153.8, 152.2, 151.9, 136.9, 135.2, 131.6, 129.8, 128.7, 128.1, 126.7, 116.6, 113.7, 86.4, 20.7.

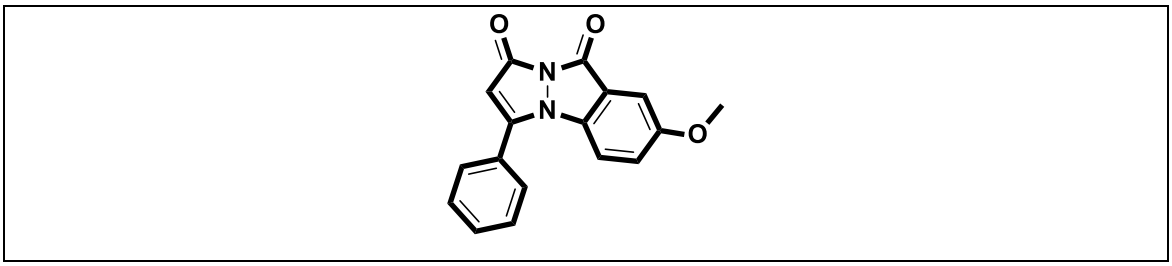

Figure 3.30. 7-methoxy-3-phenylpyrazolo[1,2-a]indazole-1,9-dione

5ad: ^{1}H NMR (400 MHz, $CDCl_3$) δ: 8.00 (d, J=6 Hz, 2H), 7.75 (d, J=2.8 Hz, 1H), 7.48-7.42 (m, 3H), 7.39-7.32 (m, 2H), 6.40 (s, 1H), 3.92 (s, 3H) ^{13}C NMR (100 MHz, $CDCl_3$) δ: 156.7, 156.1, 153.7, 152.1, 148.3, 131.6, 129.8, 128.7, 126.7, 125.2, 118.2, 114.4, 108.4, 86.2, 56.2.

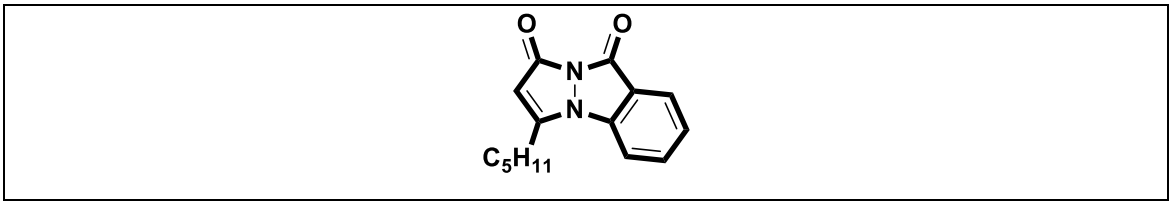

Figure 3.31. 3-pentylpyrazolo[1,2-a]indazole-1,9-dione

5ba: ^{1}H NMR (400 MHz, $CDCl_3$) δ: 8.37 (d, J= 8.4 Hz, 1H), 7.76 (t, J=8 Hz, 1H), 7.43 (t, J=8.4 Hz, 2H), 6.94 (s, 1H), 2.76 (t, J=7.6 Hz, 2H), 1.73 (pent, J= 5.6 Hz, 2H), 1.42-1.25 (m, 4H), 0.90 (t, J= 7 Hz, 3H) ^{13}C NMR (100 MHz, $CDCl_3$) δ: 159.9, 153.8, 153.5, 151.5, 135.7, 128.6, 124.9, 116.8, 88.2, 31.5, 29.4, 28.5, 22.4, 13.9.

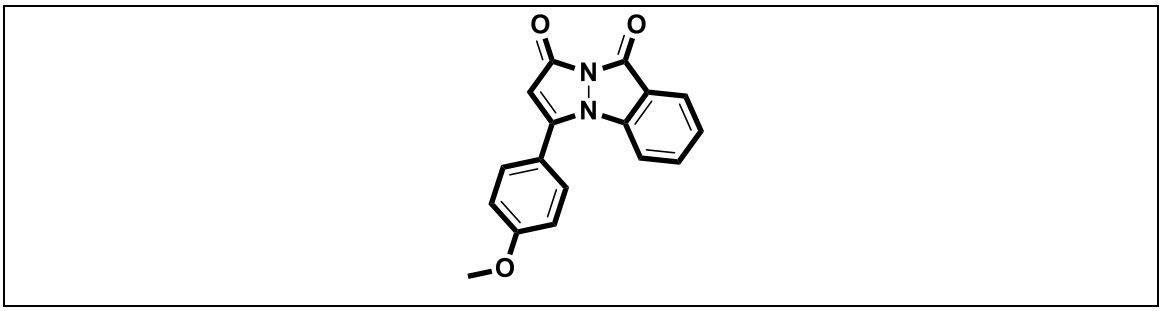

Figure 3.32. 3-(4-methoxyphenyl)pyrazolo[1,2-a]indazole-1,9-dione

5ca: ^{1}H NMR (400 MHz, $CDCl_3$) δ: 8.38 (dd, J=8.4, 2 Hz, 1H), 7.93 (d, J=9.2 Hz, 2H), 7.76 (t, J=8 Hz, 1H), 7.44 (d, J=5.6 Hz, 1H), 7.43 (d, J=7.2 Hz, 1H), 6.96 (d, J=9.2 Hz, 2H), 6.36 (s, 1H), 3.85 (s, 3H) ^{13}C NMR (100 MHz, $CDCl_3$) δ: 160.9, 155.9, 153.7, 153.6, 151.0, 135.7, 128.6, 128.2, 124.9, 124.1, 116.8, 114.2, 114.1, 86.2, 55.3.

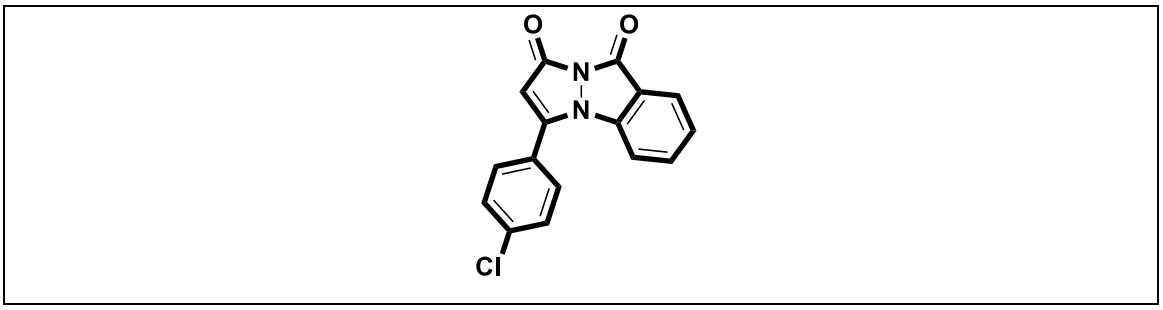

Figure 3.33. 3-(4-chlorophenyl)pyrazolo[1,2-a]indazole-1,9-dione

5da: ^{1}H NMR (400 MHz, $CDCl_3$) δ: 8.40 (d, J=6.4 Hz, 1H), 7.93 (d, J=8.8 Hz, 2H), 7.79 (t, J=8 Hz, 1H), 7.48-7.41 (m, 4H), 6.40 (s, 1H) ^{13}C NMR (100 MHz, $CDCl_3$) δ: 154.9, 153.8, 153.5, 152.1, 135.9, 135.8, 123.0, 128.9, 128.7, 127.9, 125.2, 116.9, 114.1, 86.5.

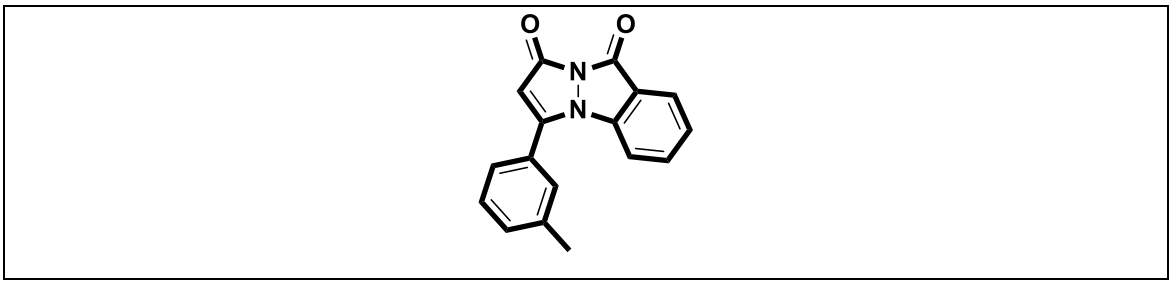

Figure 3.34. 3-(m-tolyl)pyrazolo[1,2-a]indazole-1,9-dione

5ea: ^{1}H NMR (400 MHz, $CDCl_3$) δ: 8.35 (dd, J= 7.6, 1.6 Hz, 1H), 7.85 (s, 1H), 7.76 (d, J=1.6 Hz, 1H), 7.22 (t, J=7.2 Hz, 1H), 7.43 (s, 1H), 7.40 (d, J=8 Hz, 1H), 7.31 (t, J=7.2 Hz, 1H), 7.20 (d, J=8 Hz, 1H), 6.38 (s, 1H), 2.39 (s, 3H) ^{13}C NMR (100 MHz, $CDCl_3$) δ: 156.1, 153.7, 153.6, 151.9, 138.4, 135.8, 133.6, 131.3, 130.6, 128.6, 127.2, 124.9, 123.9, 116.8, 114.1, 86.6, 21.3.

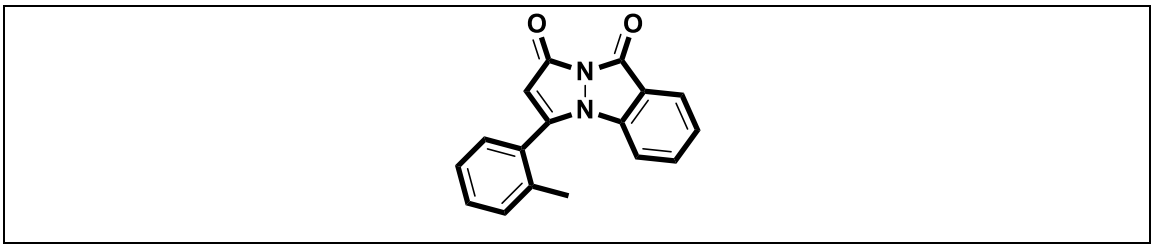

Figure 3.35. 3-(o-tolyl)pyrazolo[1,2-a]indazole-1,9-dione

5fa: ^{1}H NMR (400 MHz, $CDCl_3$) δ: 8.42 (dd, J= 2.0, 1.6 Hz, 1H), 7.82-7.77 (m, 1H), 7.68 (d, J=7.2 Hz, 1H), 7.48-7.45 (m, 2H), 7.34-7.28 (m, 3H), 6.31 (s,1H), 2.55 (s, 3H) ^{13}C NMR (100 MHz, $CDCl_3$) δ: 157.0, 153.8, 153.6, 151.4, 136.7, 135.9, 131.6, 130.9, 129.8, 129.2, 128.7, 125.9, 125.0, 116.9, 114.2, 89.7, 21.1.

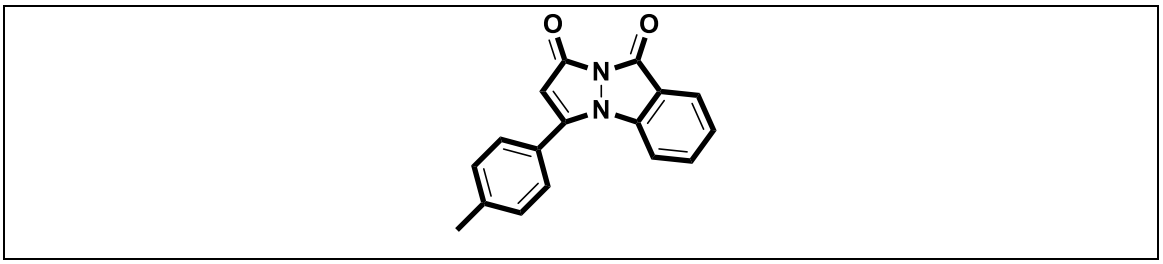

Figure 3.36. 3-(p-tolyl)pyrazolo[1,2-a]indazole-1,9-dione

5ga: ^{1}H NMR (400 MHz, $CDCl_3$) δ: 8.40 (dd, J= 1.6 Hz, 1.2 Hz, 1H), 7.90 (d, J= 8.0 Hz, 2H), 7.80-7.76 (m, 1H), 7.47-7.44 (m, 2H), 7.27 (d, J= 6.4 Hz, 2H), 6.41 (s, 1H), 2.40 (s, 3H) ^{13}C NMR (100 MHz, $CDCl_3$) δ: 156.2, 153.8, 153.6, 152.0, 140.0, 135.8, 129.4, 128.7, 128.6, 126.6, 125.0, 116.9, 114.1, 86.5, 21.4.

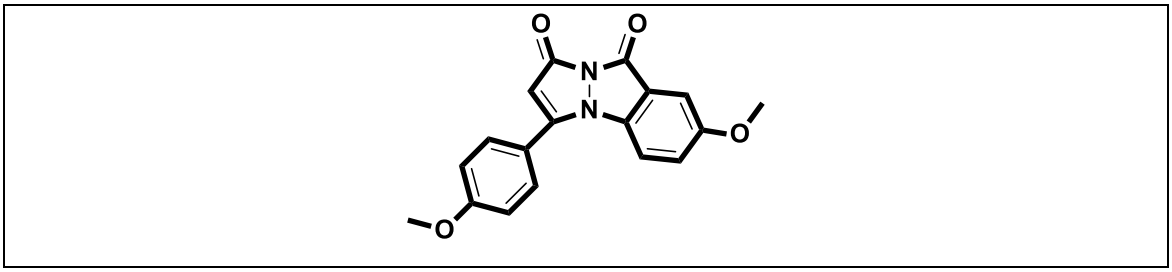

Figure 3.37. 7-methoxy-3-(4-methoxyphenyl)pyrazolo[1,2-a]indazole-1,9-dione

5cd: ^{1}H NMR (400 MHz, $CDCl_3$) δ: 7.94 (d, J= 8.8 Hz, 2H), 7.74 (d, J= 2.8 Hz, 1H), 7.36 (s, 1H), 7.34 (d, J= 2.8 Hz, 1H), 6.97 (d, J= 8.8 Hz, 2H), 6.34 (s, 1H), 3.92 (s, 3H), 3.86 (s, 3H) ^{13}C NMR (100 MHz, $CDCl_3$) δ: 160.9, 156.6, 155.9, 153.7, 152.1, 148.3, 128.2, 125.2, 124.1, 118.2, 114.4, 114.1, 108.3, 85.8, 56.2, 55.4.

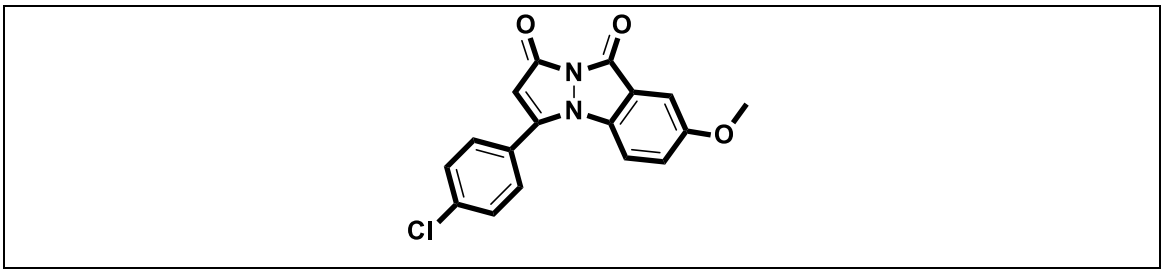

Figure 3.38. 3-(4-chlorophenyl)-7-methoxypyrazolo[1,2-a]indazole-1,9-dione

5dd: ^{1}H NMR (400 MHz, $CDCl_3$) δ: 7.94 (d, J= 8.4 Hz, 2H), 7.76 (d, J= 2.4 Hz, 1H), 7.44 (d, J= 8.4 Hz, 2H), 7.39-7.37 (m, 2H), 6.39 (s, 1H), 3.94 (s, 3H) ^{13}C NMR (100 MHz, $CDCl_3$) δ: 156.7, 155.0, 153.7, 152.2, 148.3, 135.8, 130.1, 129.0, 128.0, 125.5, 118.3, 114.3, 108.3, 86.2, 56.2.

CHAPTER 4

RESULTS & DISCUSSION

Bimane compounds hold unique photophysical and chemical properties. However, there are very few and challenging methodologies to synthesise and derivatise these important molecules. Because of this reason, development of a new and straightforward method to obtain various analogues of bimane compounds are in high demand. The major concern of thesis study is to construct new and applicable method for the synthesis of "syn" bimane derivatives.

4.1.Synthesis of Benzo-Bimane Derivatives via Copper Catalyst: Optimization and Other Studies

In the course of this study, a new method to synthesise benzo-bimanes derivatives was developed. The strategy was constructed on the synthesis of compound 4 which further undergoes to copper catalysed intramolecular cyclisation reaction. The proposed synthetic method along the way of succesful synthesis was demonstrated in figure below (Figure 4.1).

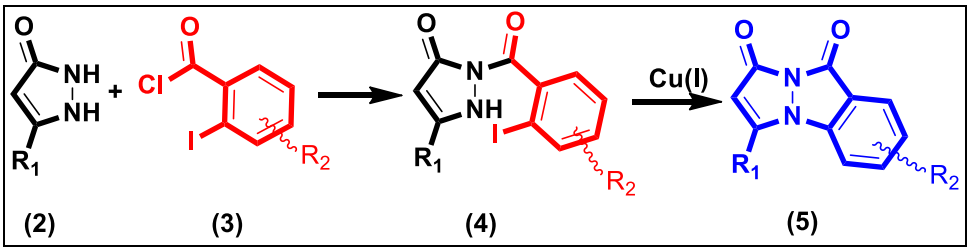

Figure 4.1. Cyclization reaction with copper-catalyst

C(aryl)-N, C(aryl)-C and C(aryl)-O cyclisation reactions via copper catalyst as indicated above (Figure 4.1) have been well-known as Ullmann condensation reactions in the literature.

4.1.1. Optimization Studies

Compound 4 bearing only phenyl ring as a substituent was chosen as probe substrate to survey optimum reaction conditions. Also, iodine substituent was used as halogen group. The reactant to be utilised in optimisation studies was shown in figure below.

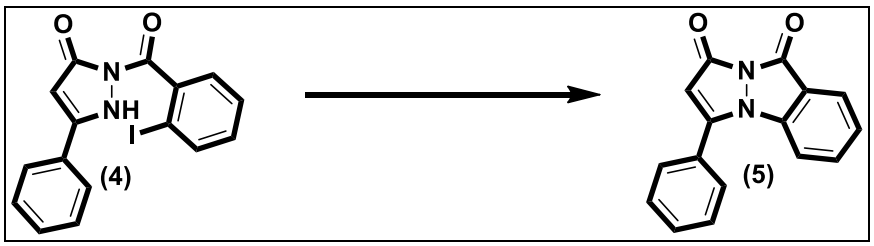

Figure 4.2. The reactant (4) to be utilized in optimization studies and final product (5)

The optimisation studies was first started with the investigation of the effect of organic/inorganic bases to the reaction yield. For this purpose, conversion of reactions was examined by switching one or more reagents used in the reaction. Copper(I) iodide (catalyst), L-proline (ligand) and K_2CO_3 (base) were vital prerequisites for reaction to proceed as seen in Table 4.1. Otherwise, the conversion occured scarcely.

Table 4.1. Conversion of reactant to Benzo-Bimane with different reagents.

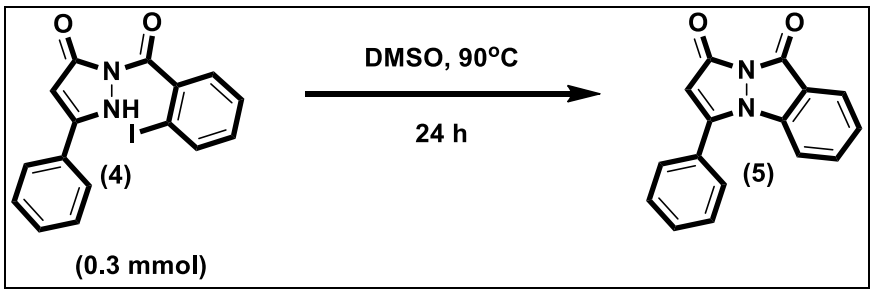

Entry	CuI (%)	L-Proline (%)	K_2CO_3	Yield (%)
1	0.5	20	2 eq.	41
2[a]	-	20	2 eq.	<3
3	-	-	2 eq.	0
4	-	-	-	0

[a] Determined by ^{1}H NMR.

In the next step, the experiments were carried out in diverse amount of copper(I) iodide to observe the catalytic activity of copper on C-N coupling reaction by holding constant the other variables of reaction such as amounts of L-proline (ligand) and potassium carbonate (base) (Table 4.2).

Table 4.2. Effect of catalyst to the reaction

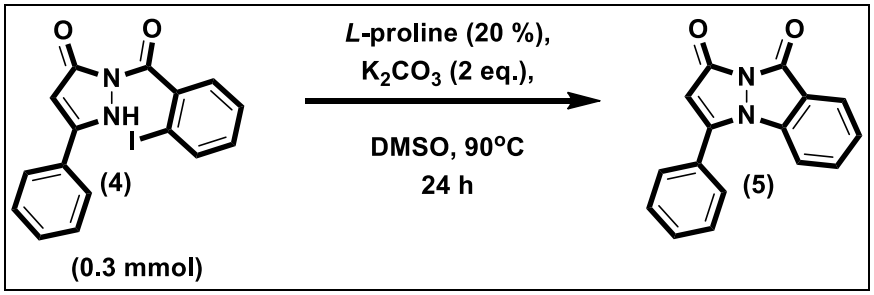

Entry	CuI (%)	Yield (%)
5	0.25	40
6	0.5	41
7	1.0	55
8	2.0	16
9	4.0	8
10	5.0	5

All experiments were isolated.

When the above table was analyzed, optimum amount of copper catalyst was established as 1 mol% to achive highest reaction yield. It should be noted that, the transformation was also possible by using small amounts of copper catalys (Table 4.2, Entries 5, 6). However, higher amounts of copper decreased the yield of the reaction that most probably caused by the deactivation of catalyst with ligands (Table 4.2, Entries 8-10).

As it is well known that the type of solvent have high impact on these type of coupling reactions. To understand the effect of solvation to the reaction yield, various organic solvents and water / solvent combinations were surveyed.

Table 4.3. Effect of solvent to the reaction

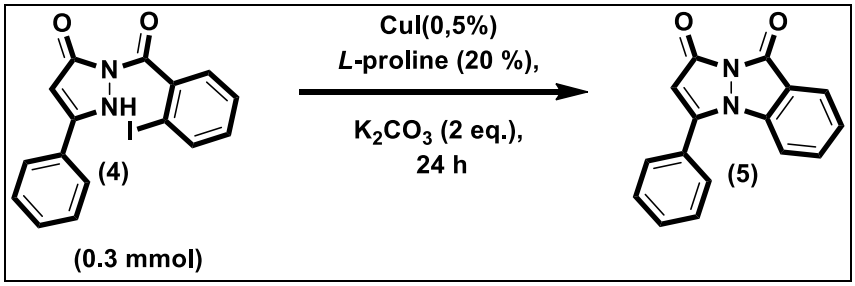

Entry	Solvent	Temperature(°C)	Yield (%)
11	Toluene	90	-
12	Dimethylformamide	90	25
13	Acetonitrile	85	25
14	Tetrahydrofuran	70	11
15	Dioxane	90	15
16	DMSO/Water (1:1, v/v)	90	-

All experiments were purified.

As shown in above table, there is no positive effect of used solvents to outcome of the reaction. Based upon this experiment, DMSO was chosen as suitable solvent for intramolecular C-N coupling reaction.

Up to this point, the reaction temperature was held constant at 90°C in all experiments (not including solvent effect experiments). The effect of temperature to the conversion was also investigated to get optimal reaction conditions. Increase in the reaction temperature reduced solely conversion time, but it had no positive contribution to isolated yield. As a result of all experiments carried out, 90°C was optimum temperature for that reaction.

Table 4.4. Effect of temperature to the reaction

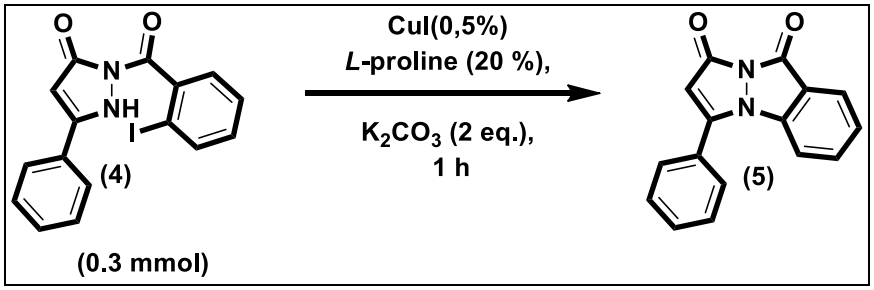

Entry	Temperature (°C)	Yield (%)
17	70	40
18	90	55
19[a]	110	25

[a] Reaction time 30 min. All experiments purified.

In general, these types of metal catalysed reactions were initiated with the metal catalyst via activation with a base and ligand species (Figure 4.3) (Li et al., 2014).

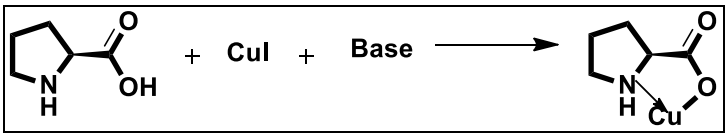

Figure 4.3. Activation of copper-catalyst by ligand and base

(Source: Li et al., 2014)

Based on this knowledge, distinctive types of ligands were exploited to obtain higher isolated yields. L-proline (ligand), one of the commercially procurable and economic aminoacids, was given priority. Feasibility of the reaction was proven in the presence of that ligand via various amounts of catalyst. Also, the reaction yield was endeavoured to increase by implementing distinctive ligands which include heteroatoms and activate copper-catalyst. It could be concluded from Table 4.5 that the highest isolated yield was obtained with triphenylphosphine (40 mol %). As known, triphenylphosphine is higly stable in air and also have some important features to be used in catalytic reactions. Compared to metal ammine complexes, metal phosphine complexes have an aptitude to be lipophilic and indicate good solubility in organic solvents. In addition to this, it is amenable with metals in variable oxidation states.

These two properties make metal phosphine complexes useful reagents for catalytic reactions.

Table 4.5. Effect of ligand to the reaction

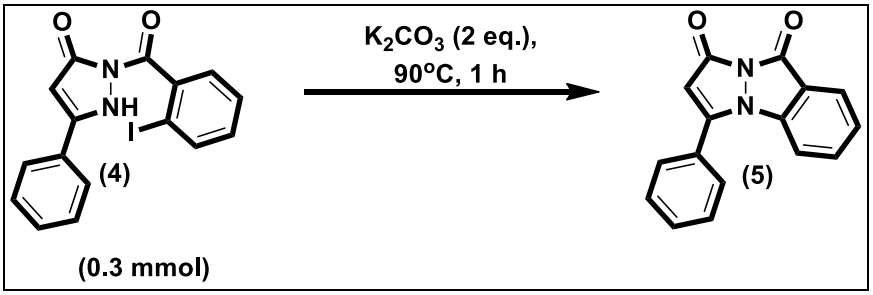

Entry	Ligand	CuI (%)	Yield (%)
20	L-proline (10 %)	1	20
21	L-proline (20 %)	1	55
22	L-proline (40 %)	1	50
23	1,10 phenanthroline (20 %)	1	65
24	1,10 phenanthroline (40 %)	1	70
25	1,10 phenanthroline (20 %)	2	32
26	N-tosylpyrolidyn-2-carboxamide (20 %)	1	51
27	Pyridine (20 %)	1	55
28	2,2'-bipyridyl (20 %)	1	63
29	Triphenylphosphine (20 %)	1	67
30	Triphenylphosphine (40 %)	1	85

All experiments isolated.

One of the most signifant factor required for reaction was sort of the base. With this object in mind, the effect of a variety of organic and inorganic bases to the reaction was researched. Although the maximum yield was achieved via addition of K_2CO_3, caesium carbonate have no constructive effect to the reaction yield. Among all organic bases employed in synthesis, 1,8-diazabicycloundec-7-ene suggested the best reaction yield. According to previous studies, differences in the amount of copper catalyst had

great influences over the reaction. Due to that reason, the effect of 1,8-diazabicycloundec-7-ene offering higher yields were examined along with a variety of copper amounts. Surprisingly, its effect to the reaction yield was fewer compared to conditon incorporating 1 mol% CuI and potassium carbonate.

Table 4.6. Effect of base to the reaction

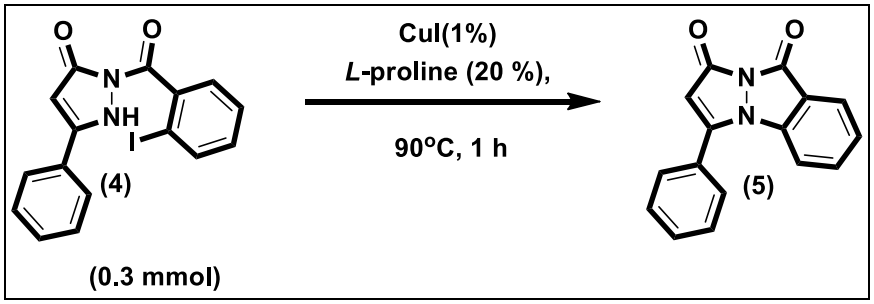

Entry	Base (2 eq.)	CuI (%)	Yield (%)
31	Cs_2CO_3	0,5	<5
32	Triethylamine	0,5	10
33	Diethylamine	0,5	<10
34	1,8-Diazabicycloundec-7-ene	0,25	55
35	1,8-Diazabicycloundec-7-ene	0,5	60
36	1,8-Diazabicycloundec-7-ene	1	40

All experiments purified.

As a consequence of optimisation studies, the optimum condition for this reaction was analysed in entry 30. Therefore, the optimum condition for that reaction was gathered under 0.3 mmol 2-iodobenzoyl-pyrazole (reactant) in dimethylsulfoxide, 1 mol% CuI, 40 mol% triphenylphosphine and 2 equivalent K_2CO_3 at 90^{o}C in 1 hour.

Subsequent to determination of optimum conditions, the availability of reaction with reactants bearing other halogens was initially tested. The results shown in Table 4.7 proved practicality of reaction with reactants bearing other halogen group.

Table 4.7. Effect of other halogens to the reaction

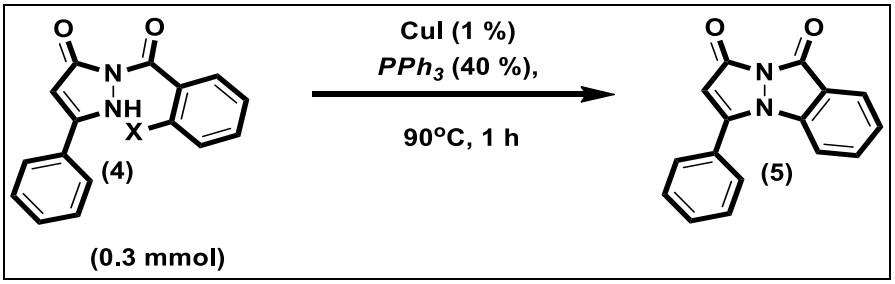

Entry	(2-halobenzoyl)-pyrazol	Yield (%)
37	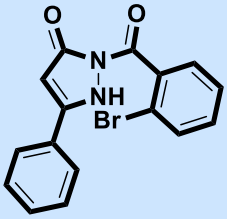	73
38	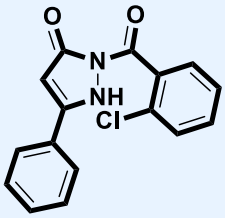	80

All experiments isolated.

4.1.2. Synthesis of Benzo-Bimane Derivatives

To understand the feasibility of reaction conditions, various substitution patterns were synthesised and subjected to copper catalyzed C-N intramolecular coupling reaction under optimum conditions. The results summarized in Table 4.8 revealed the applicability of methodology to achieve benzo-biman structure with various substitution patterns such as electron donating and withdrawing groups.

Table 4.8. Cyclization reactions of different analogs of (2-iodobenzoyl)-pyrazoles

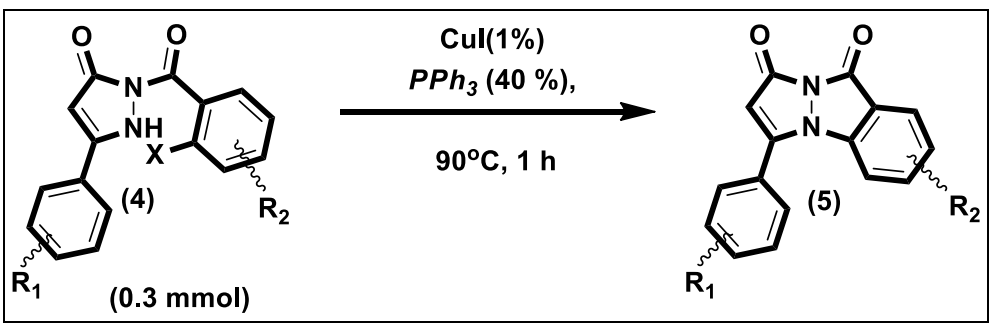

continued on next page

Table 4.8. continued

Entry	Reactant	Product	Yield (%)
30	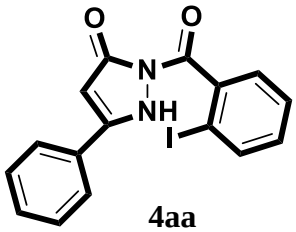 4aa	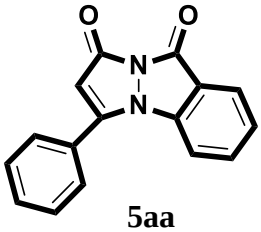 5aa	85
39	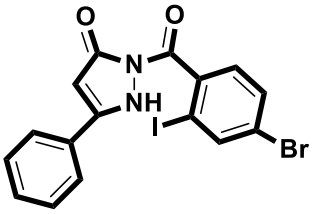 4ab	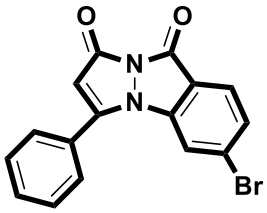 5ab	66
40	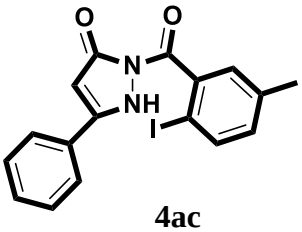 4ac	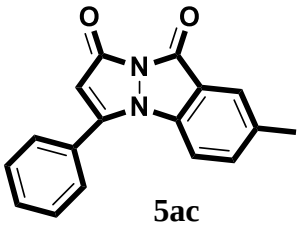 5ac	90
41	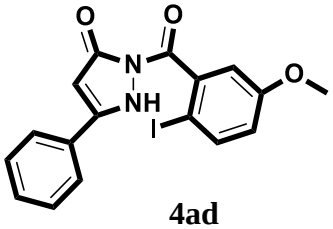 4ad	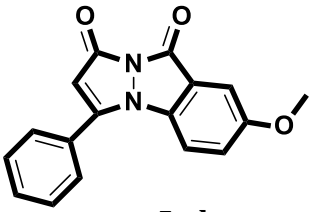 5ad	62
42	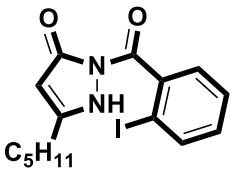 4ba	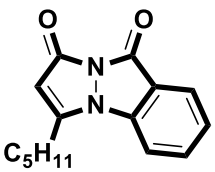 5ba	40
43	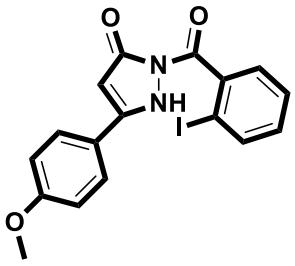 4ca	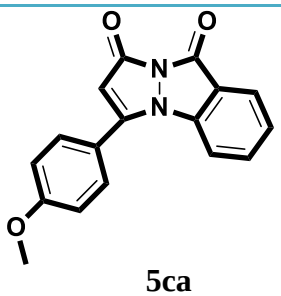 5ca	76

continued on next page

Table 4.8. continued

Entry	Reactant	Product	Yield (%)
44	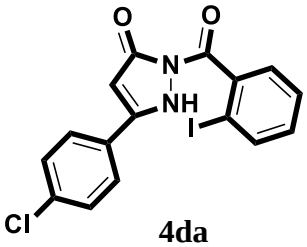 4da	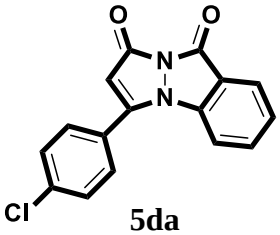 5da	61
45	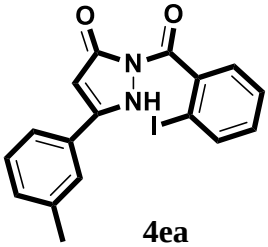 4ea	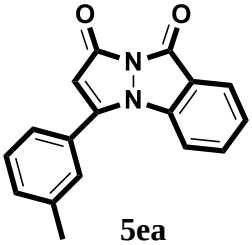 5ea	71
46	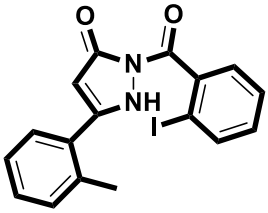 4fa	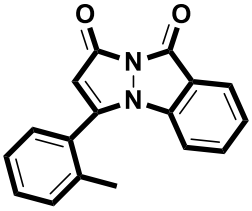 5fa	72
47	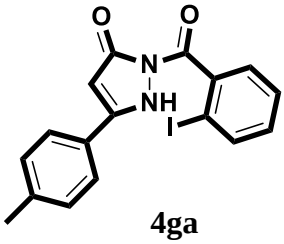 4ga	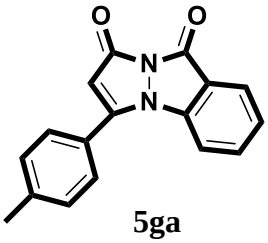 5ga	65
48	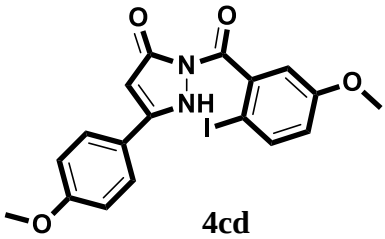 4cd	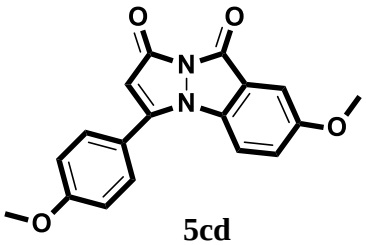 5cd	81
49	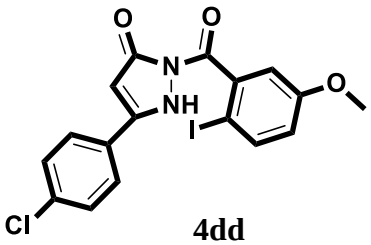 4dd	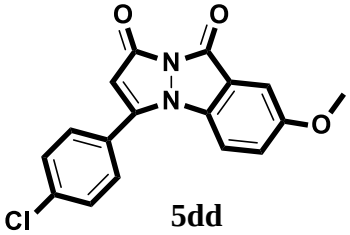 5dd	66

All experiments purified.

4.1.3. Photophysical Experiments

In addition to NMR and mass analyses, the photophysical properties of synthesised compounds were also surveyed carefully. Because of the fact that bimane compounds are highly fluorescent and used in many areas of sensor chemistry, it is important to determine photophysical properties of synthesised compounds. Fluorescence emission and UV absorption measurements were made for all benzo-bimane derivatives as shown below. Because of quantum yield measurements, dye concentration of each molecule in fluorescence graphs may vary (Appendix C).

In this study, quantum yields, extinction coefficients, λ_{ex} and λ_{em} of all synthesised benzo-bimane analogues have been cautiously established. The derivatives bearing electron donor group(s) and having conjugation system have unique, high fluorescence intensities and high quantum yields (Φ) due to the fact that there occurs electron donation in the ring conjugation system. Contrary to this, the derivatives bearing heavy atom (bromine) and aliphatic group have relatively low fluorescence intensities and low quantum yields (Φ) because of the fact that these molecules are lacking in conjugation system (phenyl ring conjugation) and their emissions are probably compressed by heavy atom effect. Determination of quantum yields, extinction coefficients, λ_{ex} and λ_{em} of all synthesized benzo-bimane derivatives have critical importance to be applied in areas such as fluorescent labelling, fluorescent bioimaging and sensing.

4.2. Photophysical Studies of Benzo-Bimane Derivatives

Photophysical measurements of benzo-bimane compounds were performed carefully. Stock solutions were prepared in acetonitrile for fluorescence and absorption measurements. UV absorption spectra were measured over the range from 250 nm to 600 nm. Upon excitation at 310 nm, fluorescence measurements of compounds were performed over the range from 320 nm to 600 nm. In measurements, dye concentrations were held constant as 20 μM and samples were handled in 10.0 mm path length quartz cuvettes (2.0 mL volume). Slit widths were adjusted to 5nm-5nm for both excitation and emission. All measurements were carried out at least in triplicate. Spectra of benzo-bimane analogs were indicated below.

4.2.1. Quantum Yield Calculation

Quantum yields of synthesised dyes were calculated with reference dye coumarin 102 by using equation number [1] (Table 4.9).

$$QY_{dye} = QY_{ref} \times (IA_{dye}/IA_{ref}) \times (OD_{ref}/OD_{dye}) \times (\eta_{dye}^2/\eta_{ref}^2) \ldots [1]$$

QY: Quantum yield

IA: Integrated area

OD: Optical density

η: refractive index

Table 4.9. Quantum yields of synthesized Benzo-Bimane analogs

Product	Quantum Yield	Product	Quantum Yield
5aa	14.9	**5da**	16.5
5ab	0.9	**5ea**	12.2
5ac	25.3	**5fa**	0.8
5ad	25.0	**5ga**	4.0
5ba	4.8	**5cd**	13.2
5ca	76.4	**5dd**	8.2

4.2.2. Extinction Coefficient Calculation

Moreover, extinction coefficients for each synthesised benzo-bimane derivatives were calculated by sketching absorption graphs. Accordingly, dye solutions were prepared in acetonitrile over concentration range from 2.5 µM to 20 µM and absorbance measurements were made. Absorbance-concentration graph was plotted by using the measurement results acquired formerly and extinction coefficients of synthesised dyes were calculated by using equation number [2] (Table 4.10).

$$\mathbf{A=Ɛ\ x\ b\ x\ c}\ldots[2]$$

A: Absorbance

Ɛ: Extinction coefficient ($cm^{-1}\ M^{-1}$)

b: Path length of light (cm)

c: Concentration (M)

Table 4.10. Extinction coefficient of synthesized Benzo-Bimane analogs

Product	Extinction Coefficient ($10^6\ M^{-1}\ cm^{-1}$)	Product	Extinction Coefficient ($10^6\ M^{-1}\ cm^{-1}$)
5aa	0.0186	**5da**	0.027
5ab	0.0164	**5ea**	0.019
5ac	0.022	**5fa**	0.066
5ad	0.016	**5ga**	0.057
5ba	0.0029	**5cd**	0.018
5ca	0.026	**5dd**	0.006

CHAPTER 5

CONCLUSION

In the literature, it is well-known that 1,5-diazabicyclo[3.3.0] octadiendione, shortly called as ‘’9,10-dioxabimane’’ or "bimane", compounds having substantial photochemical and photophysical features have been synthesized under harsh reaction conditions in extremely low yields. In this study, less harmful chemicals and simple reaction conditions are envisaged to synthesise bimane compounds. Optimisation studies and synthesis of various analogues of bimane compounds could be successfully carried out.

In the course of synthesis study by utilising Ullmann reaction, benzo-bimane compound and analogues of it are synthesised via the treatment of various 2-iodobenzoyl pyrazol compounds with copper catalyst, ligand and base in moderate to good yields. Additionally, it is experienced that the method offered for the synthesis of benzo-bimane is applicable to the benzo-bimane derivatives bearing electron withdrawing and electron donor groups.

Moreover, photophysical properties of all synthesised products have been cautiously investigated in this study. The derivatives bearing electron donor group(s) and having conjugation system have unique, high fluorescence intensities and high quantum yields (Φ). Contrary to this, the derivatives bearing heavy atom (bromine) and lacking in conjugation system have low fluorescence intensities and low quantum yields (Φ). All synthesised benzo-bimane analogues hold unique photophysical properties to be applied in areas such as fluorescent labelling, fluorescent bioimaging and sensing.

REFERENCES

Carpino, A. L., Terry, P. H. 1958. ‘’Thatt S. D., A New Synthesis of Unsaturated Acids. IV. Further Aspects of the Scope and Mechanism of the Conversion of Halopyrazolones to α,β-Acetylenic and Olefinic Acids’’, J. Am. Chem. Soc., 31, 2867-2873.

Pazhenchevsky, B., Kosower, M. A., Hershkowitz, E. 1978. ‘’1,5-Diazabicyclo[3.3.0]octadienediones (9,10-Dioxabimanes). Strongly Fluorescent Syn Isomers’’, J. Am. Chem. Soc., 6516-6518.

Kosower, M. A., Pazhenchevsky, B. 1980. ‘’Bimanes. 5. Synthesis and Properties of syn- and anti-1,5-Diazabicyclo[3.3.0]octadienediones (9,10-Dioxabimanes)’’, J. Am. Chem. Soc., 102, 4983-4993.

Zheng, Z., Yu, Z., Luo, N., Han, X. 2006. ‘’Tautomerism-Dependent Ring Construction of N-Heterocyclic Compounds from the Reactions of 1-Alkynyl Fischer Carbene Complexes and Substituted Pyrazolinones’’, J. Org. Chem., 71, 9695-9700.

Ranney, H. M., Newton, L. G., Kosower, N. S., Kosower, E. M. 1979. ‘’Bimane fluorescent labels: Labeling of normal human red cells under physiological conditions’’, Proc. Natl. Acad. Sci., 76, 3382-3386.

Shoshan, M. B., Kosower, M. A. 1996. ‘’Bimane Acetylenes and Diacetylenes. Bimanes. 33’’, J. Org. Chem., 61, 5871-5884.

Radkowsky, E. A., Kosower, E. M. 1986. ‘’Bimanes.17. (Haloalky1)- 1,5-Diazabicyclo[3.3.0]octadienediones (Halo-9,10-dioxabimanes): Reactivity toward the Tripeptide Thiol, Glutathione’’, J. Am. Chem. Soc., 108, 4527-4531.

Nicholas, G. M., Kovac, P., Bewley, C. A. 2002. ‘’Total Synthesis and Proof of Structure of Mycothiol Bimane’’, J. Am. Chem. Soc., 124, 3492-3493.

Mansoor, S. E., Farrens, D. L. 2004. “High-Throughput Protein Structural Analysis Using Site-Directed Fluorescence Labeling and the Bimane Derivative (2-Pyridyl)dithiobimane”, Biochemistry, 43, 9426-9438.

Islas, L. D., Zagotta, W. N. 2006. ‘’Short-range Molecular Rearrangements in Ion Channels Detected by Tryptophan Quenching of Bimane Fluorescence’’, J. Gen. Physiol., 128, 337–346.

Wintner, E. A., Deckwerth, T. L., Langston, W., Bengtsson, A., Leviten, D., Hill, P., Insko, M. A., Dumpit, R., VandenEkart, E., Toombs, C. F., Szabo, C. 2010. ‘’A monobromobimane-based assay to measure the pharmacokinetic profile of reactive sulphide species in blood’’, British Journal of Pharmacology, 160, 941–957.

Montoya, L. A., Shen, X., McDermott, J. J., Kevil, C. G., Pluth, M. D. 2014. “Mechanistic investigations reveal that dibromobimane extrudes sulfur from biological sulfhydryl sources other than hydrogen sulfide”, Chem. Sci., 6, 294-300.

Sigmaaldrichhttp://www.sigmaaldrich.com/catalog/search?term=bimane&interface=All&N=0&mode=match%20partialmax&lang=en&region=TR&focus=product Last Accessed: 31.05.2016.

Ley S. V., Thomas A. W. 2003. ‘’Modern Synthetic Methods for Copper-Mediated C(aryl)-O, C(aryl)-N, and C(aryl)-S Bond Formation’’, Angew. Chem. Int. Ed., 42, 5400 – 5449.

Ullmann F. 1904. ‘’Ueber eine neue Darstellungsweise von Phenyläthersalicylsäure’’, Eur. J. Inorg. Chem., 37, 853-854.

Ullmann F. 1901. ‘’Ueber Synthesen in der Biphenylreihe’’, Eur. J. Inorg. Chem., 34, 2174-2185.

Ullmann F. 1903. ‘’Ueber eine neue Bildungsweise von Diphenylaminderivaten’’, Eur. J. Inorg. Chem., 36, 2382-2384.

Klapars A., Antilla J. C., Huang X., Buchwald S. L., 2001. ‘’A General and Efficient Copper Catalyst for the Amidation of Aryl Halides and the N-Arylation of Nitrogen Heterocycles’’, J. Am. Chem. Soc., 123, 7727-7729.

Ma. D., Cai Q, Zhang H., 2003. ‘’Mild Method for Ullmann Coupling Reaction of Amines and Aryl Halides’’, Org. Lett., 5, 2453-2455.

Cristau H. J., Cellier P. P., Spindler J. F., Taillefer M., 2004. ‘’Highly Efficient and Mild Copper-Catalyzed N- and C-Arylations with Aryl Bromides and Iodides’’, Chem. Eur. J., 10, 5607 – 5622.

Beletskaya I. P., Cheprakov A. V., 2004. ‘’Copper in cross-coupling reactions The post-Ullmann chemistry’’, Coordination Chemistry Reviews, 248, 2337–2364.

Tanimori S., Kobayashi Y., Iesaki Y., Ozaki Y., Kirihata M., 2012. ‘’Copper-catalyzed synthesis of substituted indazoles from 2-chloroarenes at low catalyst-loading’’, Org. Biomol. Chem., 10, 1381-1387.

Xiong X., Jiang Y., Ma. D., 2012. ‘’Assembly of *N,N*-Disubstituted Hydrazines and 1-Aryl-1*H*-indazoles via Copper-Catalyzed Coupling Reactions’’, Org. Lett., 14, 2552-2555.

Li C., Zhang W. T., Wang X. S., 2014. ‘’CuI-Catalyzed C−N Bond Formation and Cleavage for the Synthesis of Benzimidazo[1,2-*a*]quinazoline Derivatives’’, J. Org. Chem., 79, 5847−5851.

Cheng, H., Zhao, B., Yao, Y., Lua, C. 2015. “Carboxylation of terminal alkynes with CO2 catalyzed by bis(amidate) rare-earth metal amides”, Green Chem., 17, 1675-1682.

Tanaka, K., Nishida, G., Wada, A., Noguchi, K. 2004. “Enantioselective Synthesis of Axially Chiral Phthalides through Cationic [RhI(H8-binap)]-Catalyzed Cross Alkyne Cyclotrimerization” Angew. Chem. Int. Ed. Engl., 43, 6510-6512.

O’Rourke, N. F., Wulff, J. E. 2014. ‘’Investigation of quantitative structure–reactivity relationship in the aliphatic Claisen rearrangement of bis-vinyl ethers reveals a dipolar, dissociative mechanism’’, Org. Biomol. Chem.,12, 1292-1308.

APPENDIX A

^{1}H-NMR AND ^{13}C-NMR SPECTRA OF COMPOUNDS

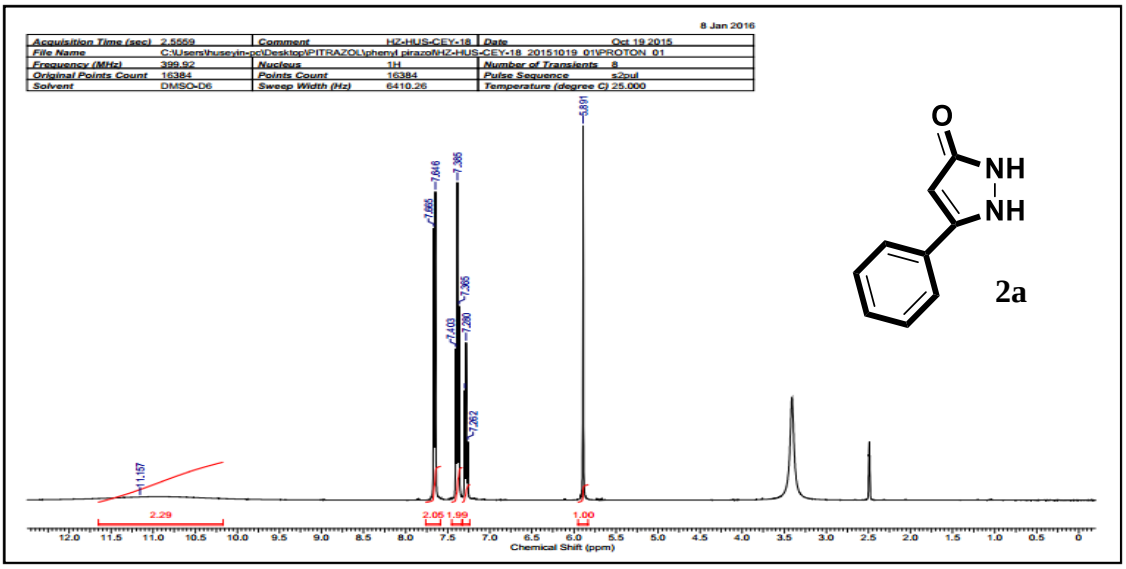

Figure A.1. ^{1}H-NMR of 5-phenyl-1*H*-pyrazol-3(2*H*)-one

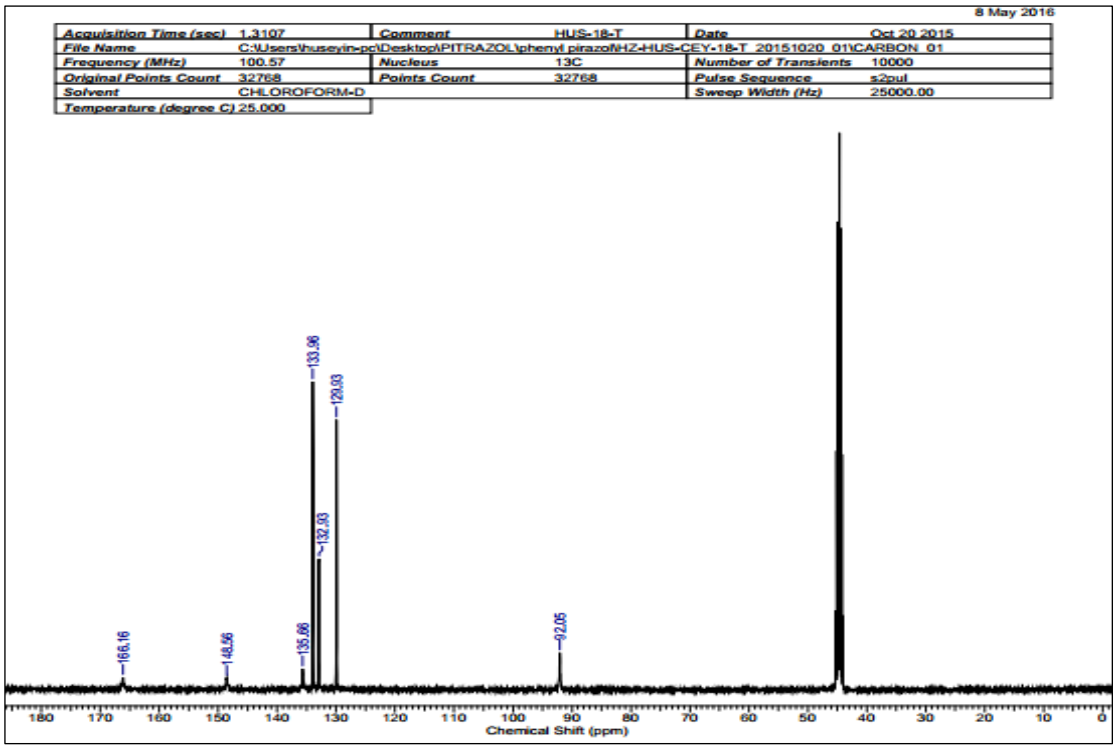

Figure A.2. ^{13}C-NMR of 5-phenyl-1*H*-pyrazol-3(2*H*)-one

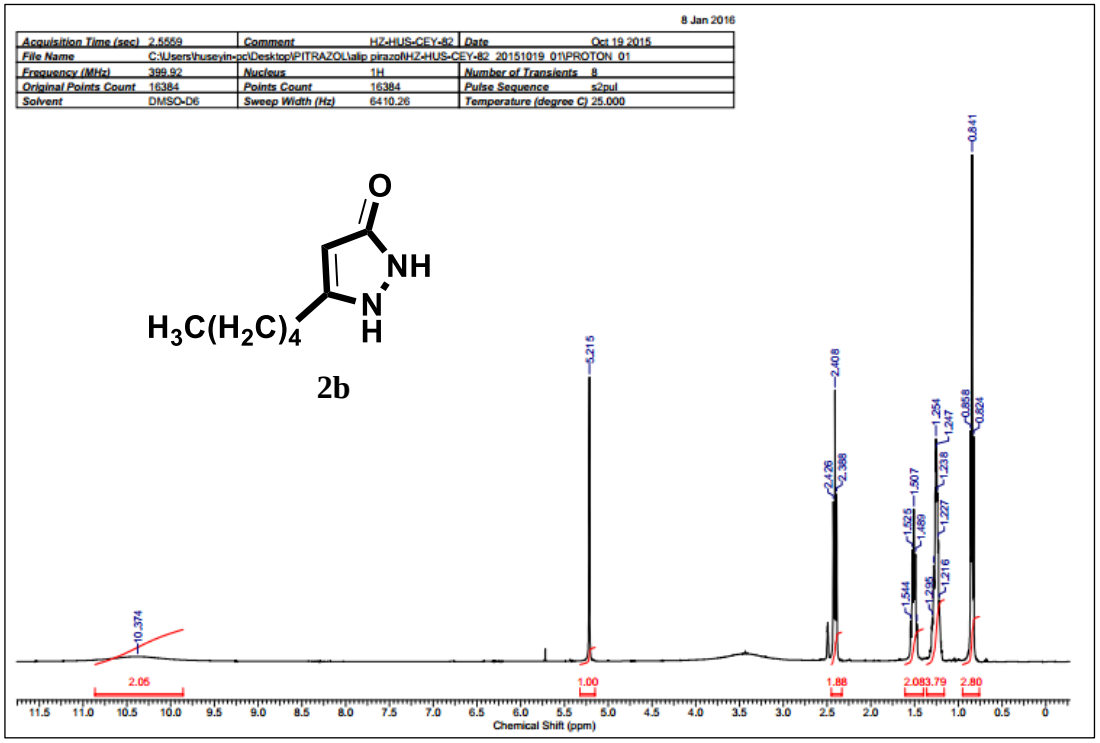

Figure A.3. ^{1}H-NMR of 5-pentyl-1*H*-pyrazol-3(2*H*)-one

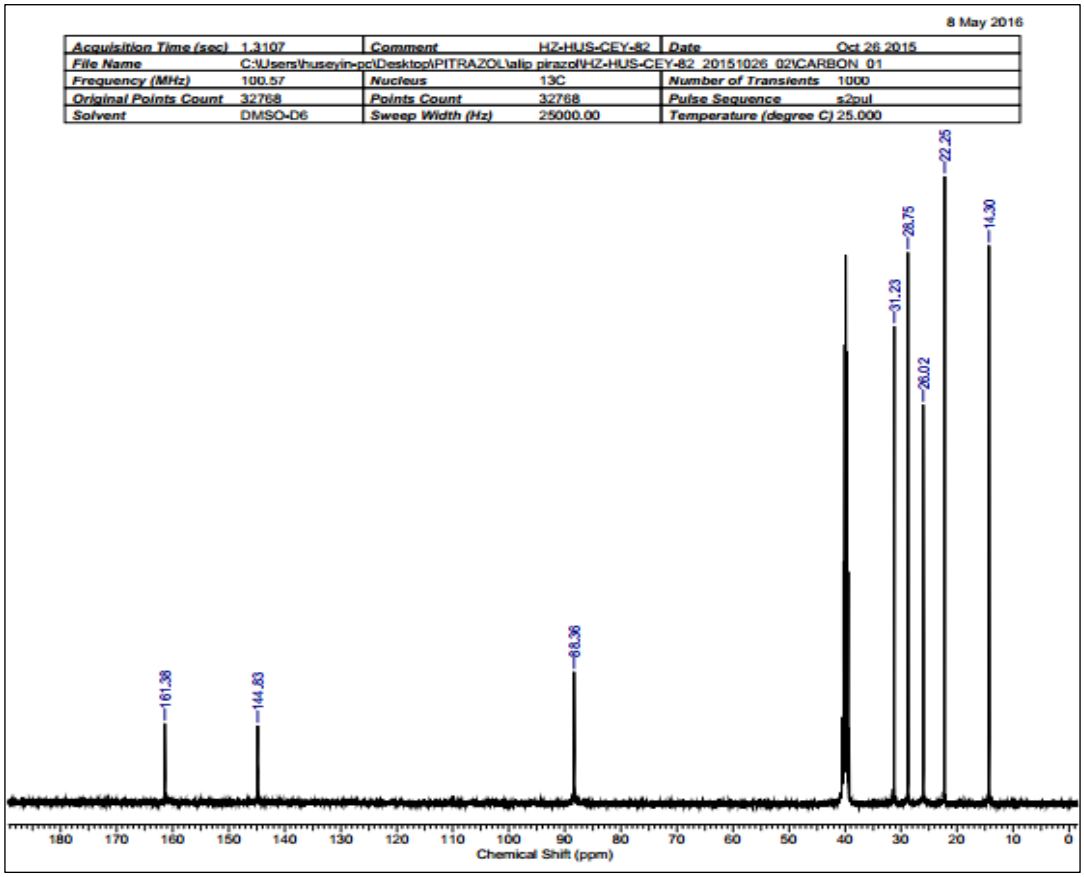

Figure A.4. ^{13}C-NMR of 5-pentyl-1*H*-pyrazol-3(2*H*)-one

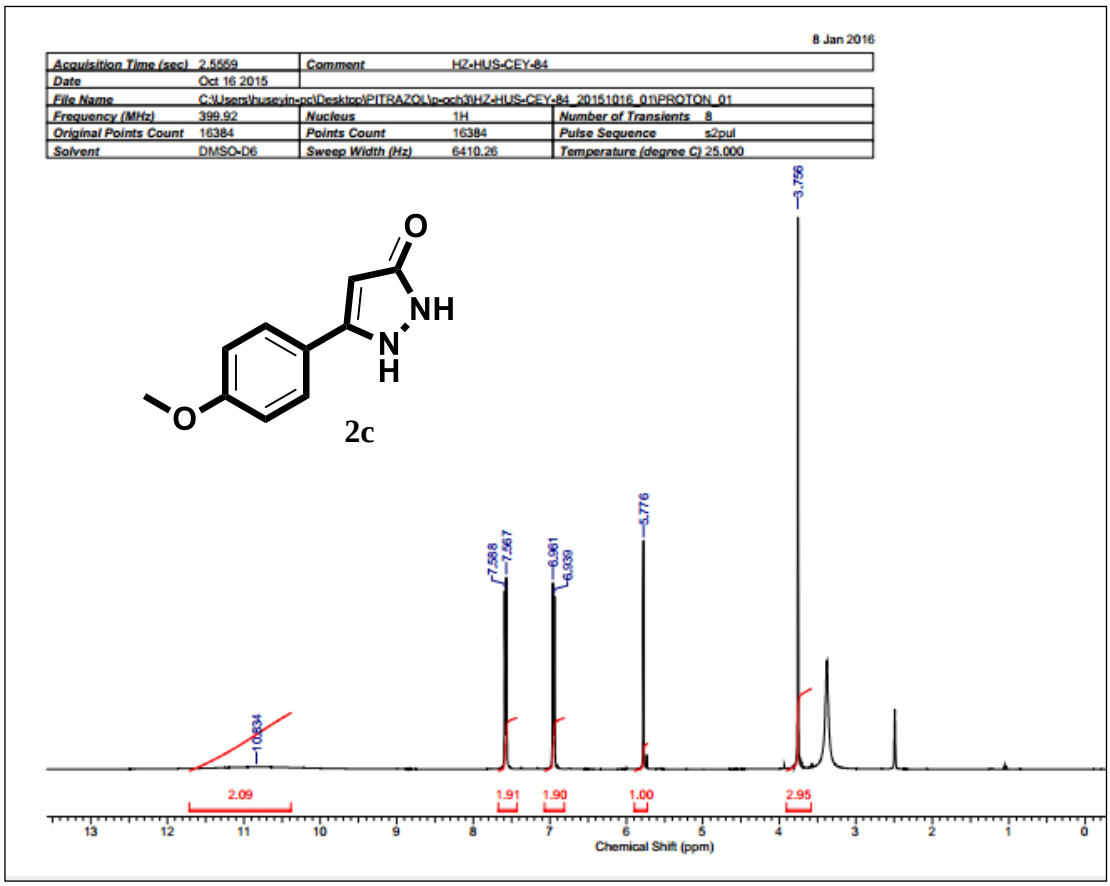

Figure A.5. [1]H-NMR of 5-(4-methoxyphenyl)-1*H*-pyrazol-3(2*H*)-one

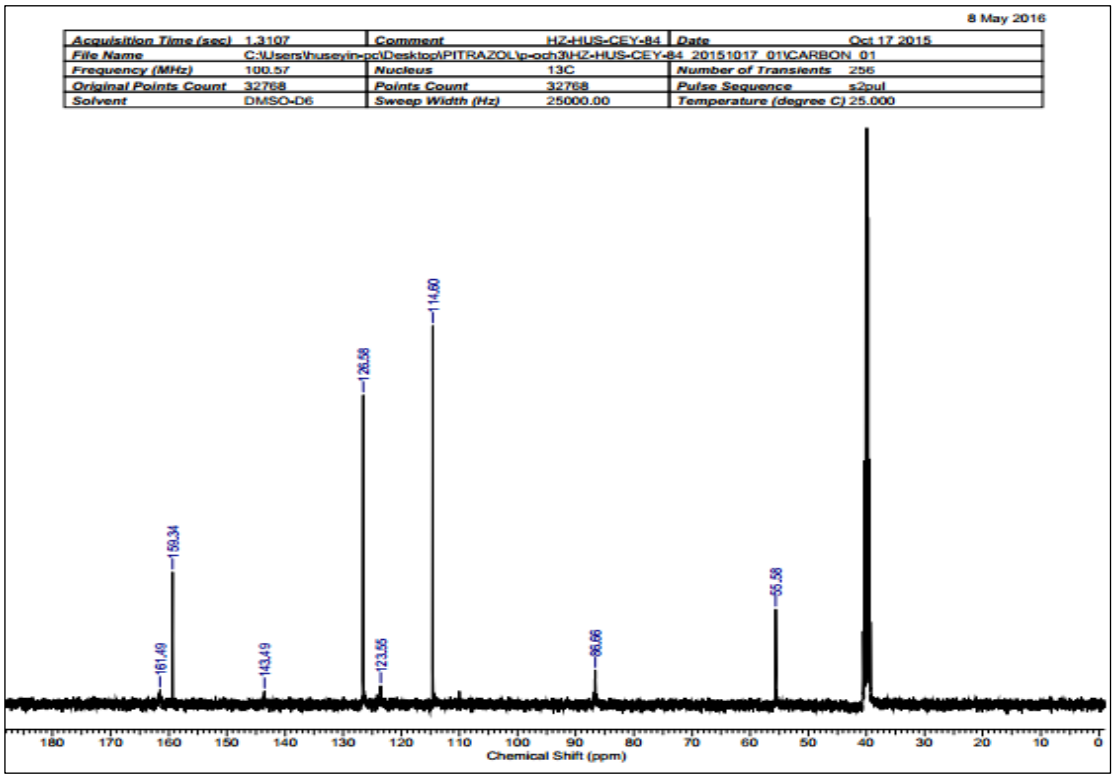

Figure A.6. [13]C-NMR of 5-(4-methoxyphenyl)-1*H*-pyrazol-3(2*H*)-one

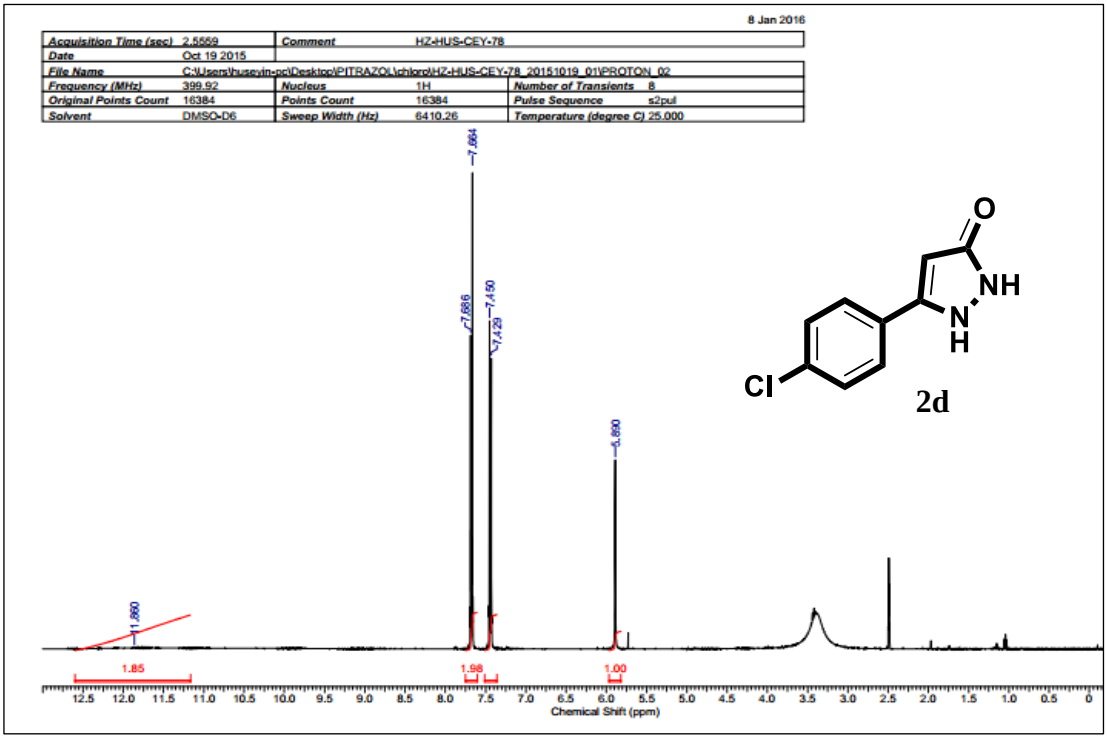

Figure A.7. [1]H-NMR of 5-(4-chlorophenyl)-1*H*-pyrazol-3(2*H*)-one

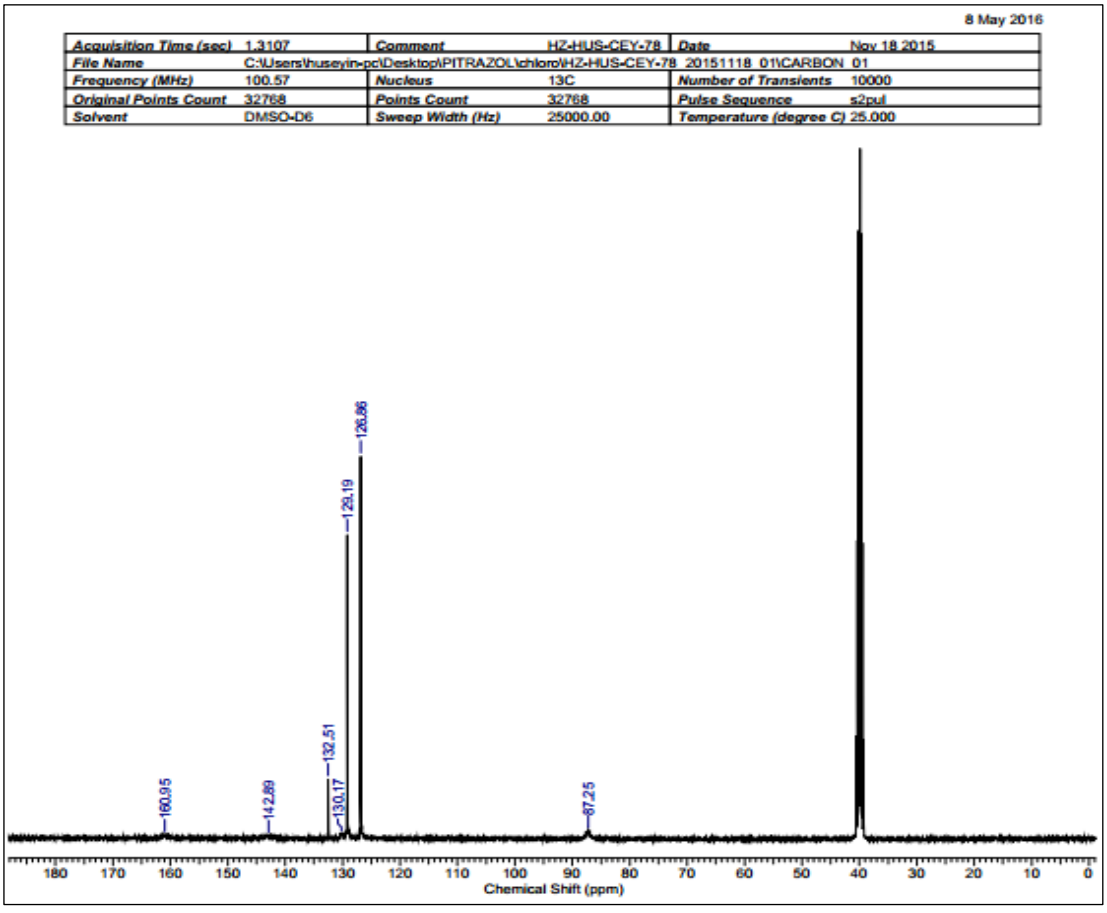

Figure A.8. [13]C-NMR of 5-(4-chlorophenyl)-1*H*-pyrazol-3(2*H*)-one

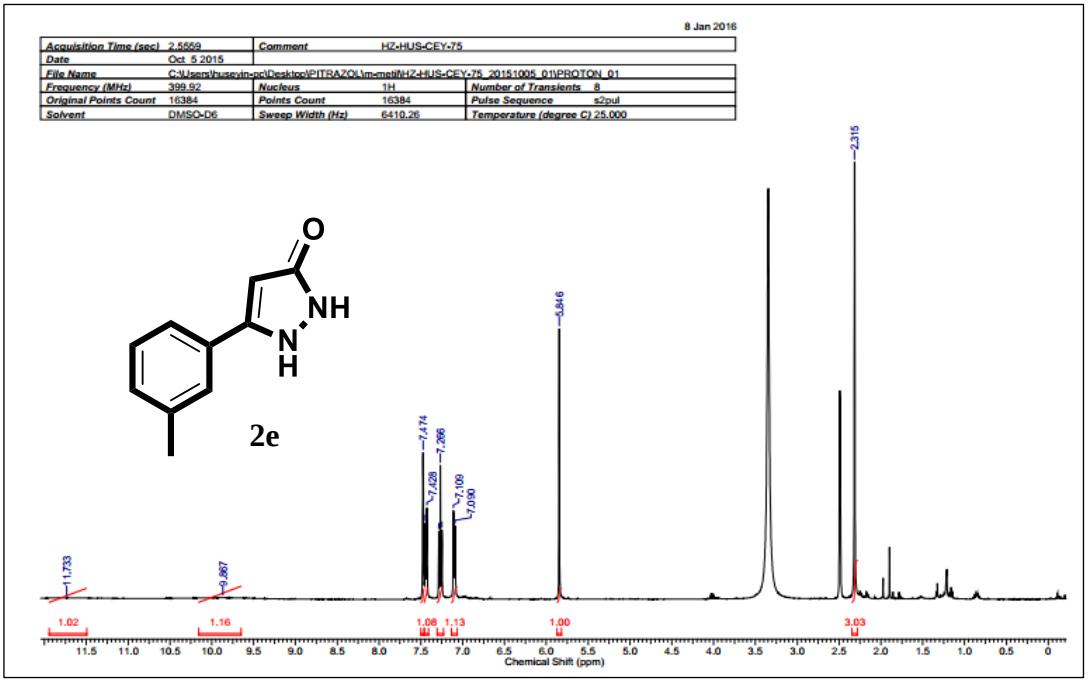

Figure A.9. ^{1}H-NMR of 5-(m-tolyl)-1*H*-pyrazol-3(2*H*)-one

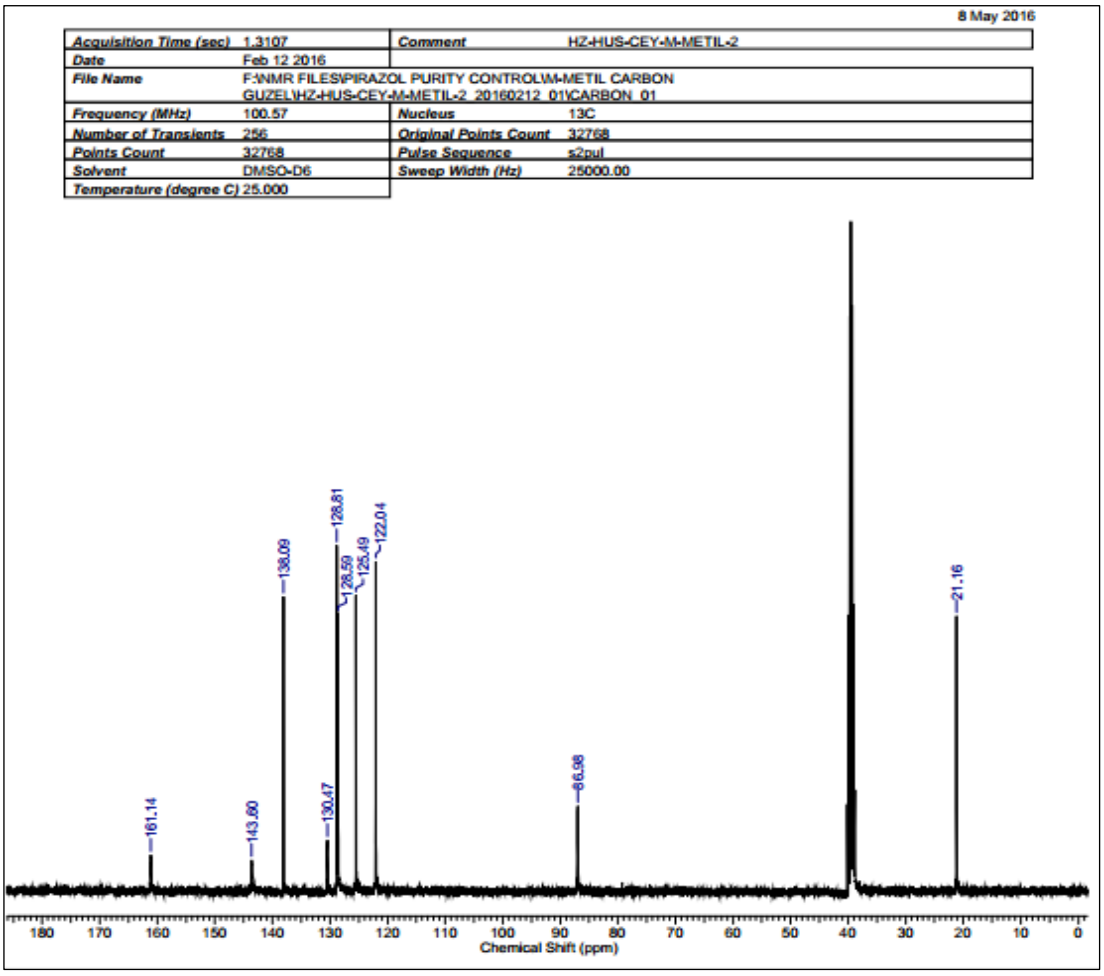

Figure A.10. ^{13}C-NMR of 5-(m-tolyl)-1*H*-pyrazol-3(2*H*)-one

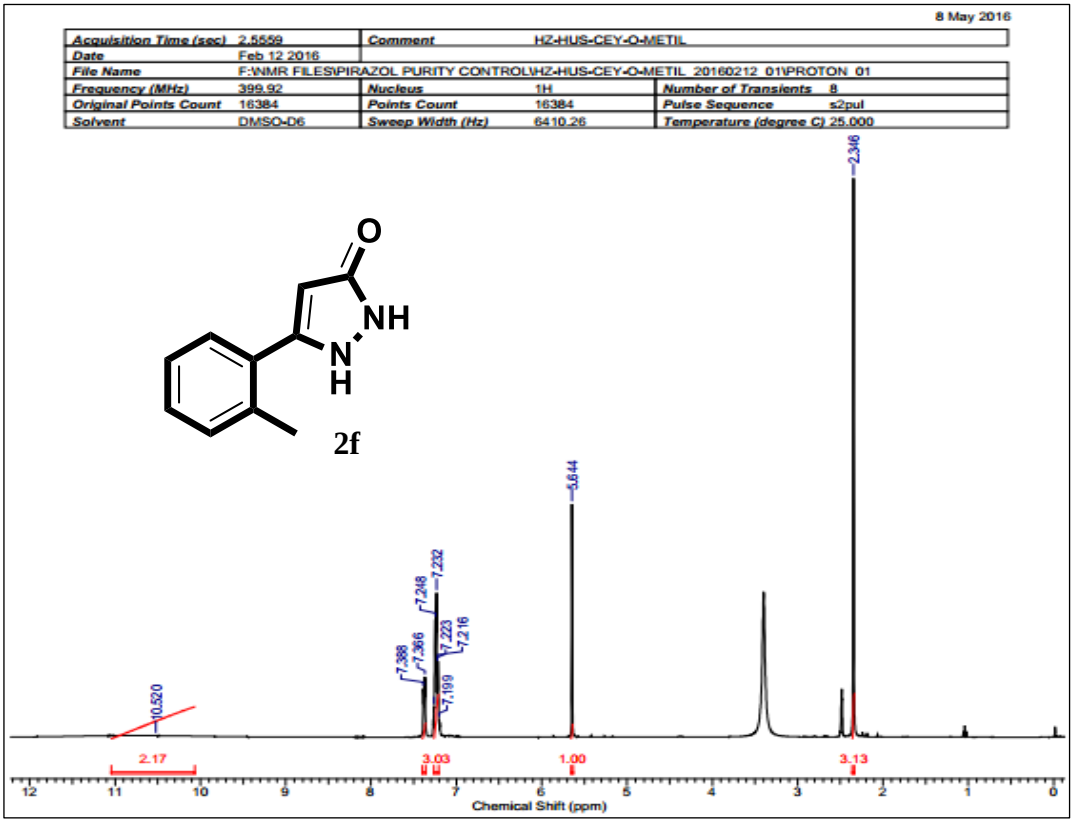

Figure A.11. ^{1}H-NMR of 5-(o-tolyl)-1*H*-pyrazol-3(2*H*)-one

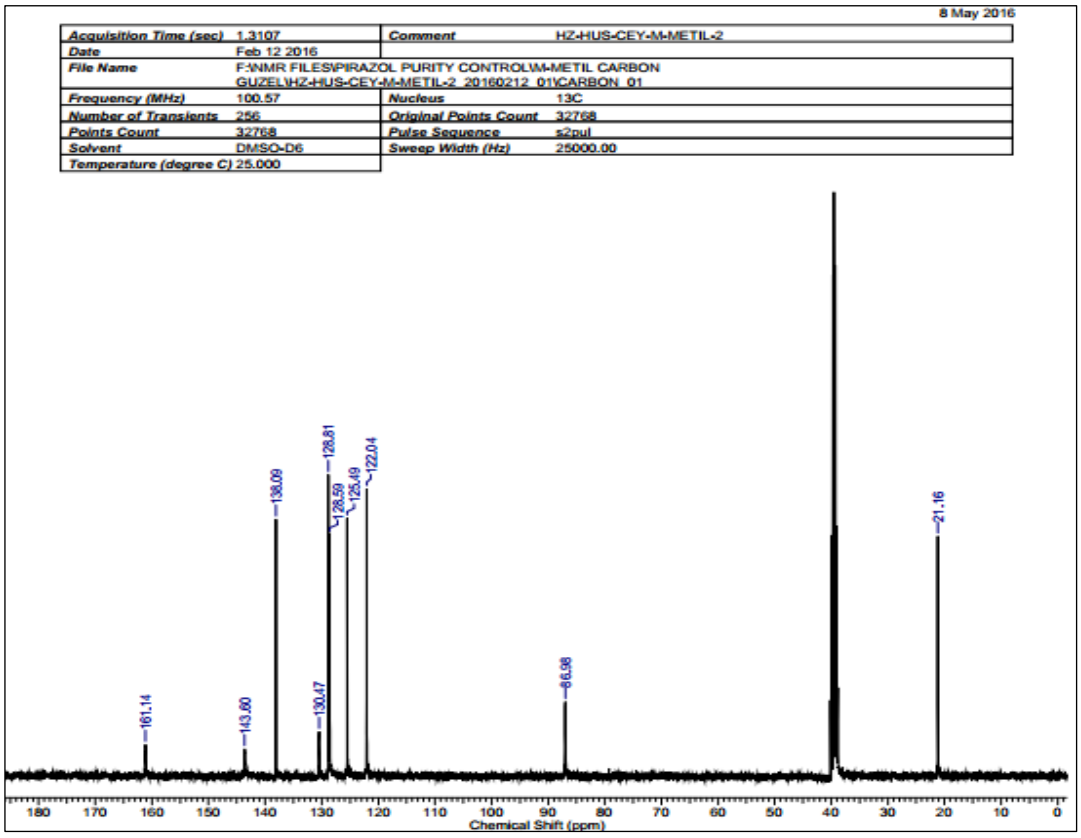

Figure A.12. ^{13}C-NMR of 5-(o-tolyl)-1*H*-pyrazol-3(2*H*)-one

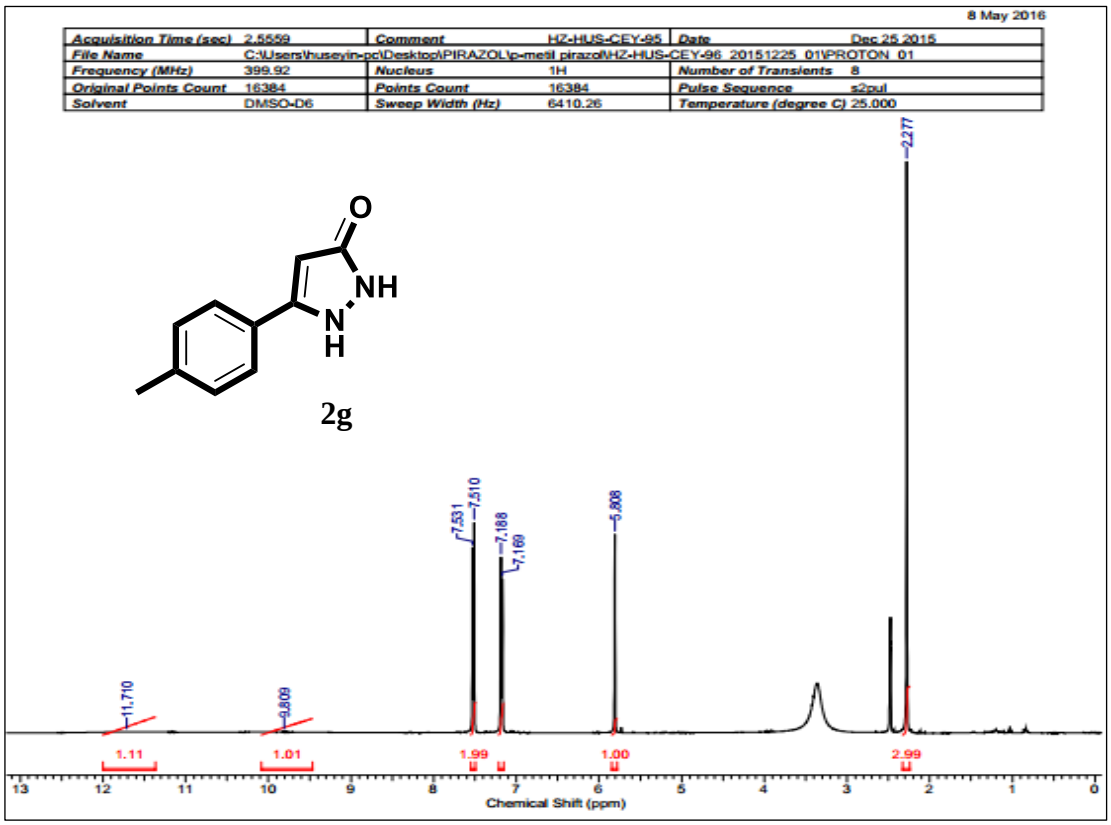

Figure A.13. ^{1}H-NMR of 5-(p-tolyl)-1*H*-pyrazol-3(2*H*)-one

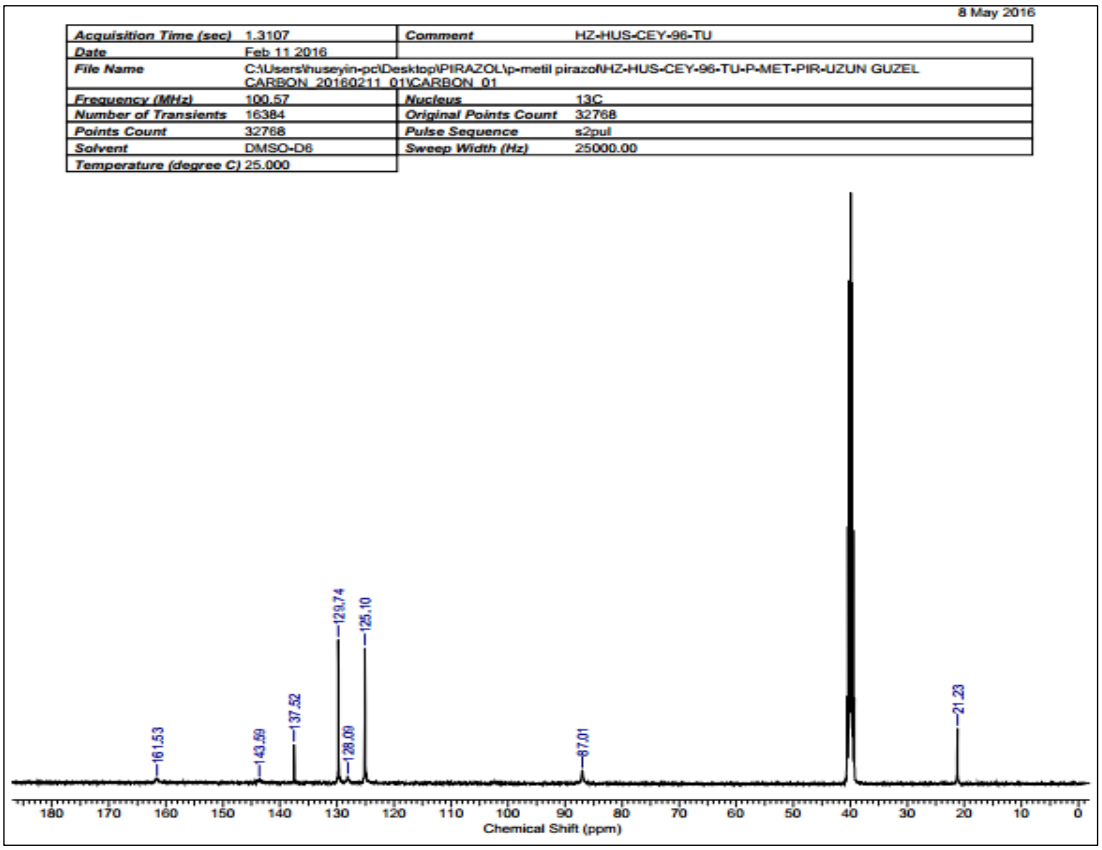

Figure A.14. ^{13}C-NMR of 5-(p-tolyl)-1*H*-pyrazol-3(2*H*)-one

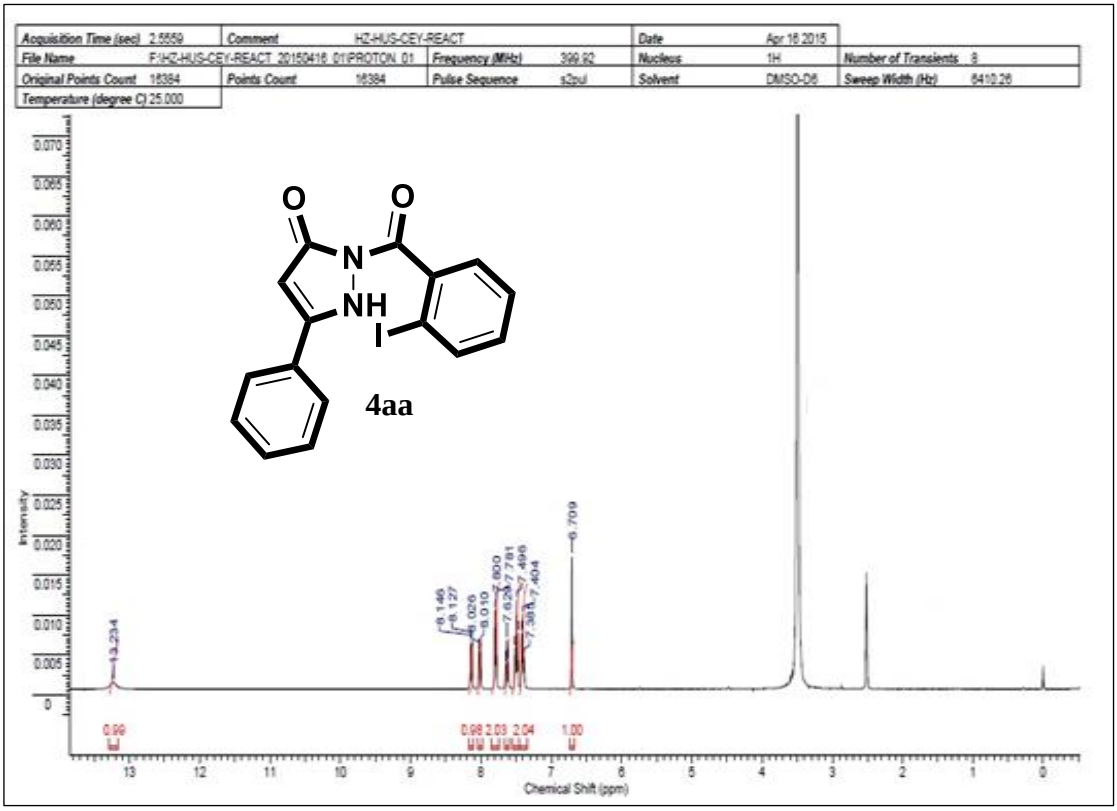

Figure A.15. [1]H-NMR of 2-(2-iodobenzoyl)-5-phenyl-1*H*-pyrazol-3(2*H*)-one

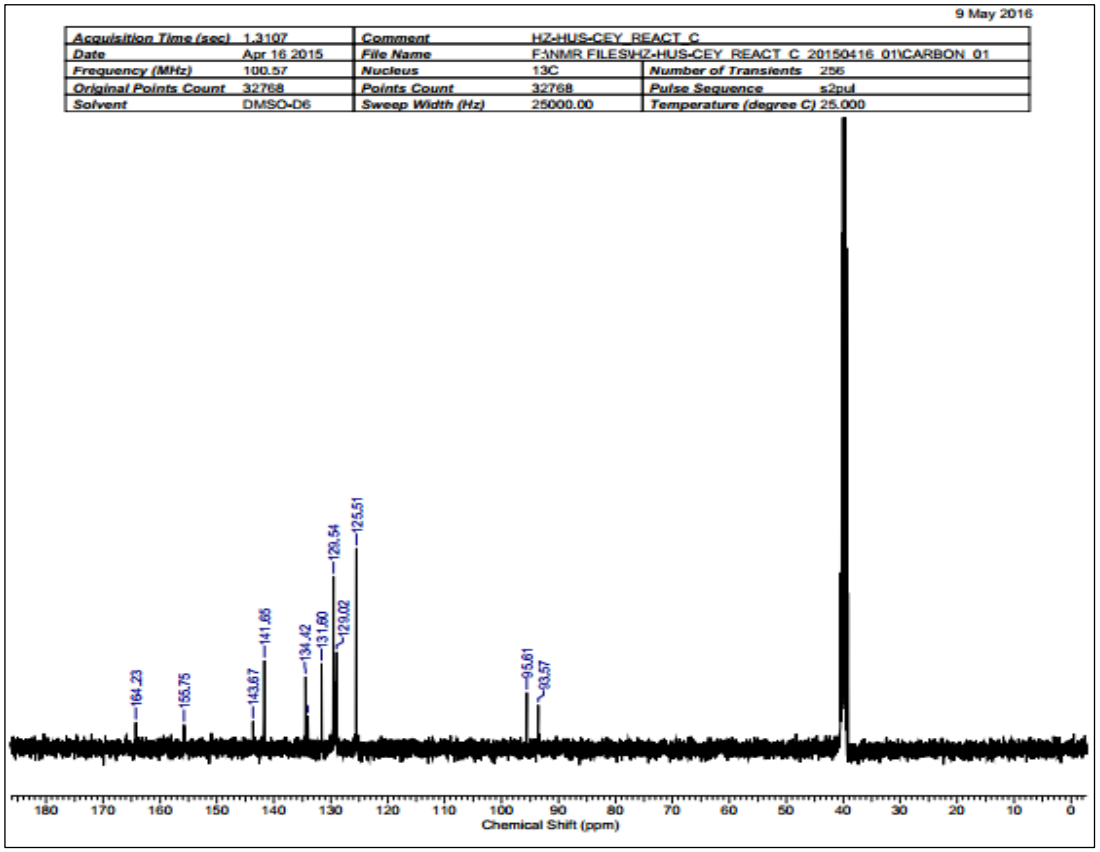

Figure A.16. [13]C-NMR of 2-(2-iodobenzoyl)-5-phenyl-1*H*-pyrazol-3(2*H*)-one

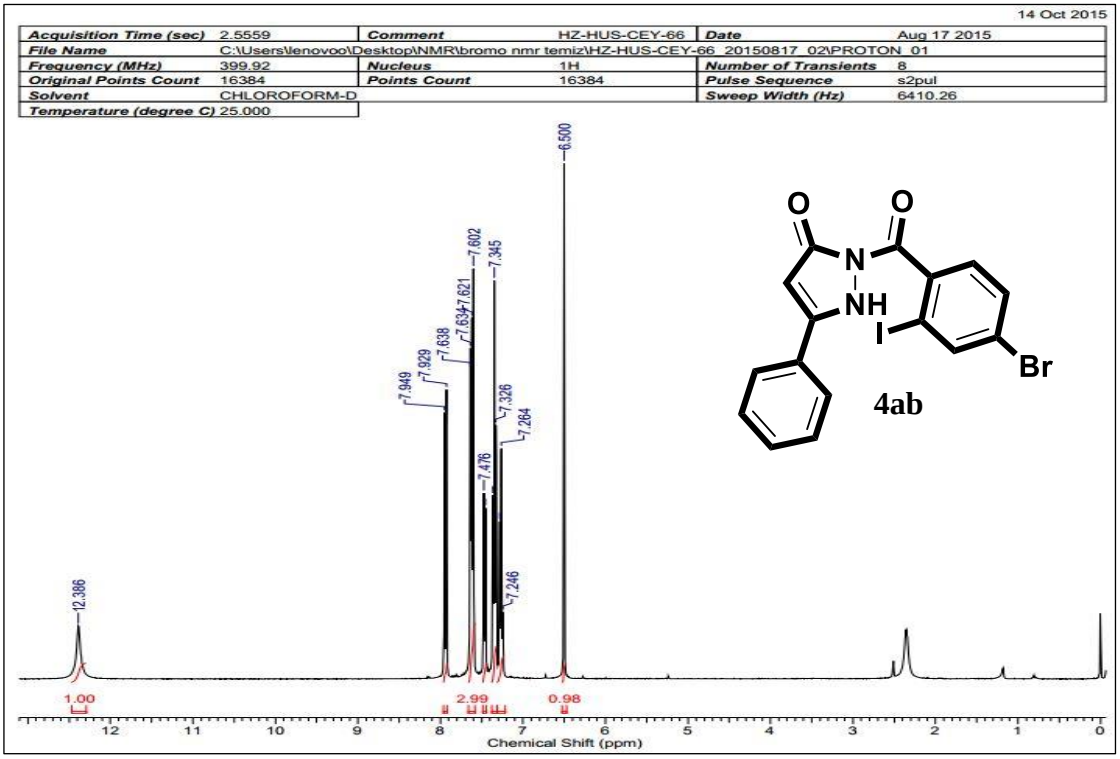

Figure A.17. [1]H-NMR of 2-(4-bromo-2-iodobenzoyl)-5-phenyl-1*H*-pyrazol-3(2*H*)-one

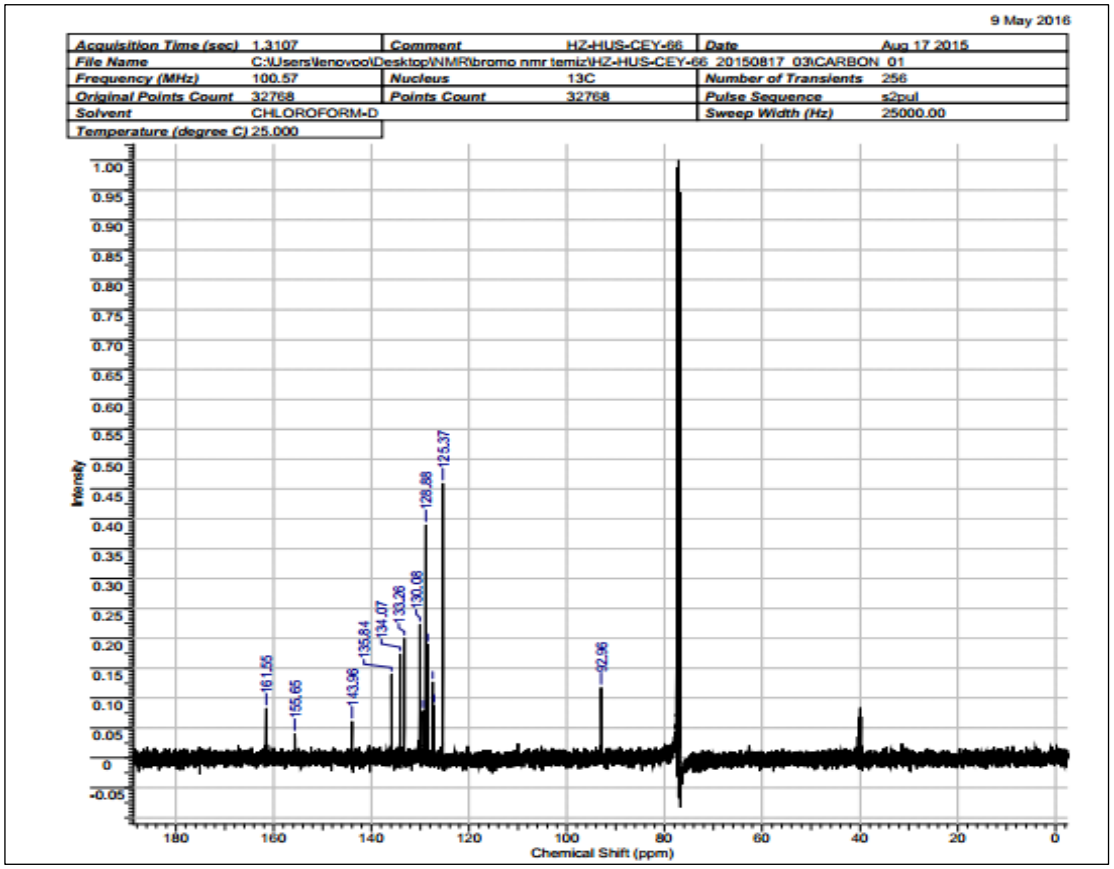

Figure A.18. [13]C-NMR of 2-(4-bromo-2-iodobenzoyl)-5-phenyl-1*H*-pyrazol-3(2*H*)-one

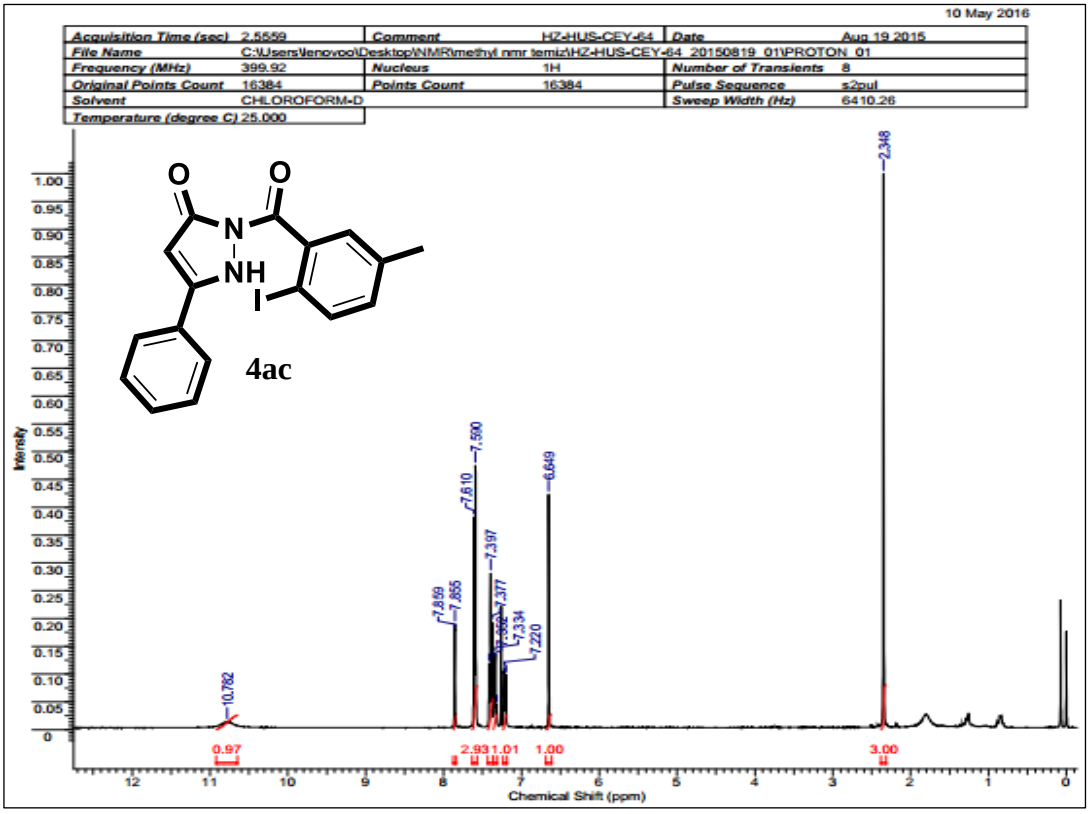

Figure A.19. ^{1}H-NMR of 2-(2-iodo-5-metylbenzoyl)-5-phenyl-1*H*-pyrazol-3(2*H*)-one

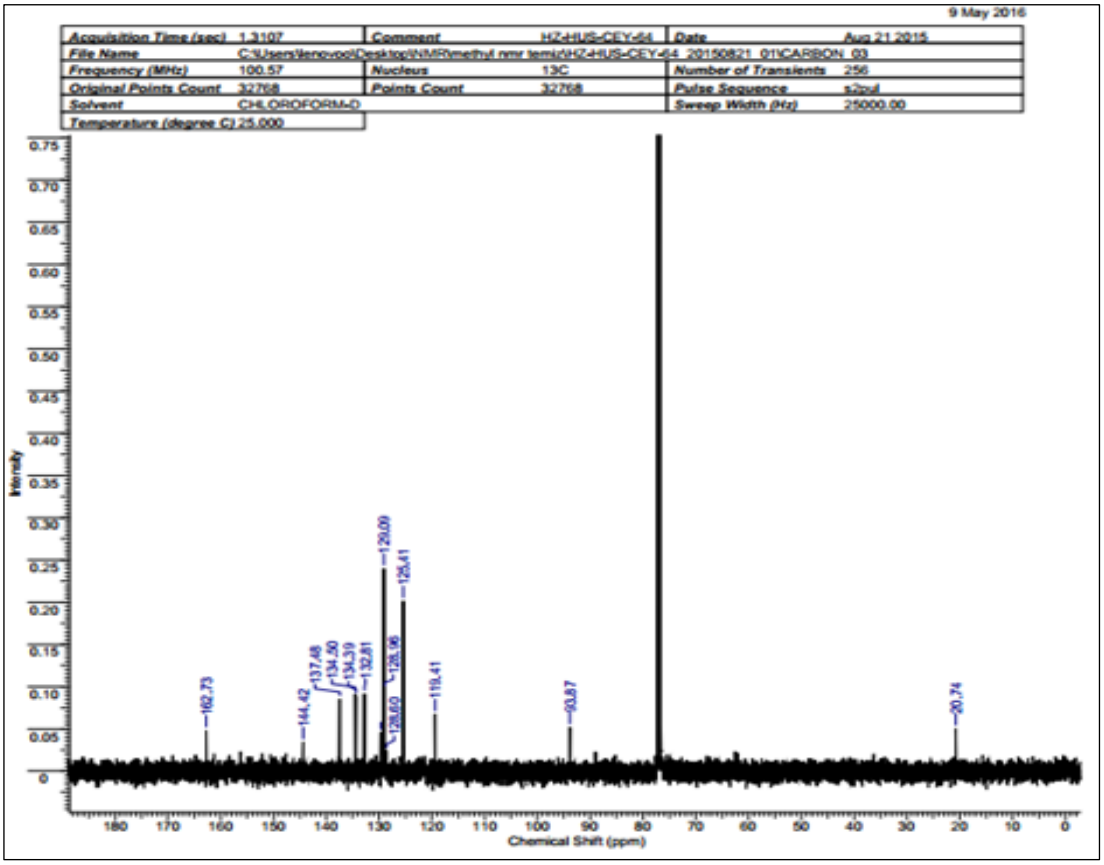

Figure A.20. ^{13}C-NMR of 2-(2-iodo-5-metylbenzoyl)-5-phenyl-1*H*-pyrazol-3(2*H*)-one

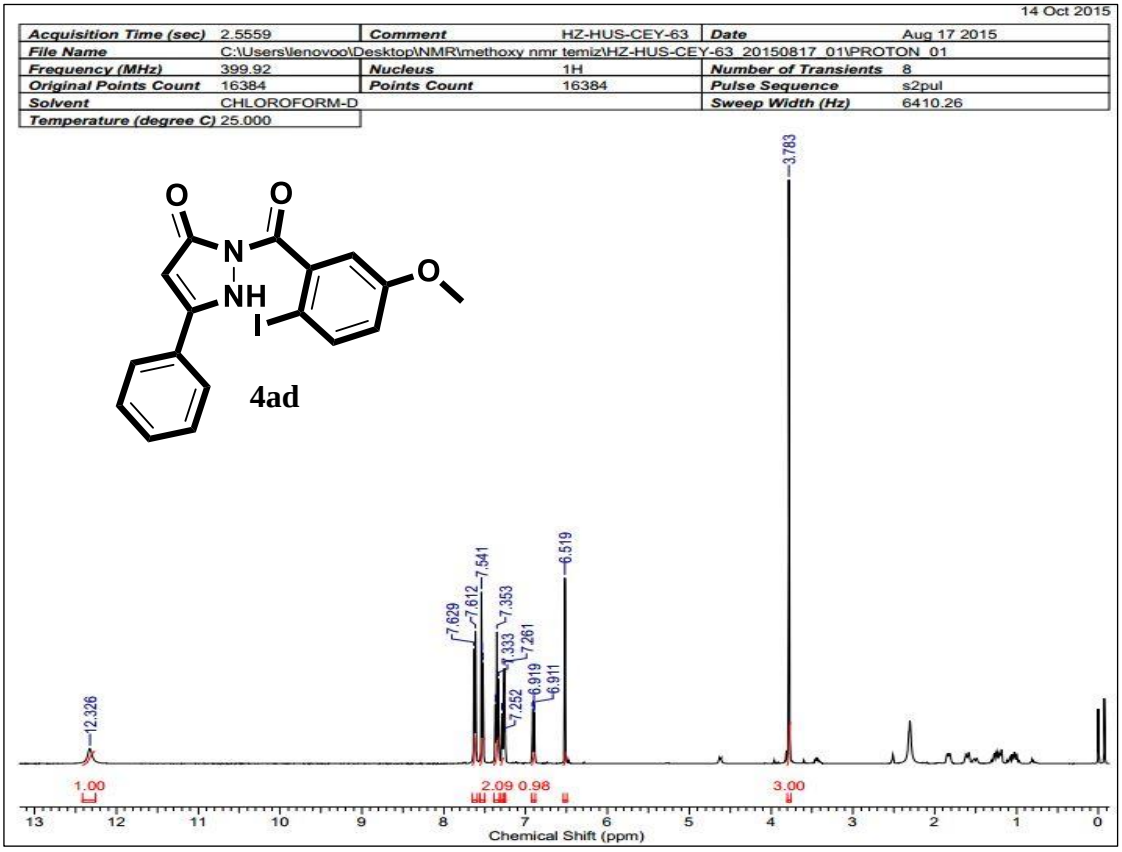

Figure A.21. [1]H-NMR of 2-(2-iodo-5-methoxybenzoyl)-5-phenyl-1*H*-pyrazol-3(2*H*)-one

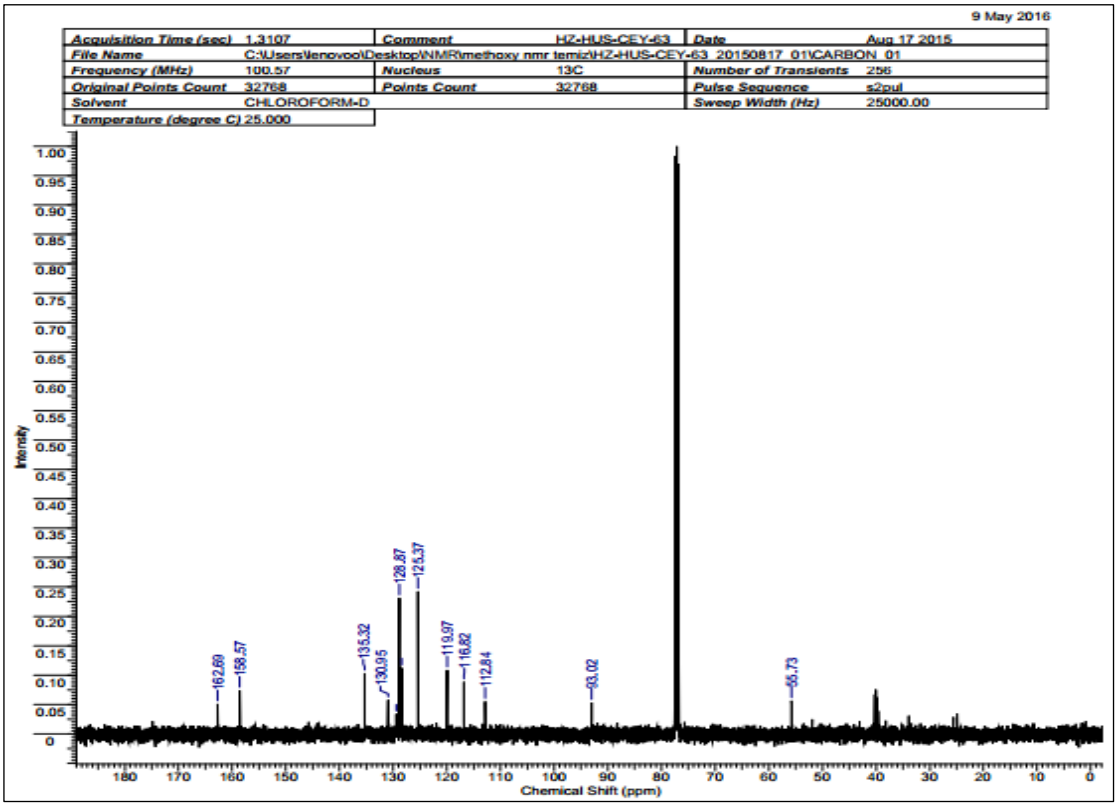

Figure A.22. [13]C-NMR of 2-(2-iodo-5-methoxybenzoyl)-5-phenyl-1*H*-pyrazol-3(2*H*)-one

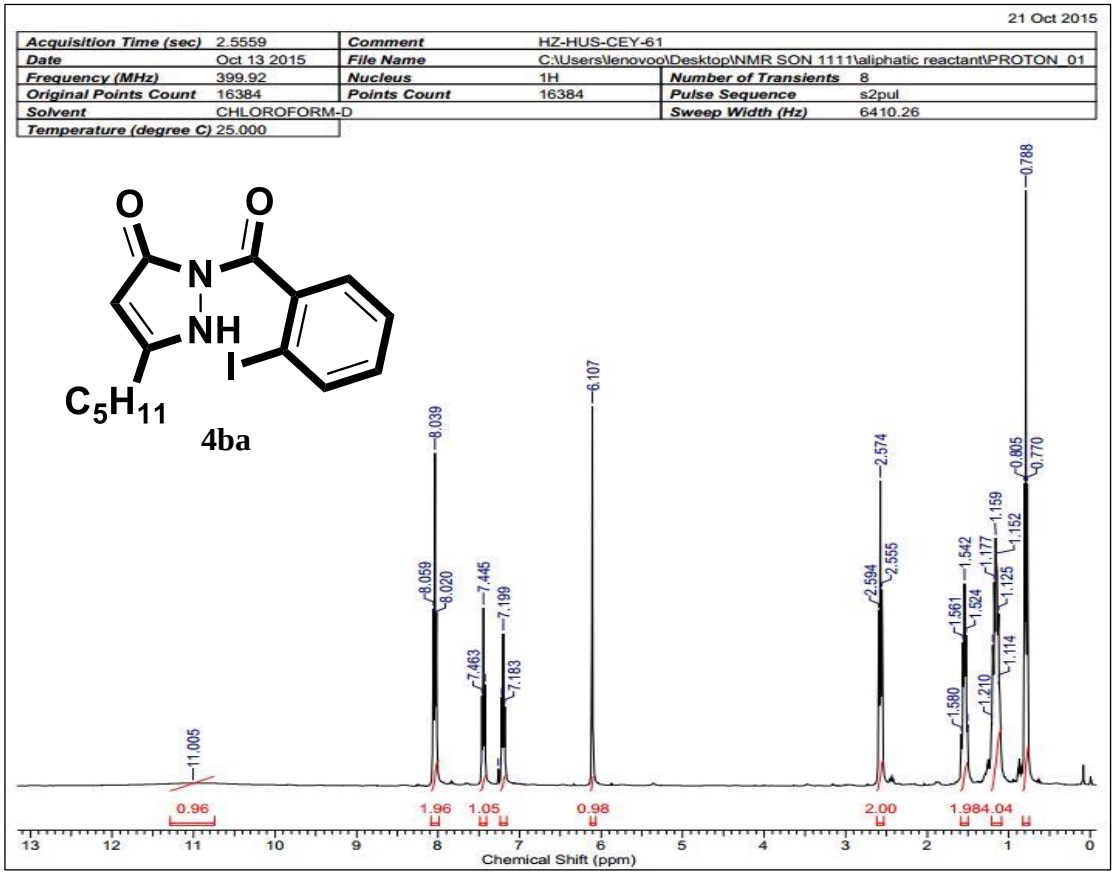

Figure A.23. ^{1}H-NMR of 5-pentyl-2-(2-iodobenzoyl)-1*H*-pyrazol-3(2*H*)-one

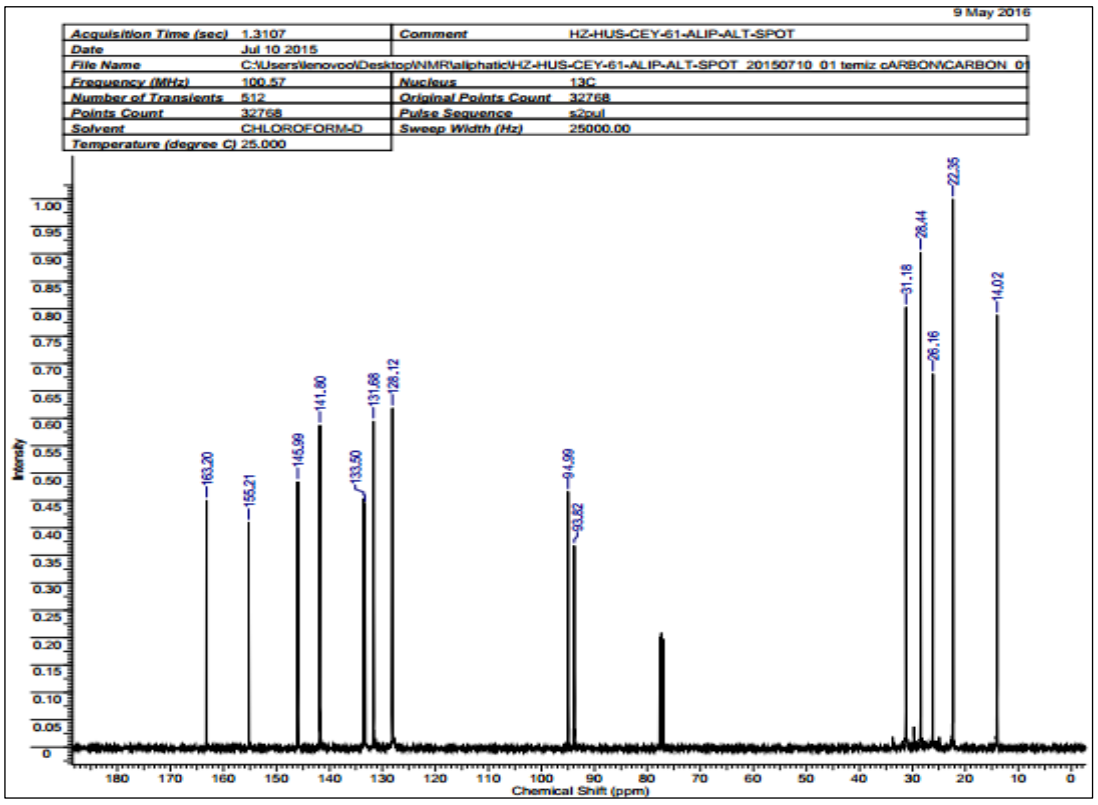

Figure A.24. ^{13}C-NMR of 5-pentyl-2-(2-iodobenzoyl)-1*H*-pyrazol-3(2*H*)-one

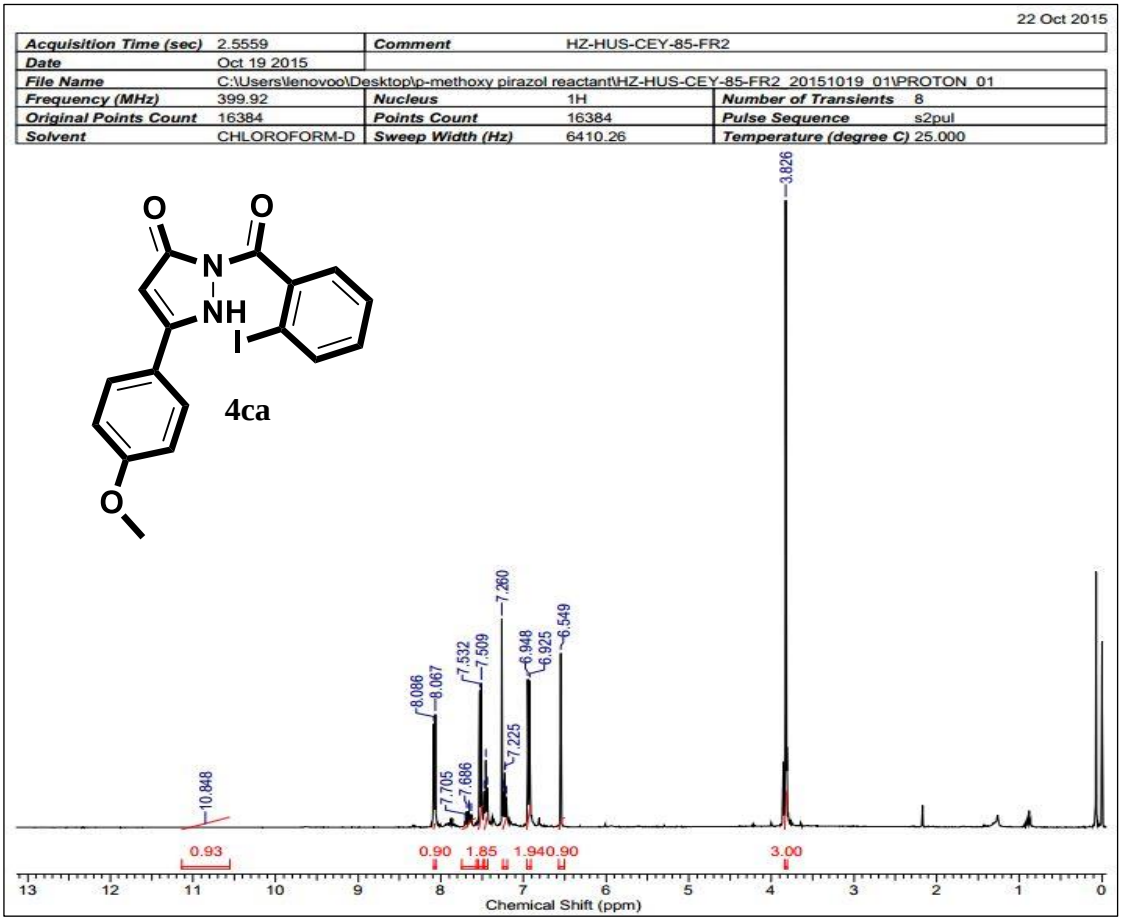

Figure A.25. [1]H-NMR of 2-(2-iodobenzoyl)-5-(4-methoxyphenyl)-1*H*-pyrazol-3(2*H*)-one

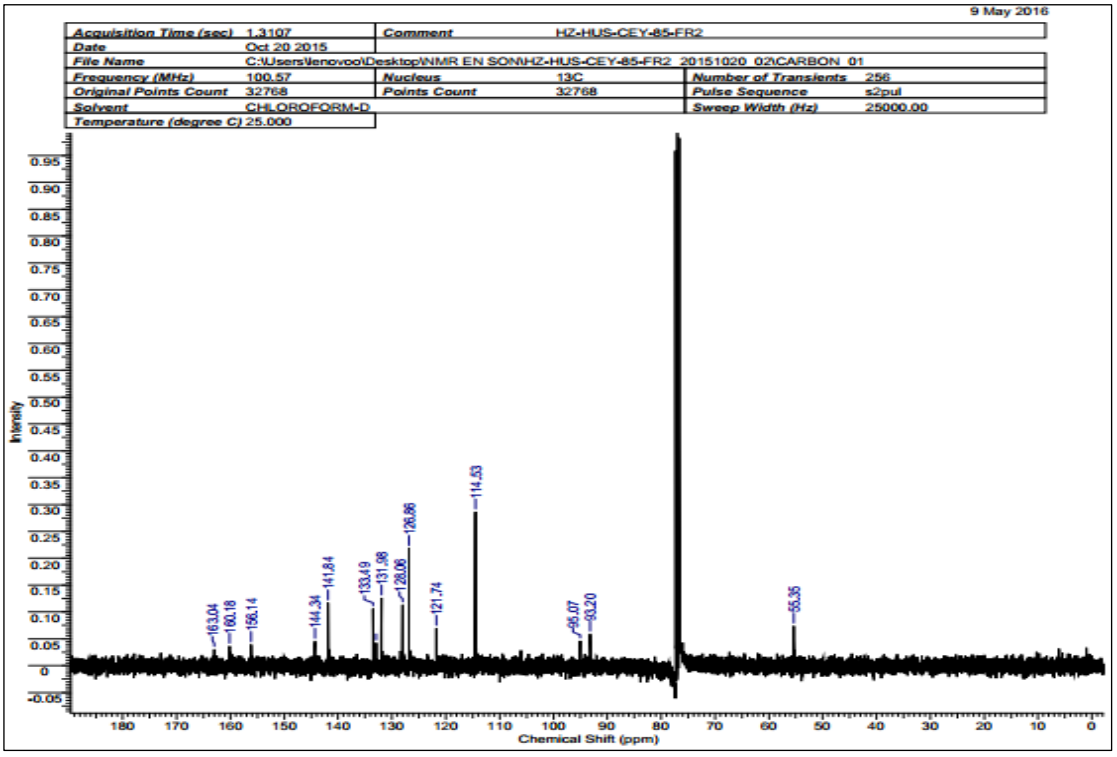

Figure A.26. [13]C-NMR of 2-(2-iodobenzoyl)-5-(4-methoxyphenyl)-1*H*-pyrazol-3(2*H*)-one

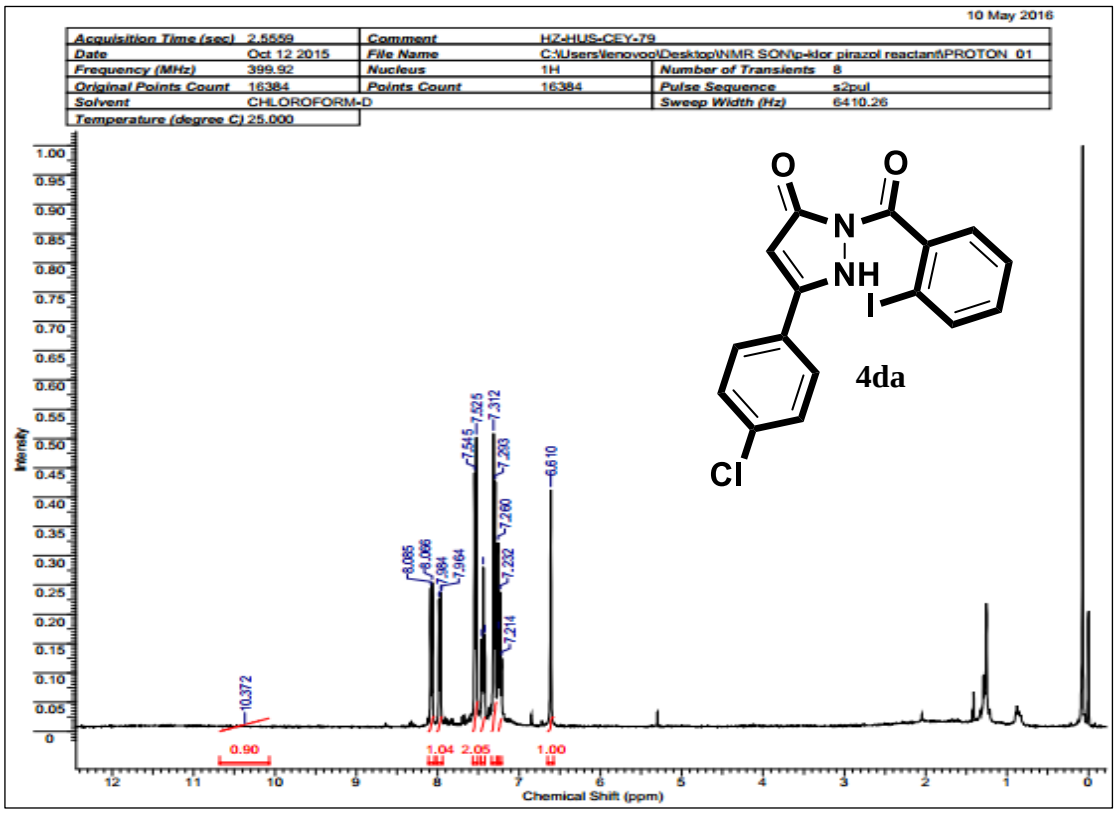

Figure A.27. ^{1}H-NMR of 2-(2-chlorobenzoyl)-5-(4-iodophenyl)-1*H*-pyrazol-3(2*H*)-one

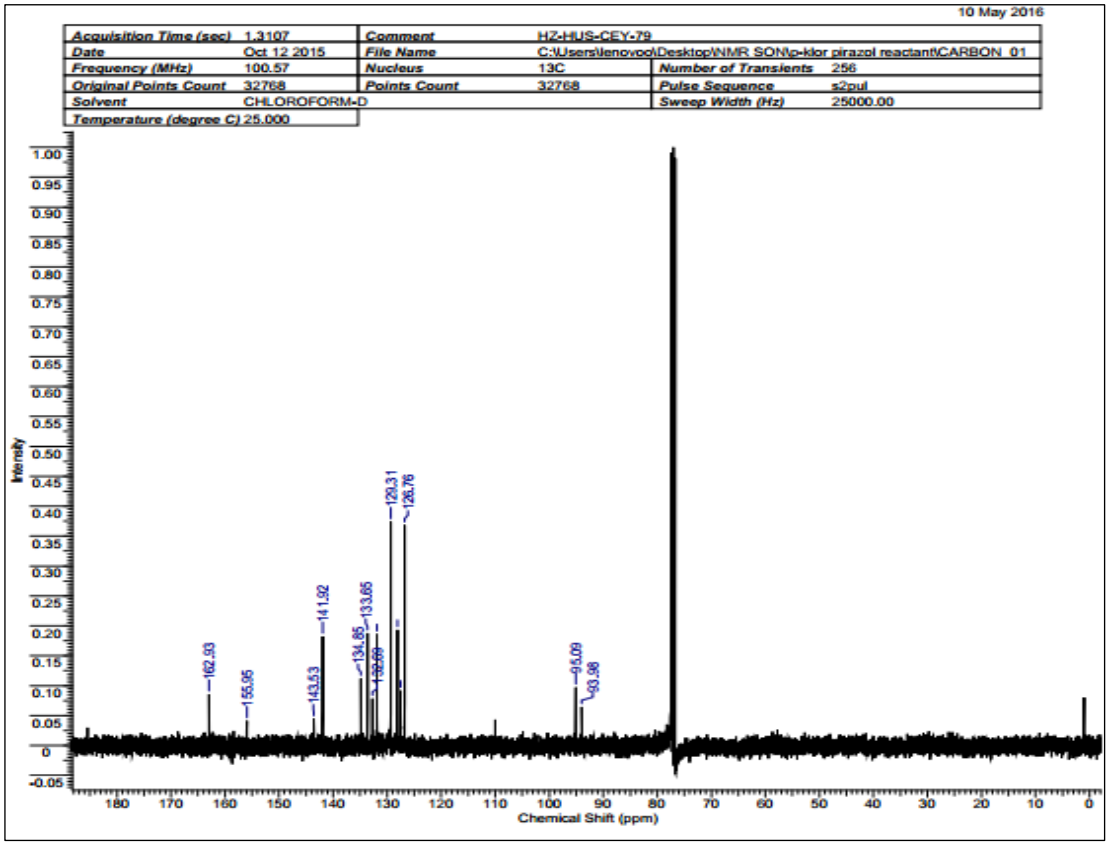

Figure A.28. ^{13}C-NMR of 2-(2-chlorobenzoyl)-5-(4-iodophenyl)-1*H*-pyrazol-3(2*H*)-one

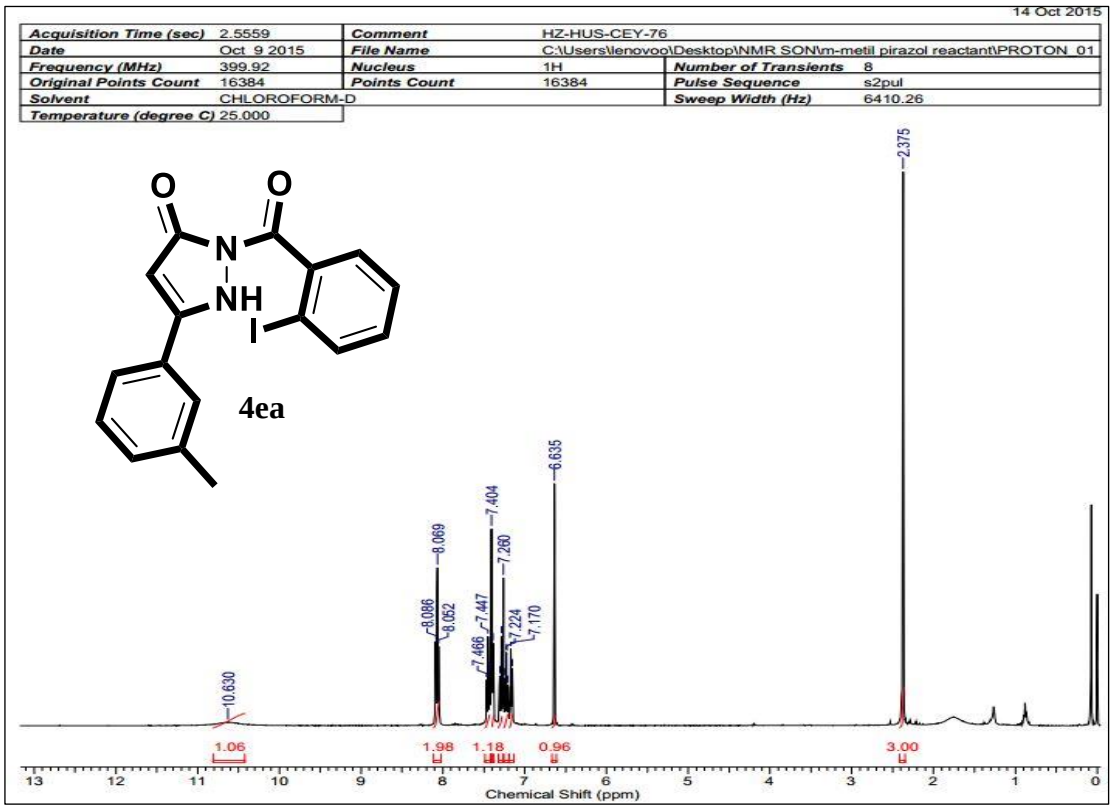

Figure A.29. [1]H-NMR of 2-(2-iodobenzoyl)-5-(m-tolyl)-1*H*-pyrazol-3(2*H*)-one

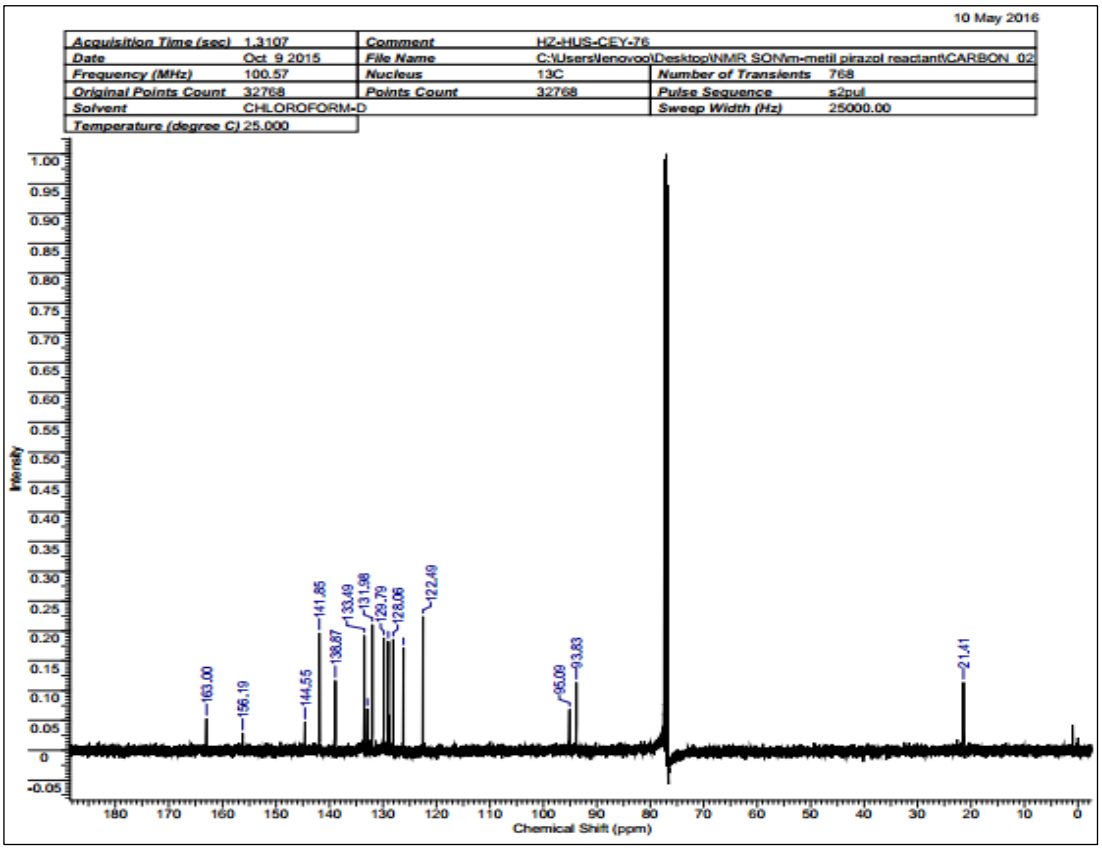

Figure A.30. [13]C-NMR of 2-(2-iodobenzoyl)-5-(m-tolyl)-1*H*-pyrazol-3(2*H*)-one

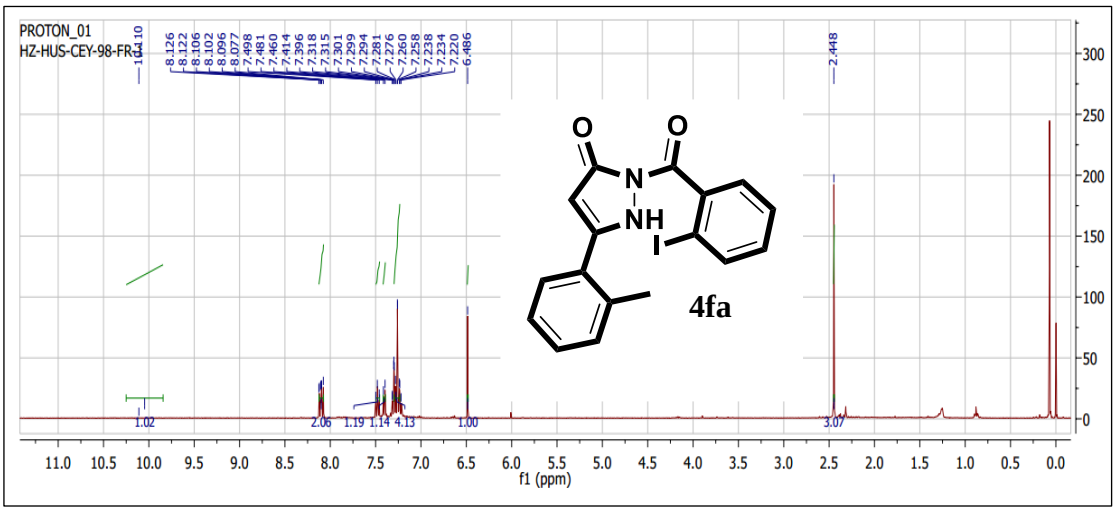

Figure A.31. ^{1}H-NMR of 2-(2-iodobenzoyl)-5-(o-tolyl)-1*H*-pyrazol-3(2*H*)-one

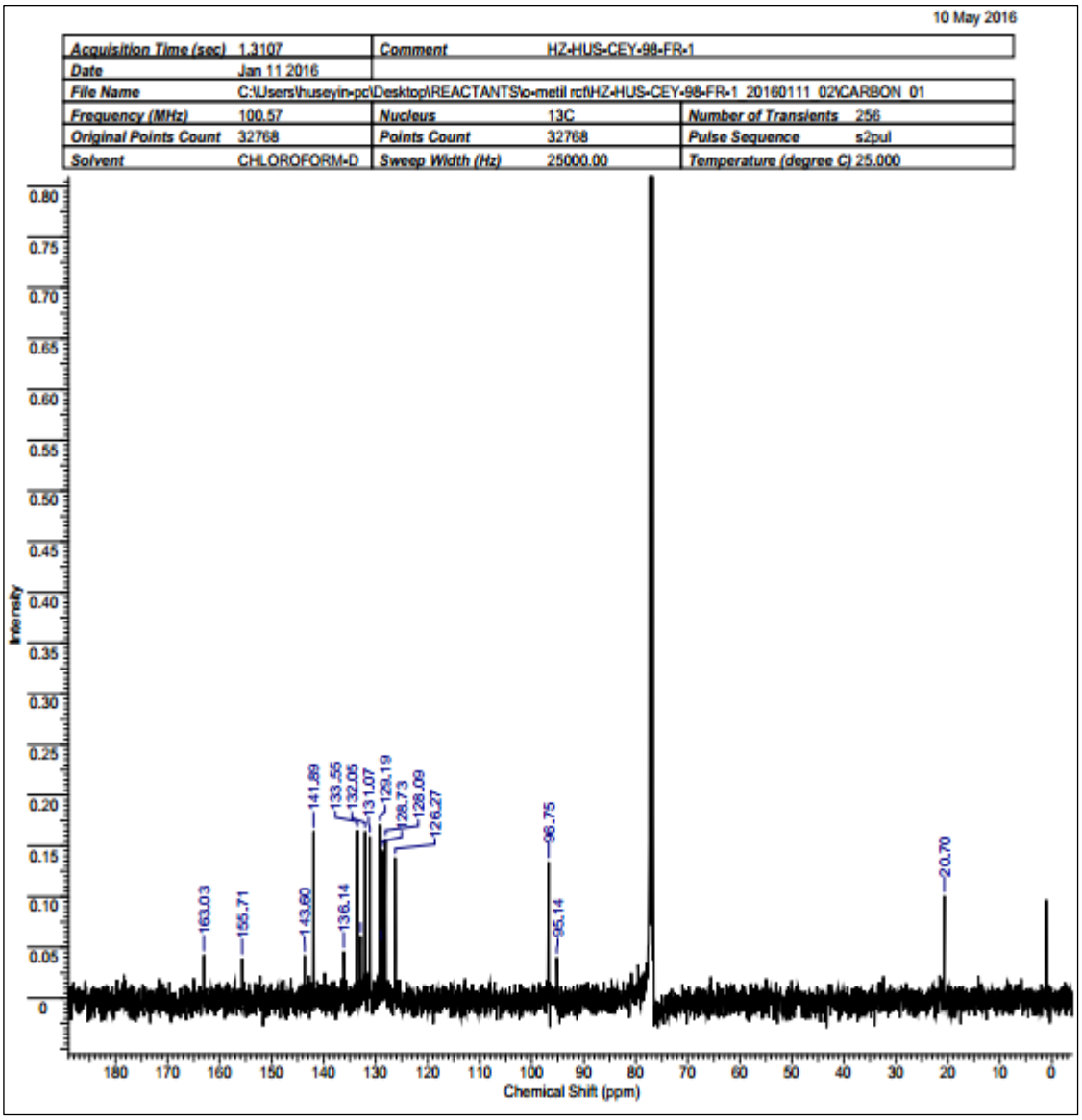

Figure A.32. ^{13}C-NMR of 2-(2-iodobenzoyl)-5-(o-tolyl)-1*H*-pyrazol-3(2*H*)-one

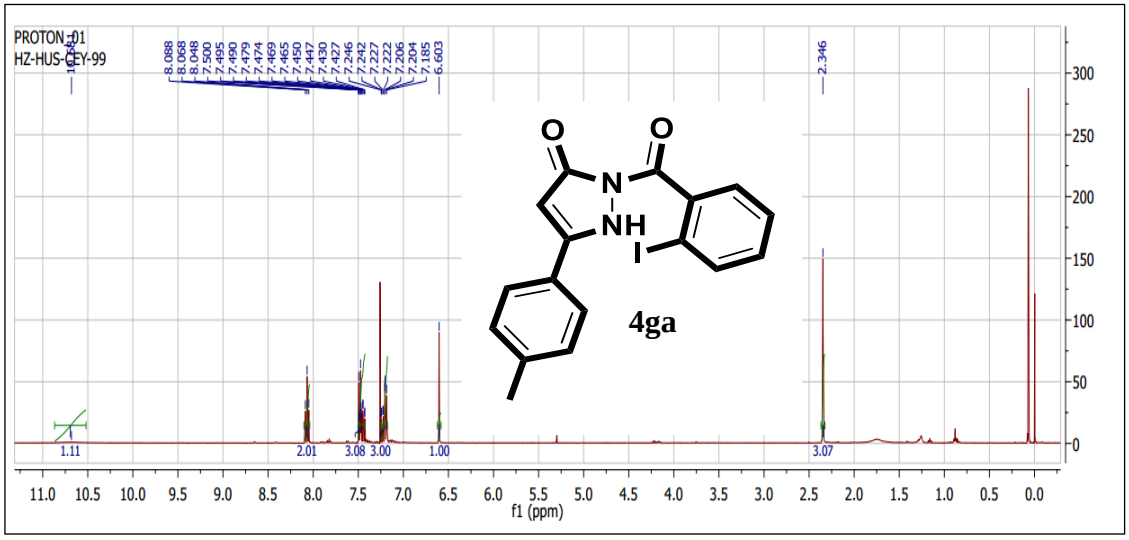

Figure A.33. ^{1}H-NMR of 2-(2-iodobenzoyl)-5-(p-tolyl)-1*H*-pyrazol-3(2*H*)-one

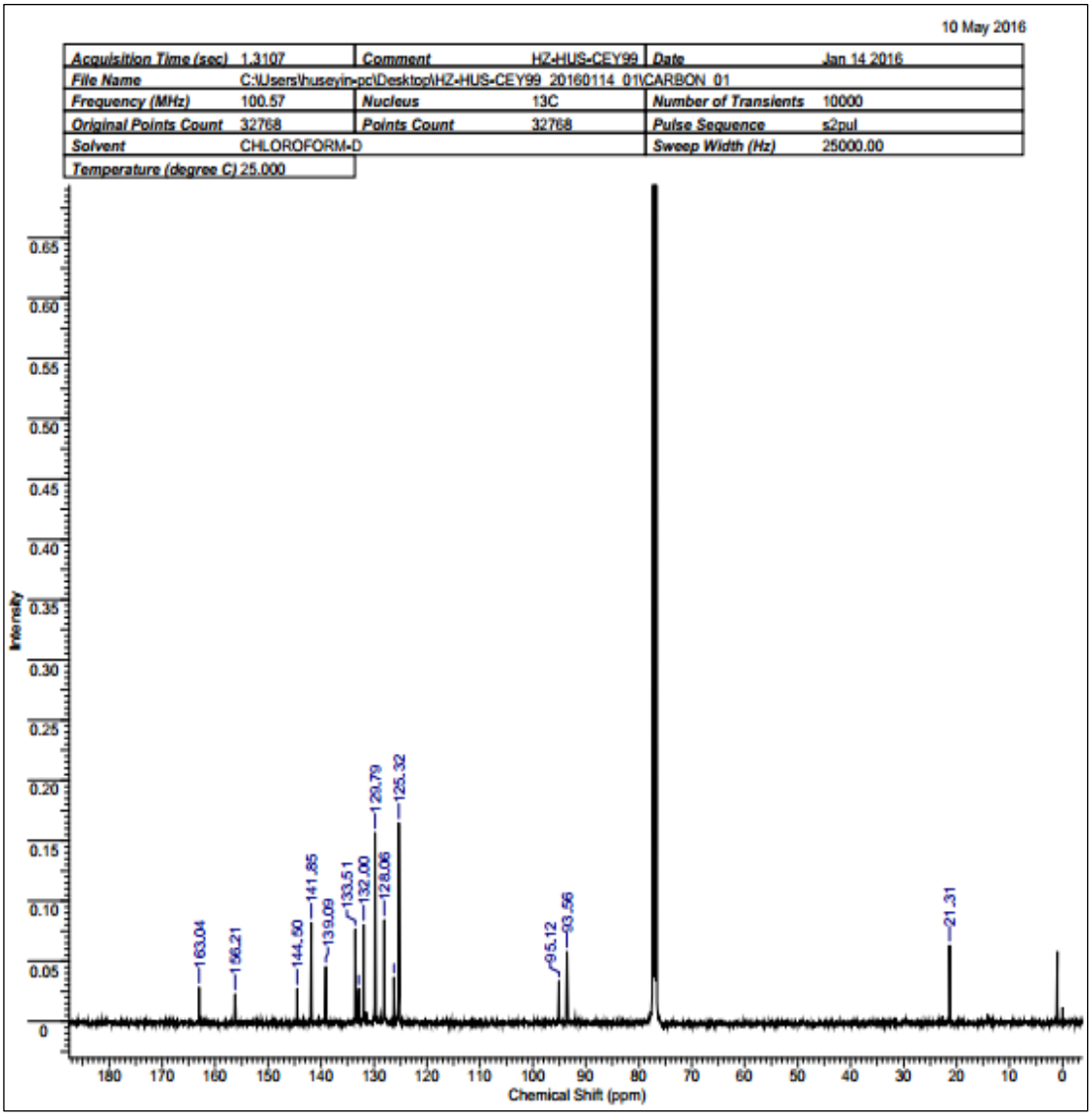

Figure A.34. ^{13}C-NMR of 2-(2-iodobenzoyl)-5-(p-tolyl)-1*H*-pyrazol-3(2*H*)-one

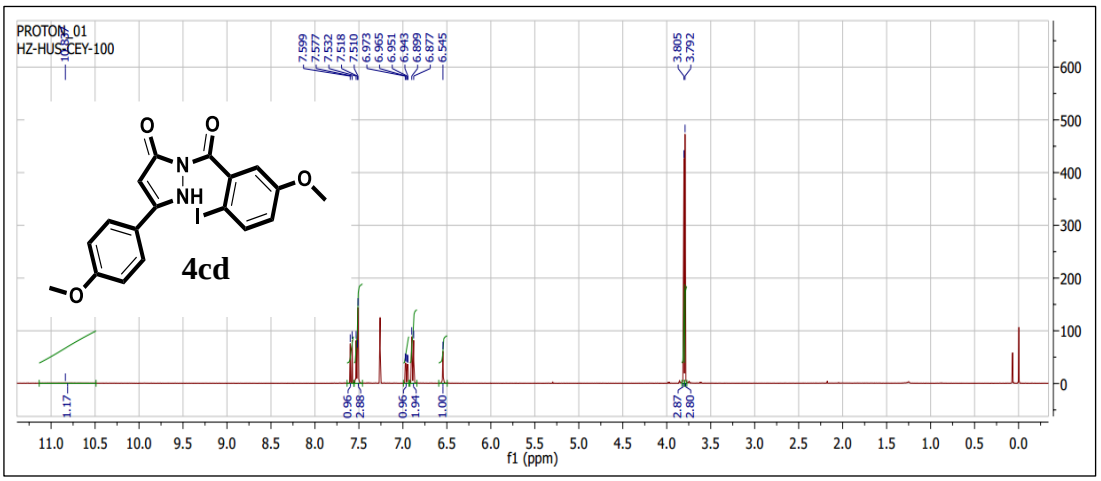

Figure A.35. [1]H-NMR of 2-(2-iodo-5-methoxybenzoyl)-5-(4-methoxyphenyl)-1*H*-pyrazol-3(2*H*)-one

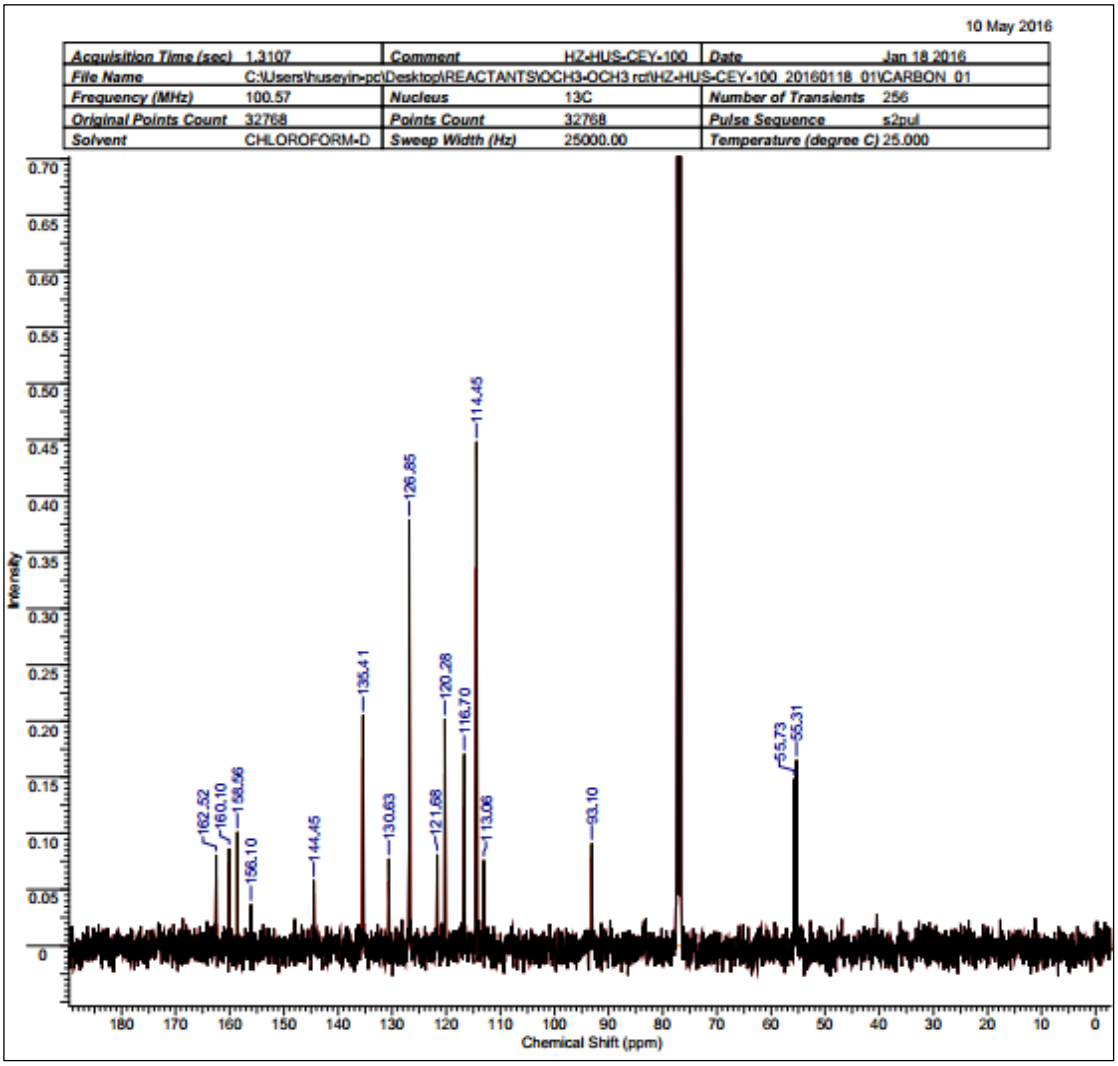

Figure A.36. [13]C-NMR of 2-(2-iodo-5-methoxybenzoyl)-5-(4-methoxyphenyl)-1*H*-pyrazol-3(2*H*)-one

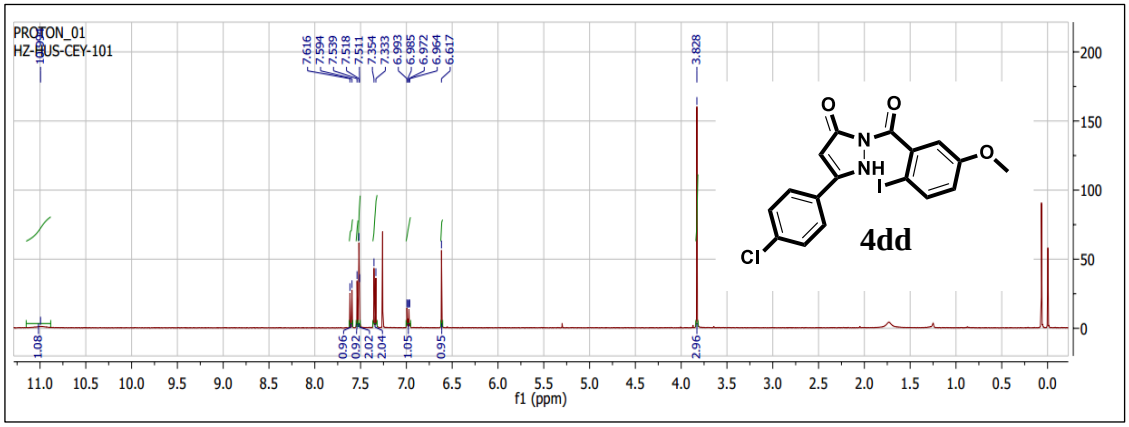

Figure A.37. ^{1}H-NMR of 5-(4-chlorophenyl)-2-(2-iodo-5-methoxybenzoyl)-1*H*-pyrazol-3(2*H*)-one

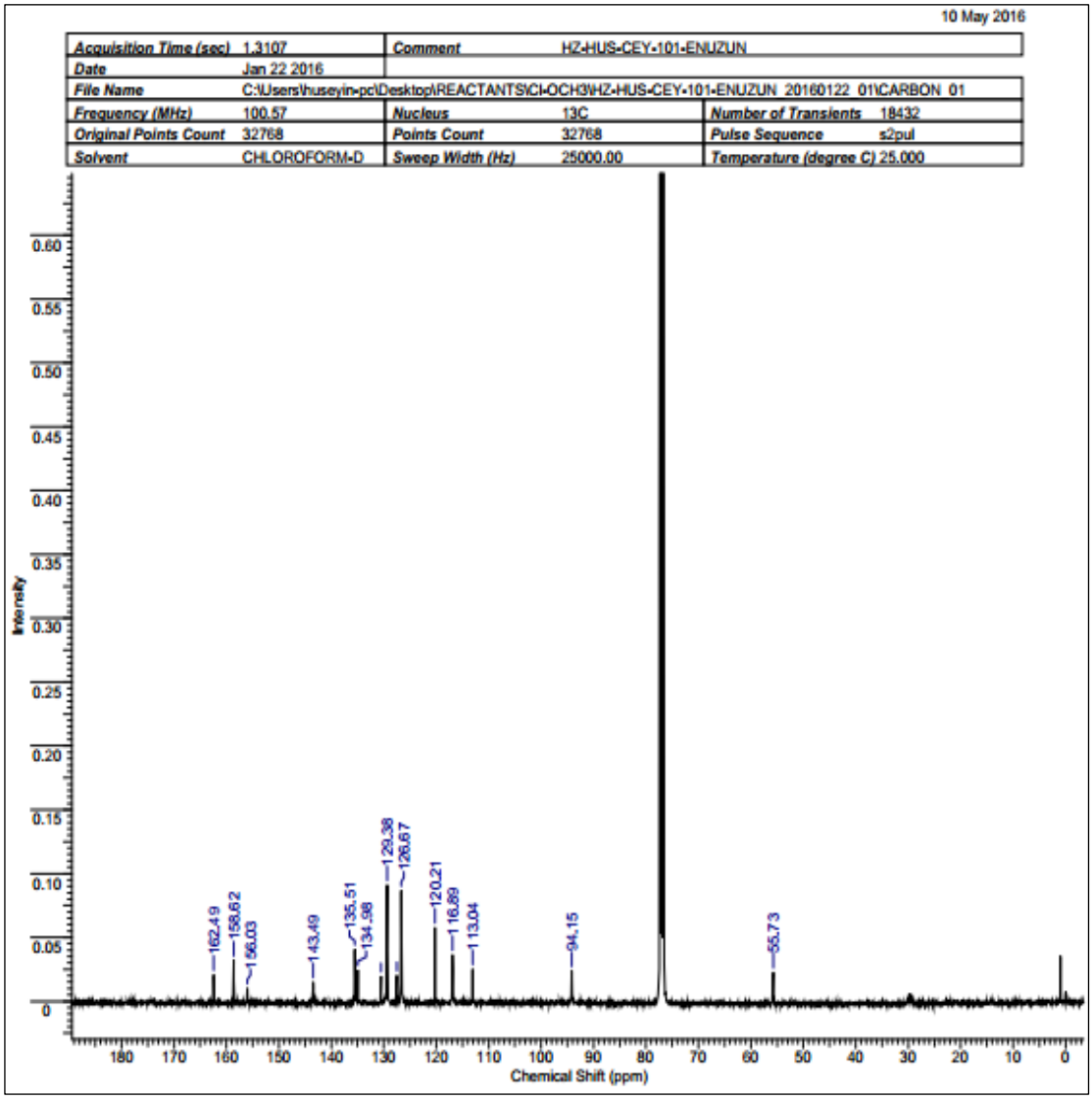

Figure A.38. ^{13}C-NMR of 5-(4-chlorophenyl)-2-(2-iodo-5-methoxybenzoyl)-1*H*-pyrazol-3(2*H*)-one

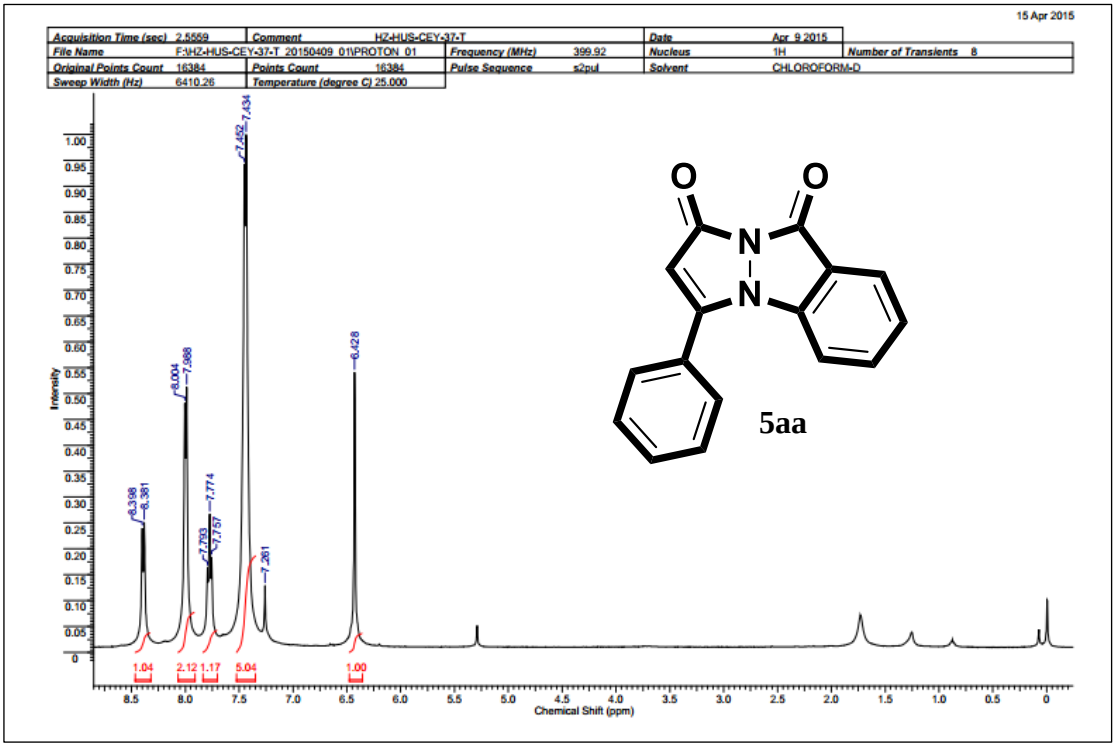

Figure A.39. [1]H-NMR of 3-phenylpyrazolo[1,2-a]indazole-1,9-dione

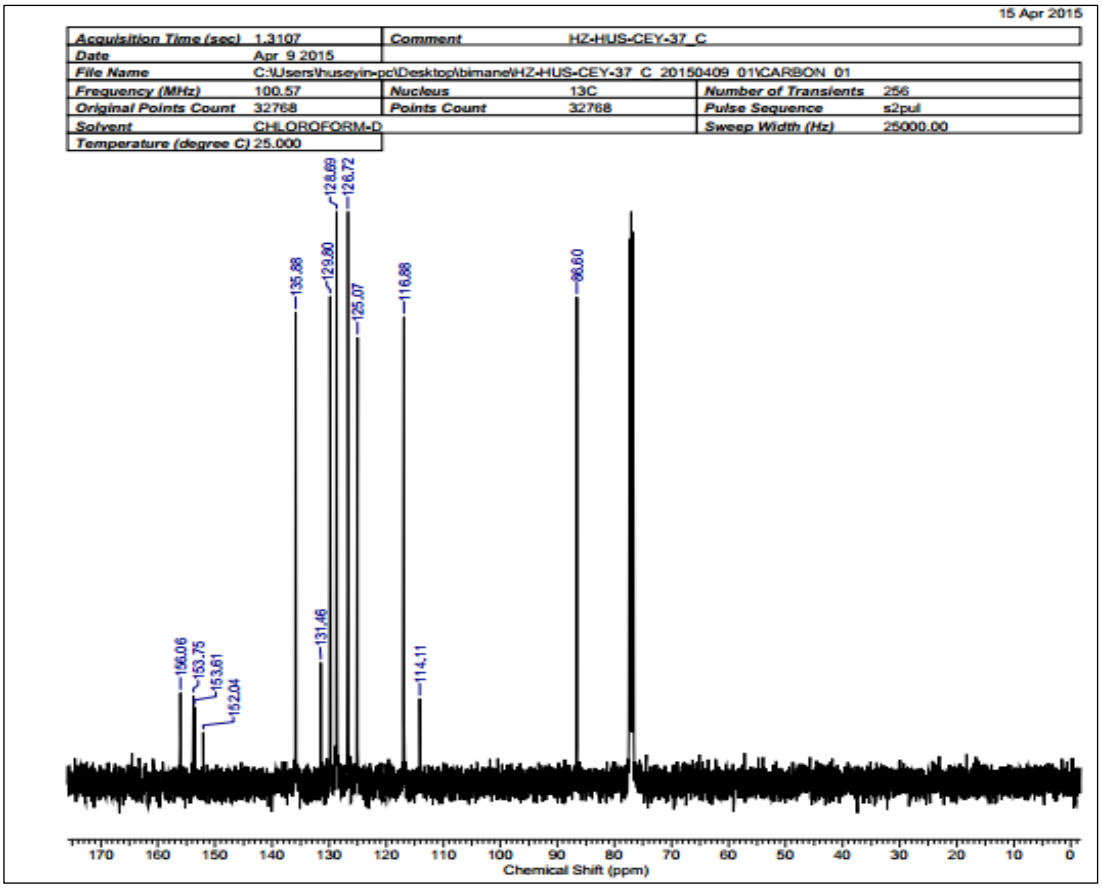

Figure A.40. [13]C-NMR of 3-phenylpyrazolo[1,2-a]indazole-1,9-dione

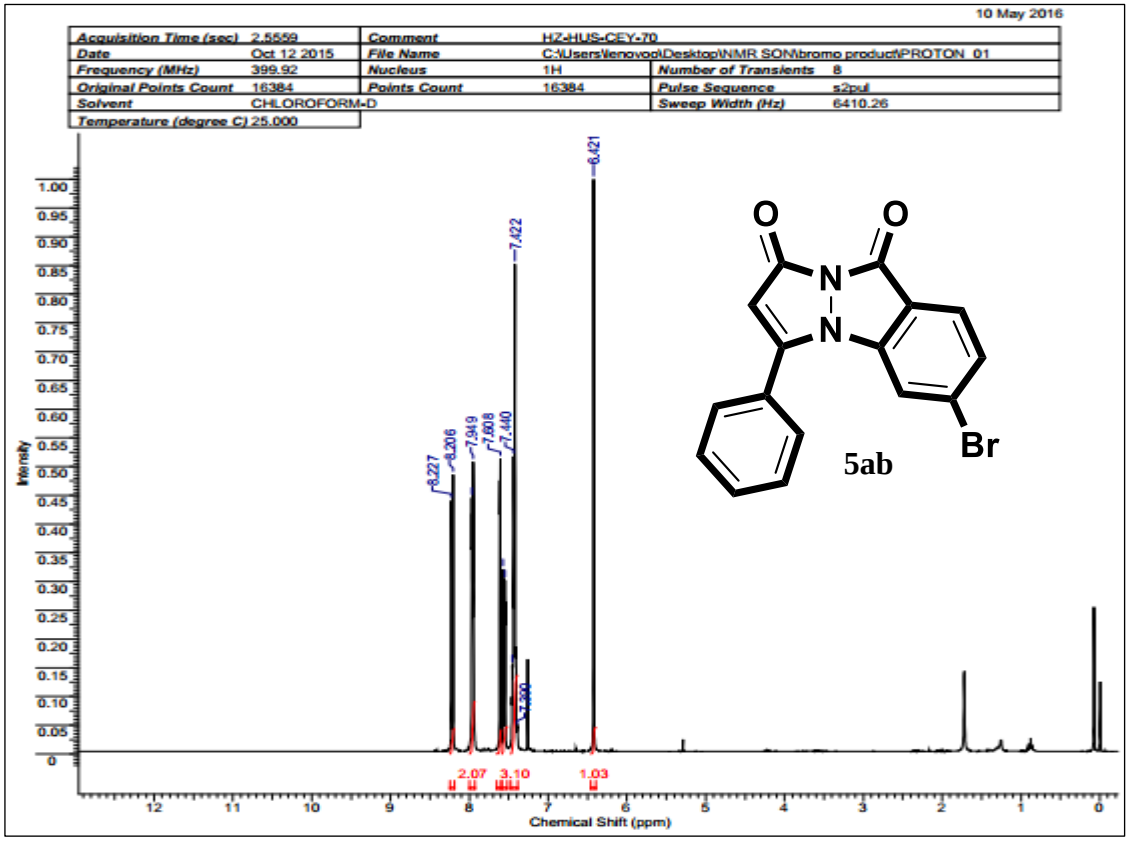

Figure A.41. [1]H-NMR of 6-bromo-3-phenylpyrazolo[1,2-a]indazole-1,9-dione

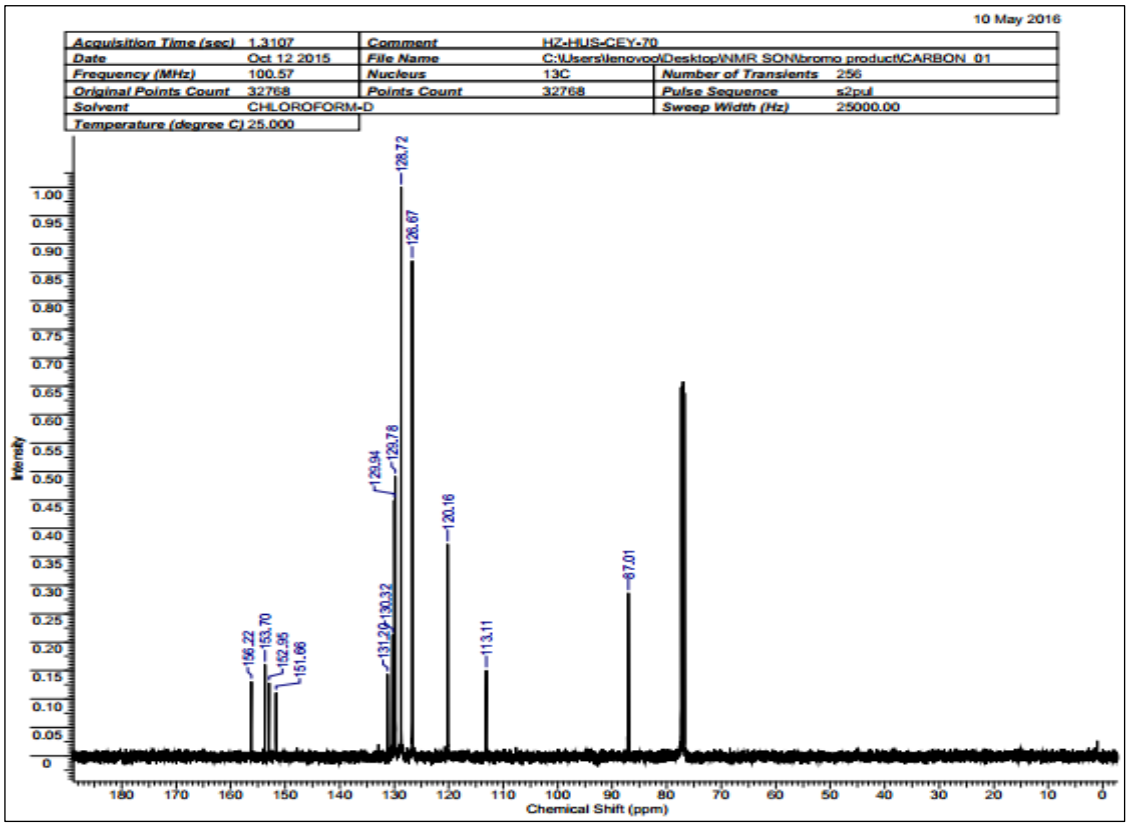

Figure A.42. [13]C-NMR of 6-bromo-3-phenylpyrazolo[1,2-a]indazole-1,9-dione

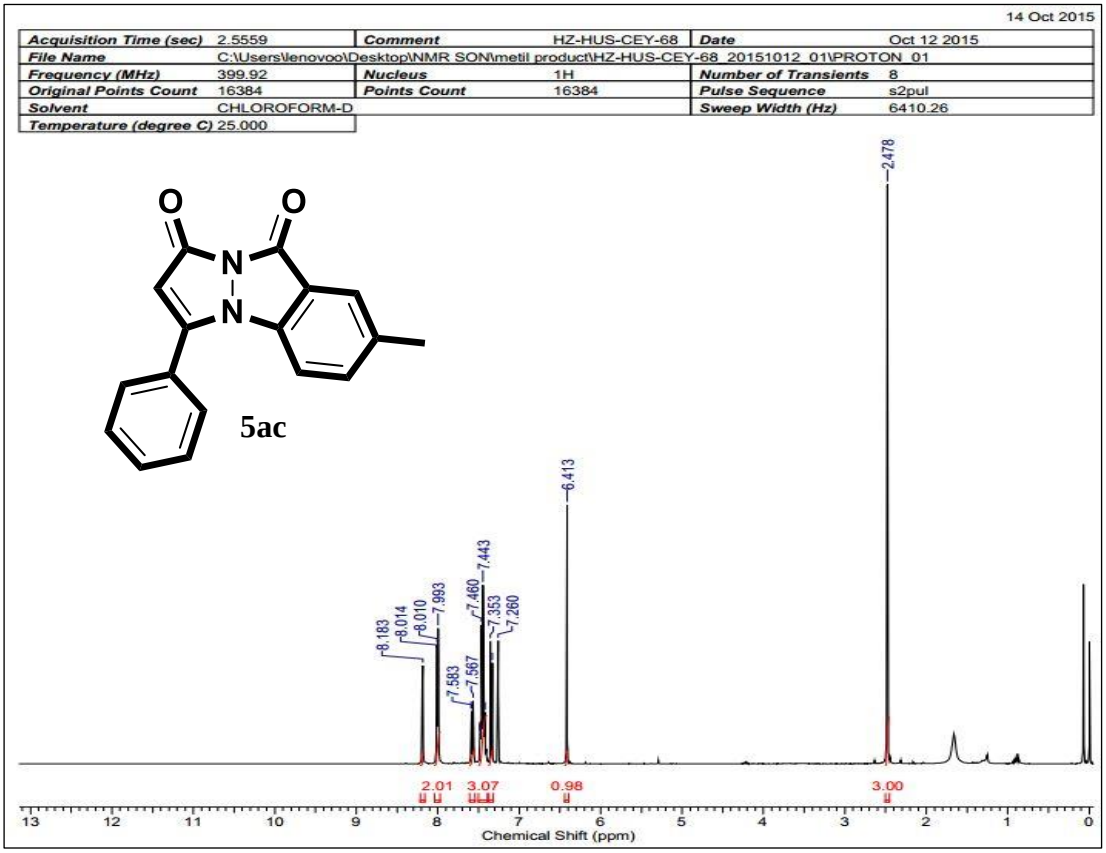

Figure A.43. [1]H-NMR of 7-methyl-3-phenylpyrazolo[1,2-a]indazole-1,9-dione

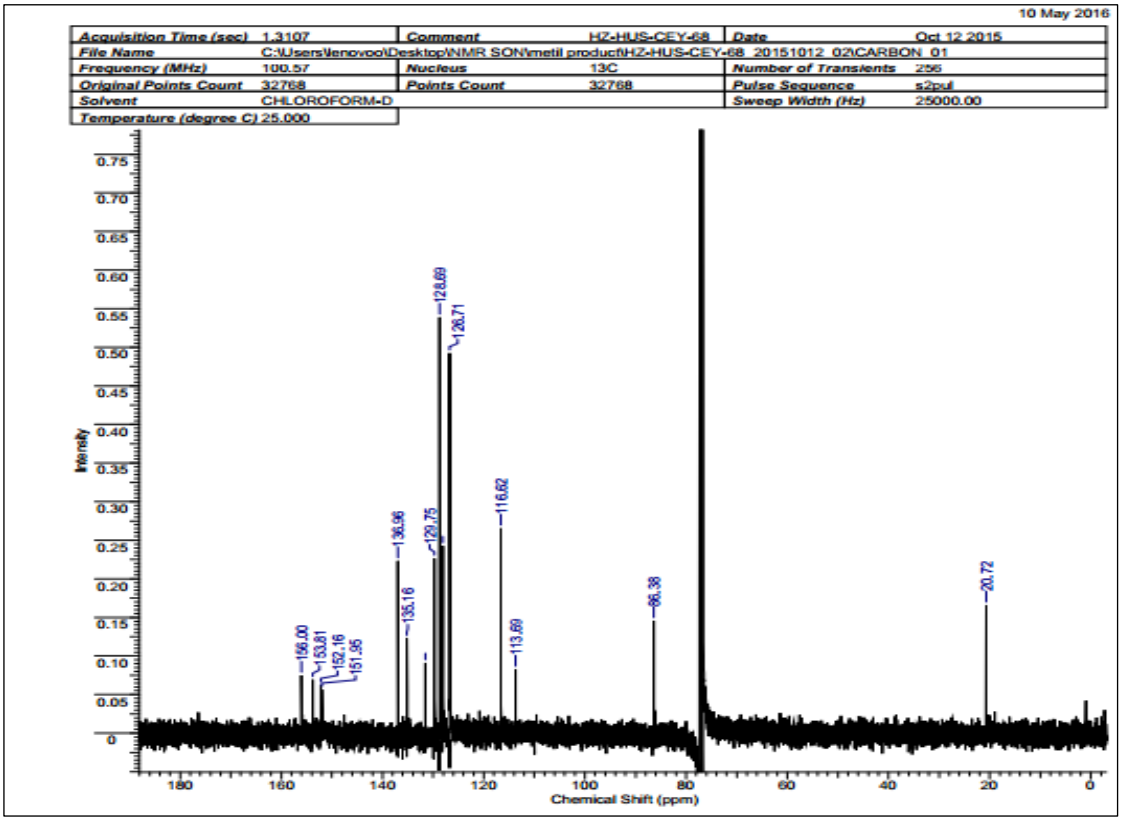

Figure A.44. [13]C-NMR of 7-methyl-3-phenylpyrazolo[1,2-a]indazole-1,9-dione

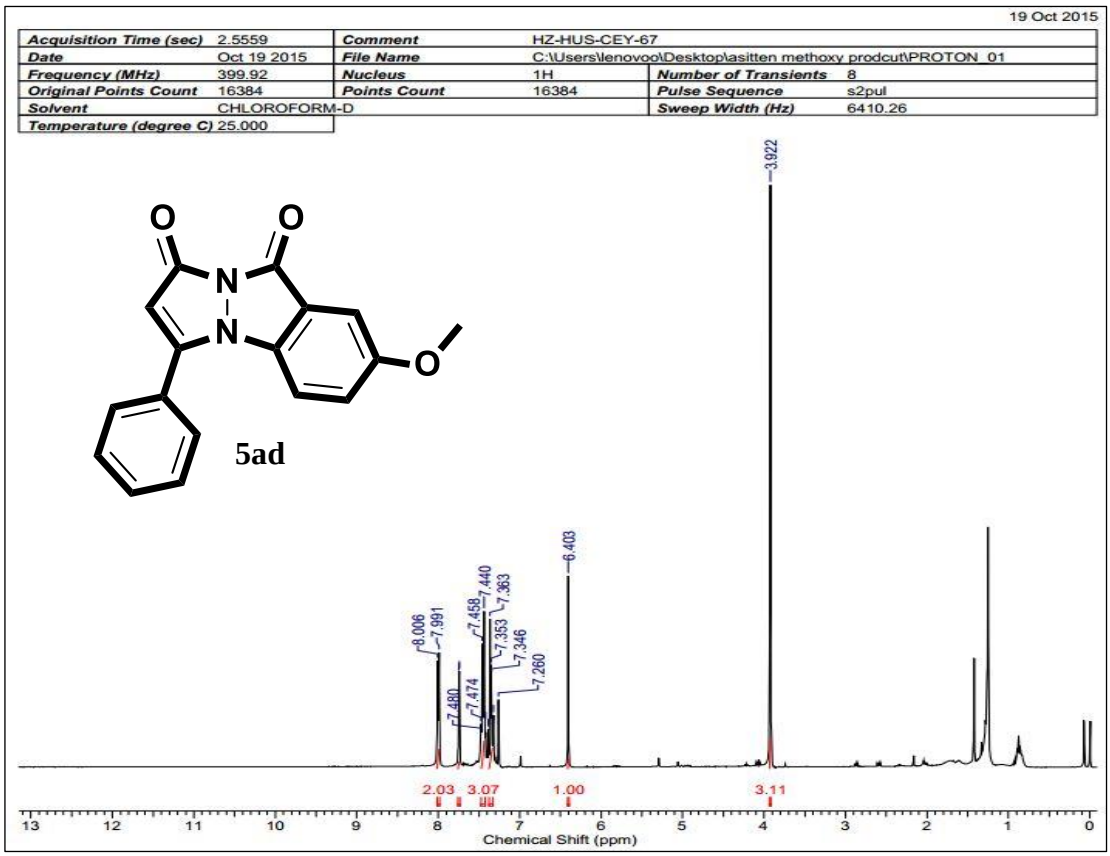

Figure A.45. [1]H-NMR of 7-methoxy-3-phenylpyrazolo[1,2-a]indazole-1,9-dione

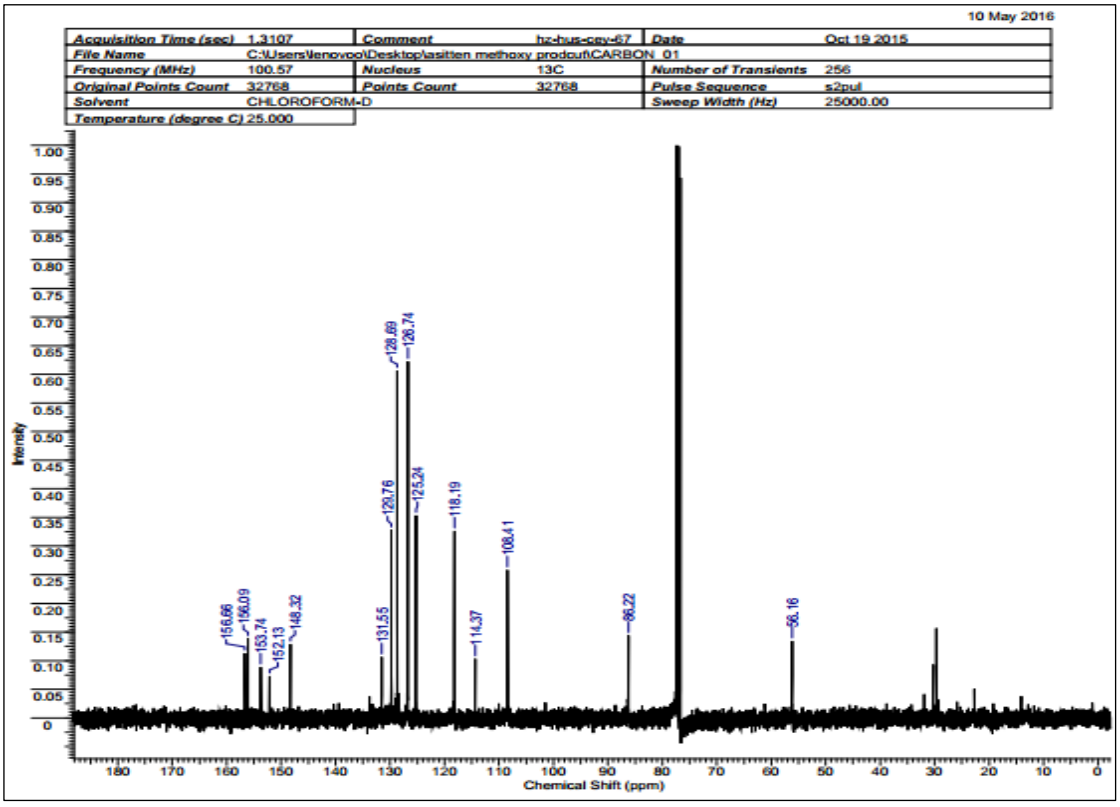

Figure A.46. [13]C-NMR of 7-methoxy-3-phenylpyrazolo[1,2-a]indazole-1,9-dione

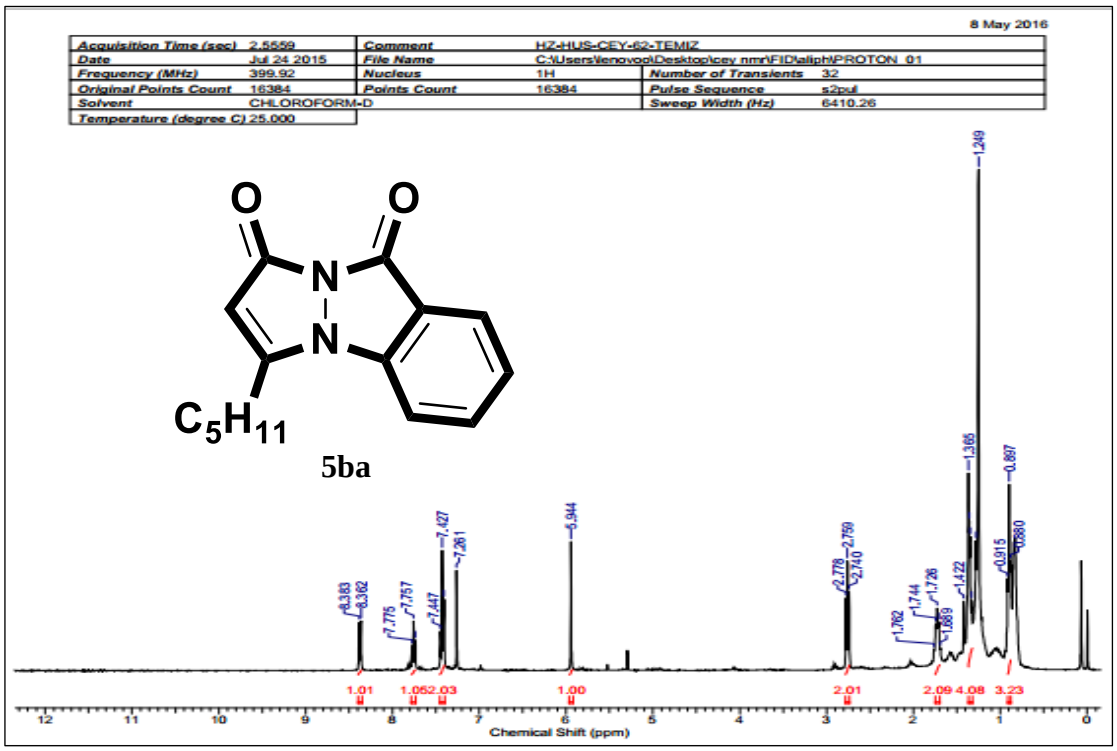

Figure A.47. [1]H-NMR of 3-pentylpyrazolo[1,2-a]indazole-1,9-dione

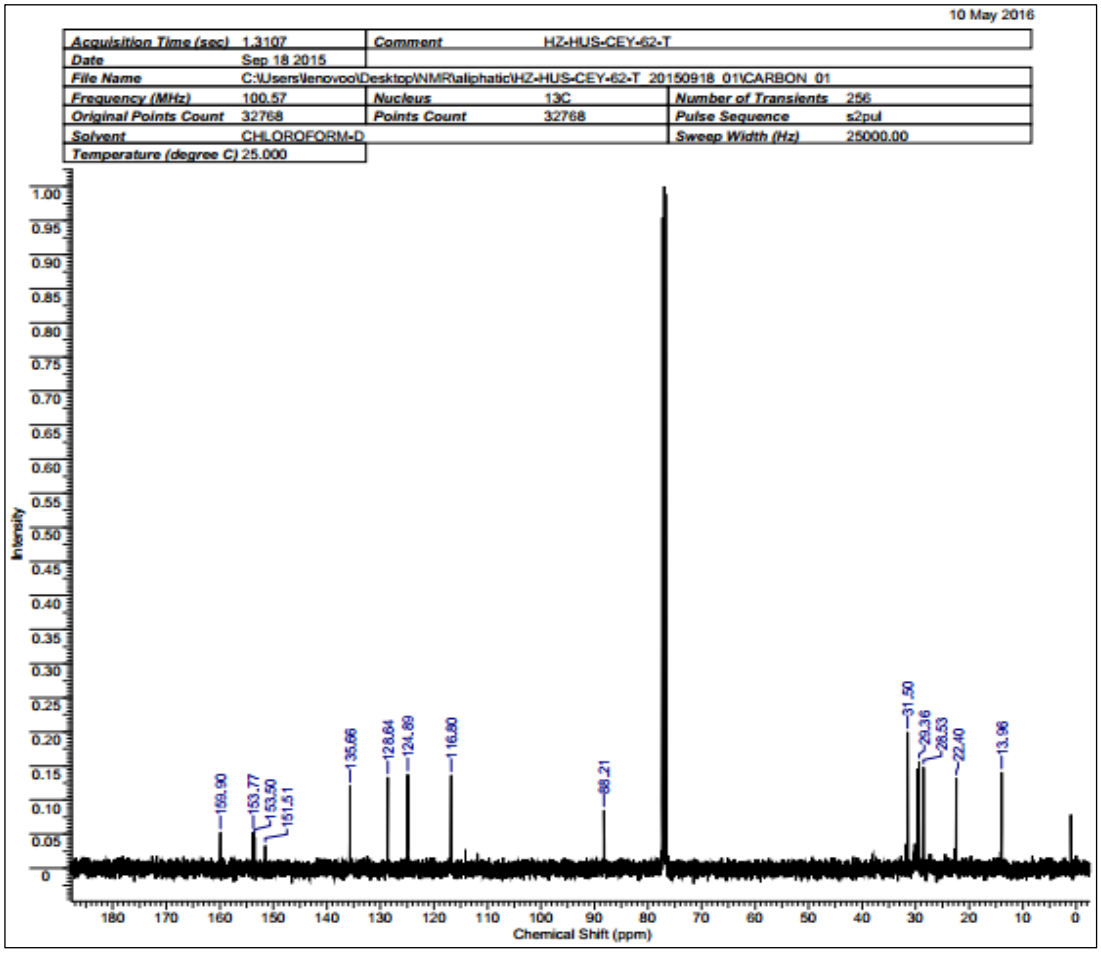

Figure A.48. [13]C-NMR of 3-pentylpyrazolo[1,2-a]indazole-1,9-dione

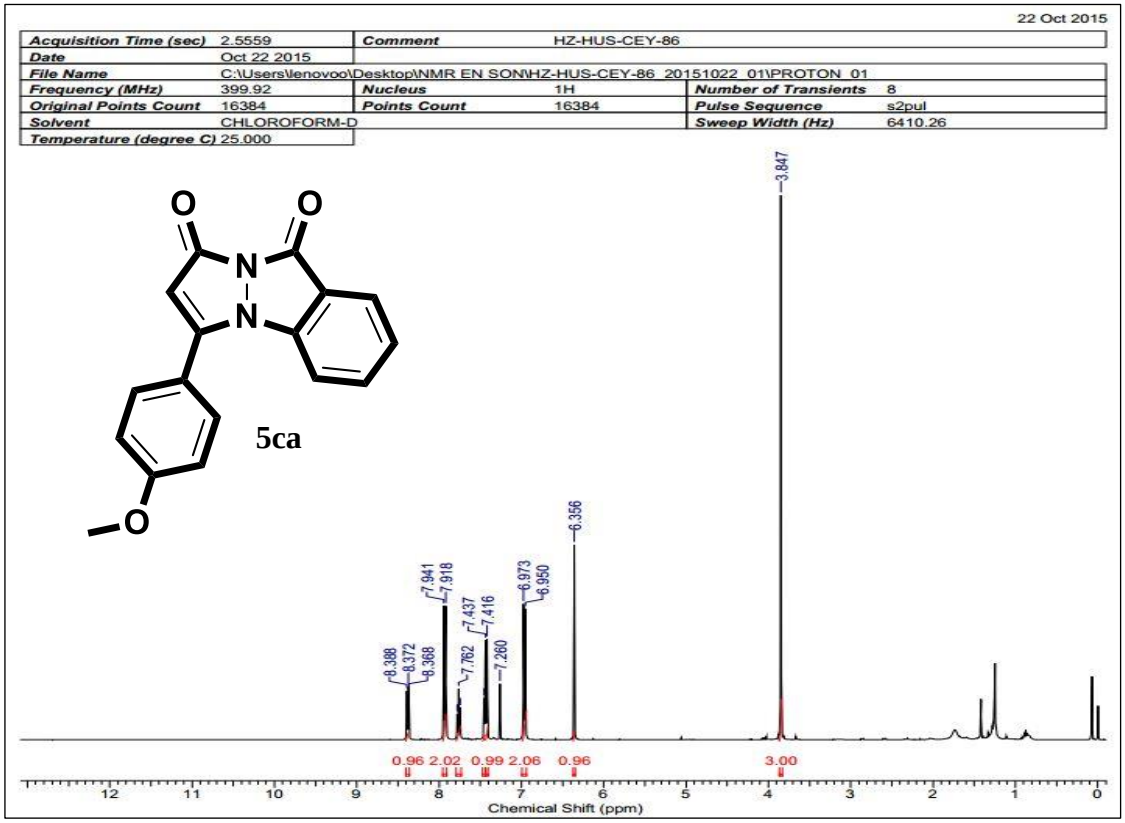

Figure A.49. [1]H-NMR of 3-(4-methoxyphenyl)pyrazolo[1,2-a]indazole-1,9-dione

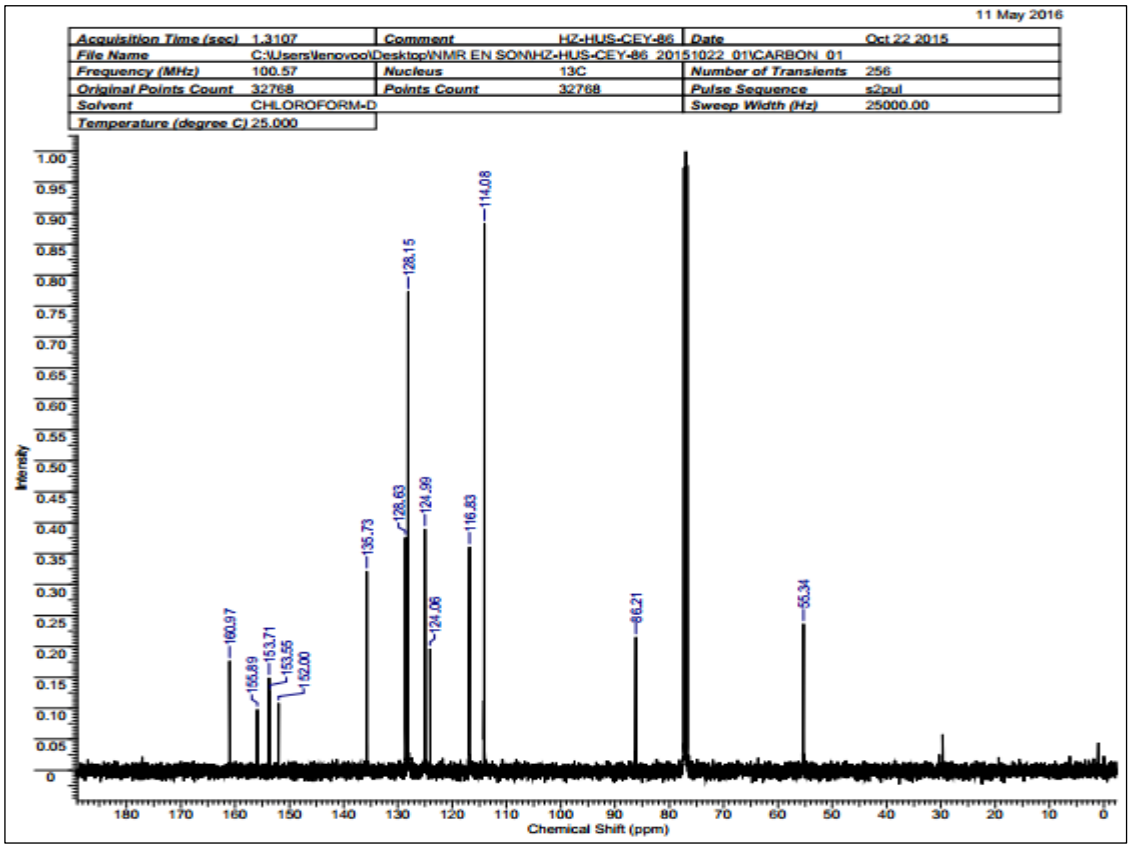

Figure A.50. [13]C-NMR of 3-(4-methoxyphenyl)pyrazolo[1,2-a]indazole-1,9-dione

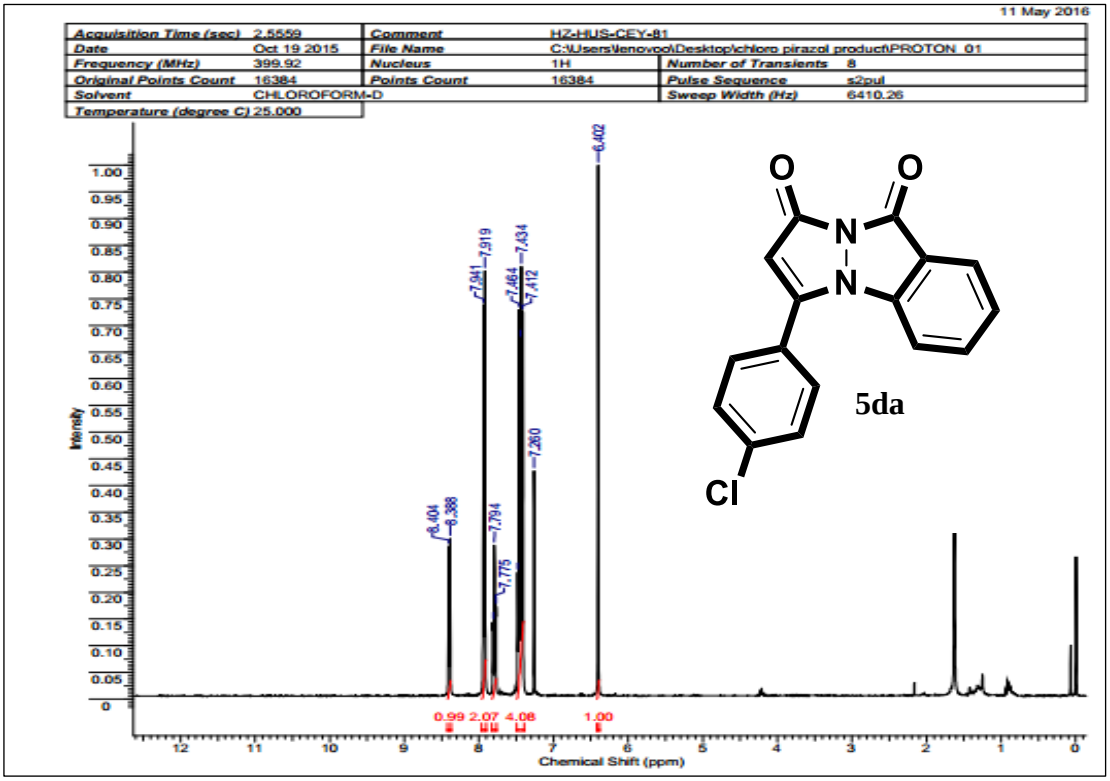

Figure A.51. ^{1}H-NMR of 3-(4-chlorophenyl)pyrazolo[1,2-a]indazole-1,9-dione

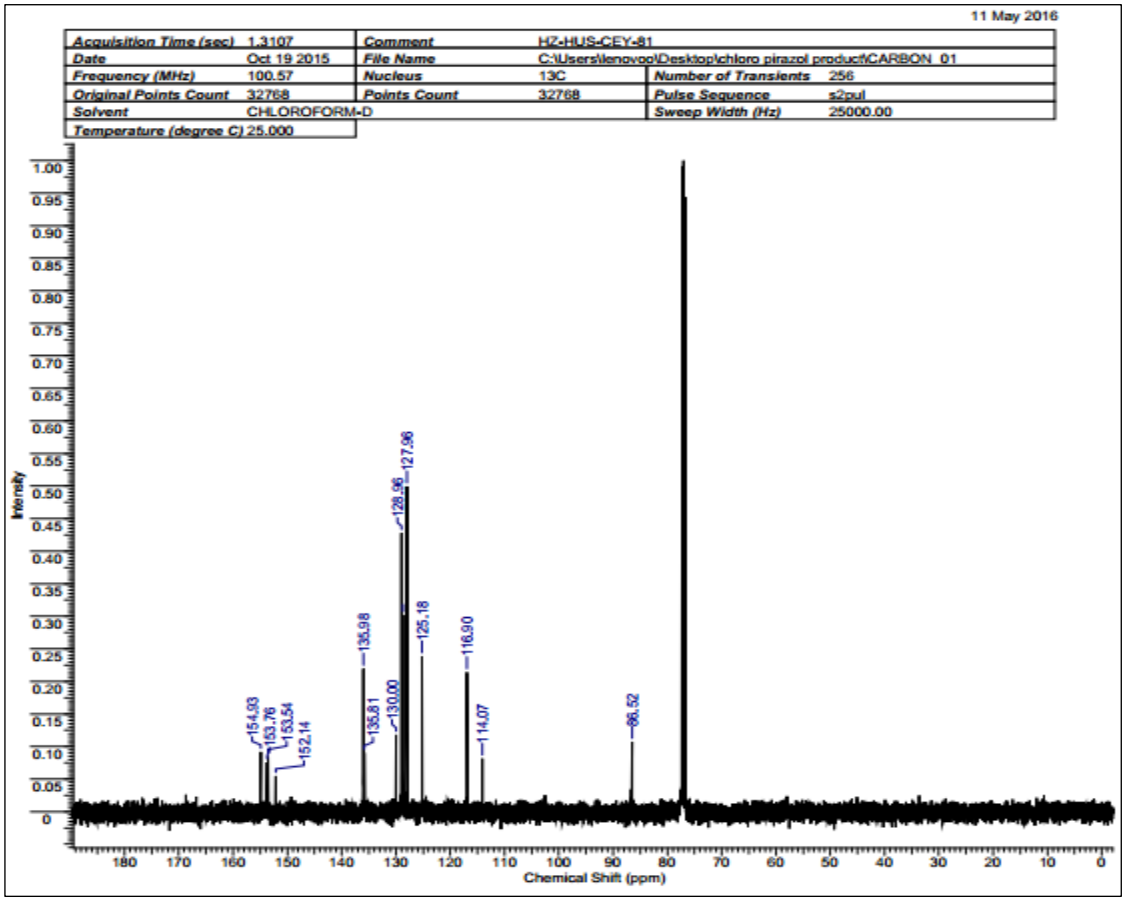

Figure A.52. ^{13}C-NMR of 3-(4-chlorophenyl)pyrazolo[1,2-a]indazole-1,9-dione

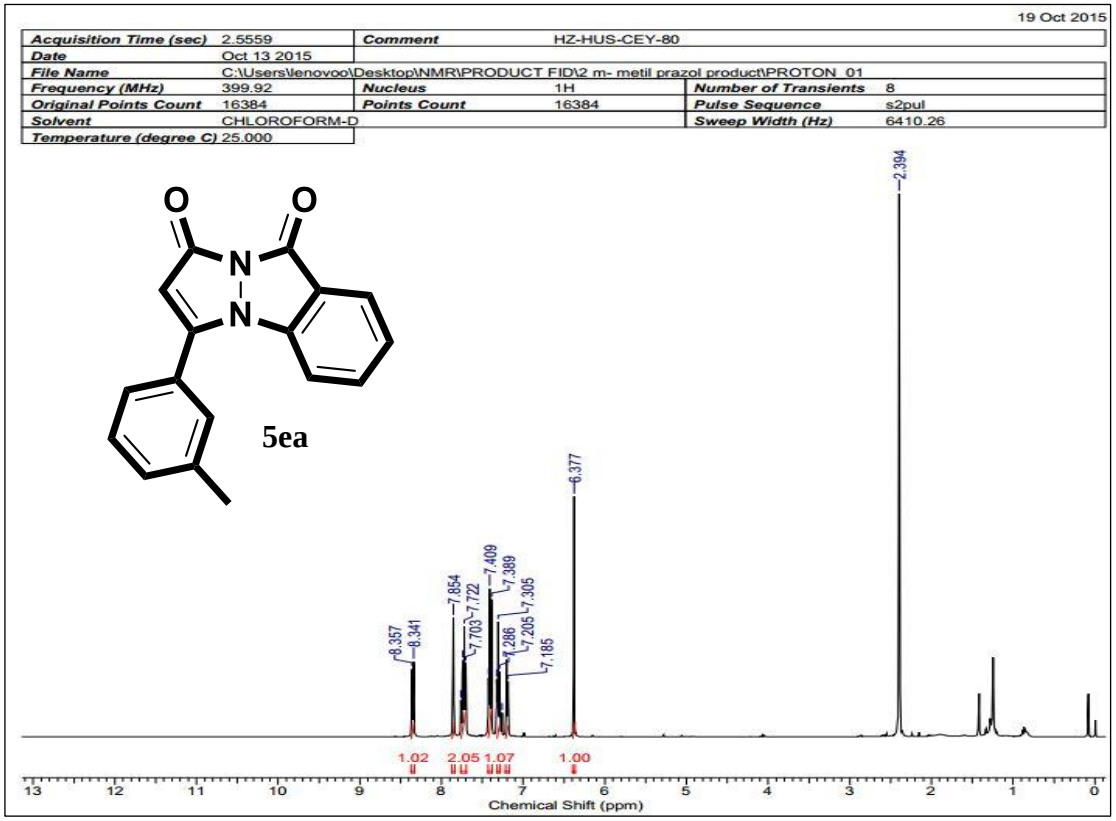

Figure A.53. ^{1}H-NMR of 3-(m-tolyl)pyrazolo[1,2-a]indazole-1,9-dione

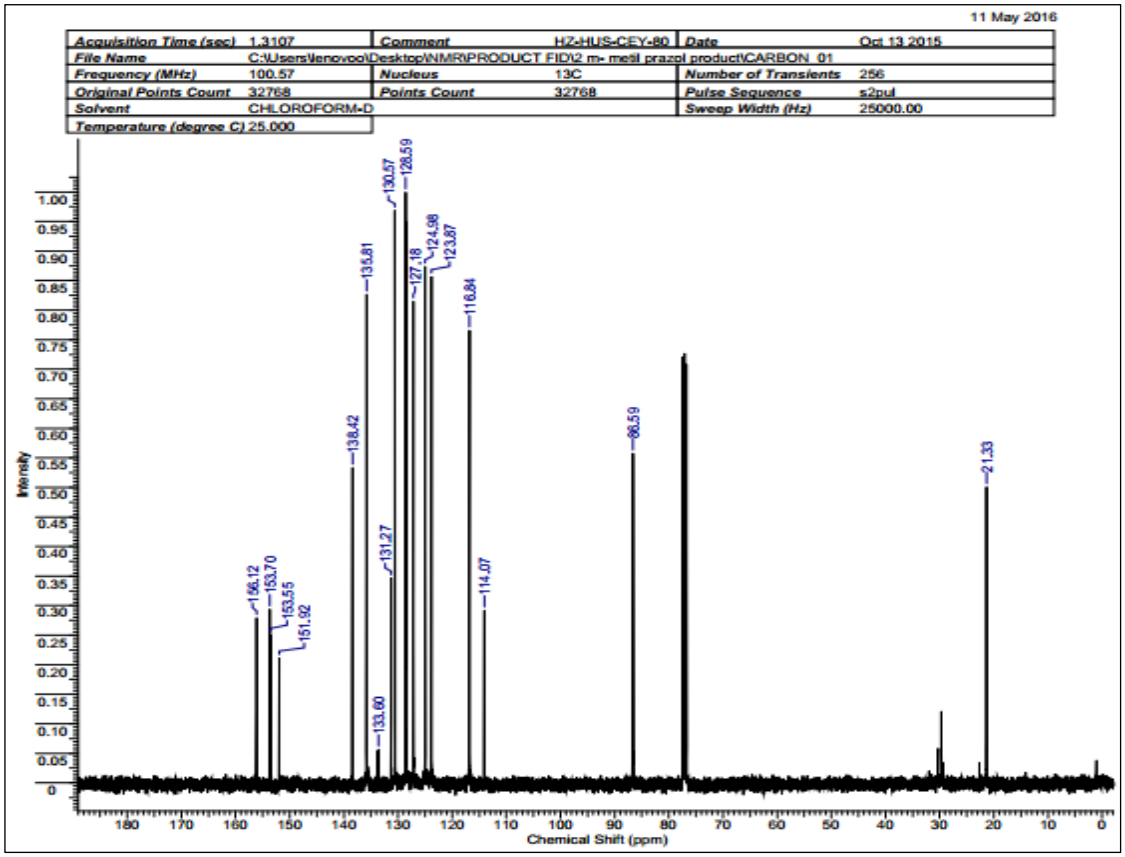

Figure A.54. ^{13}C-NMR of 3-(m-tolyl)pyrazolo[1,2-a]indazole-1,9-dione

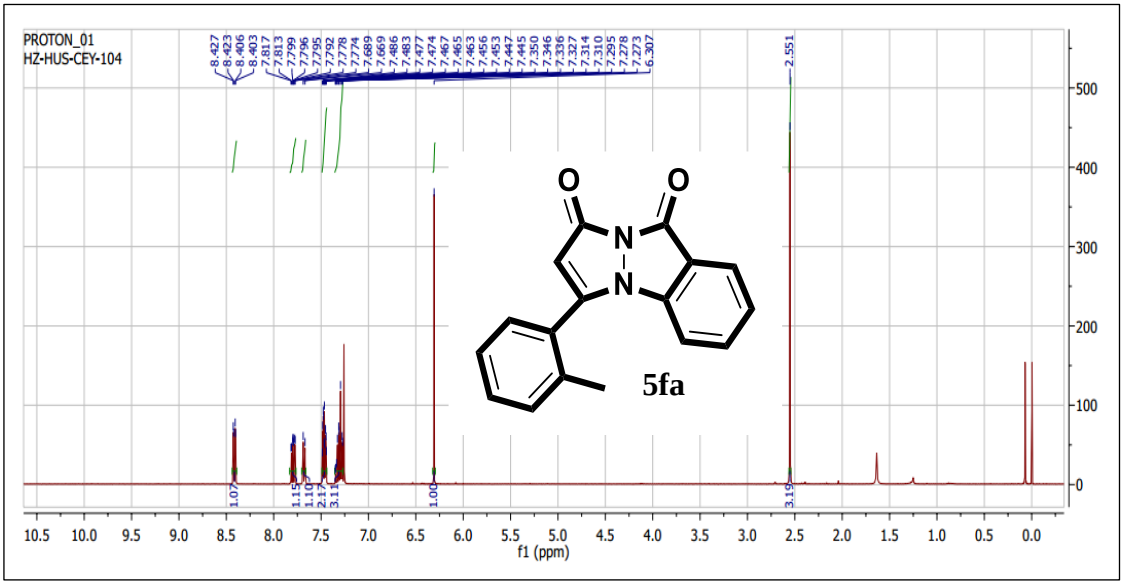

Figure A.55. [1]H-NMR of 3-(o-tolyl)pyrazolo[1,2-a]indazole-1,9-dione

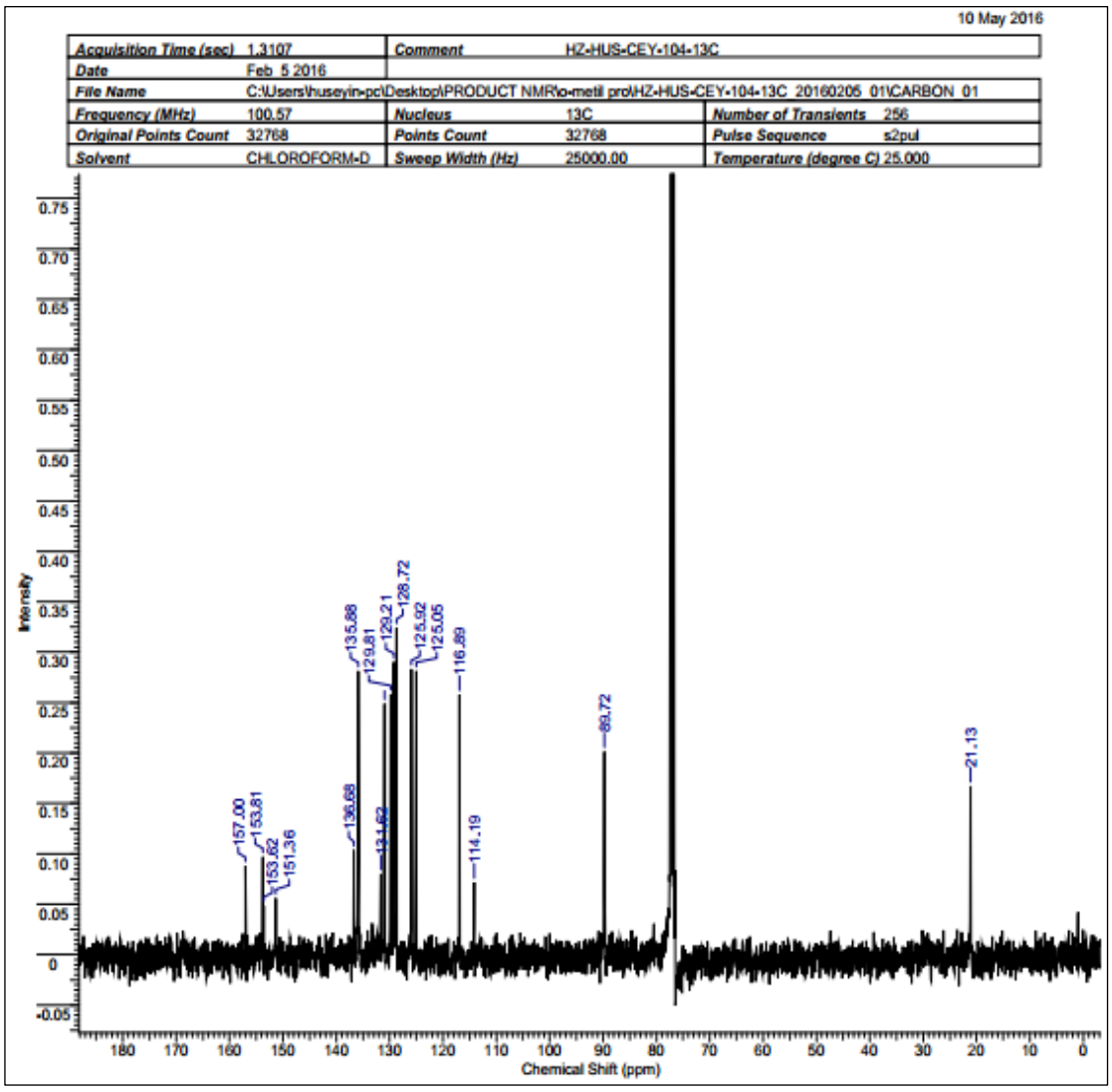

Figure A.56. [13]C-NMR of 3-(o-tolyl)pyrazolo[1,2-a]indazole-1,9-dione

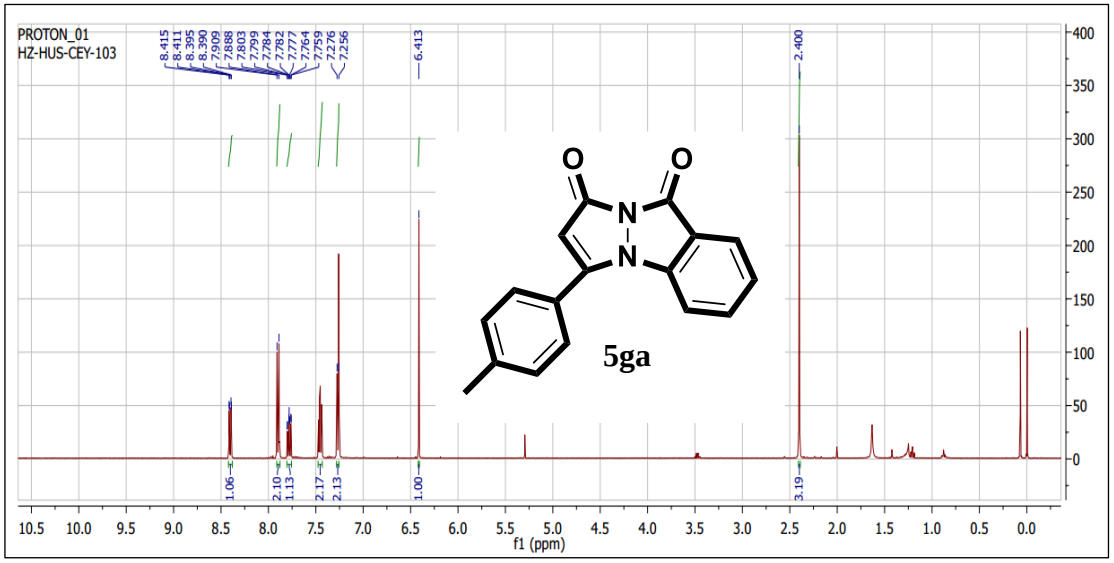

Figure A.57. ^{1}H-NMR of 3-(p-tolyl)pyrazolo[1,2-a]indazole-1,9-dione

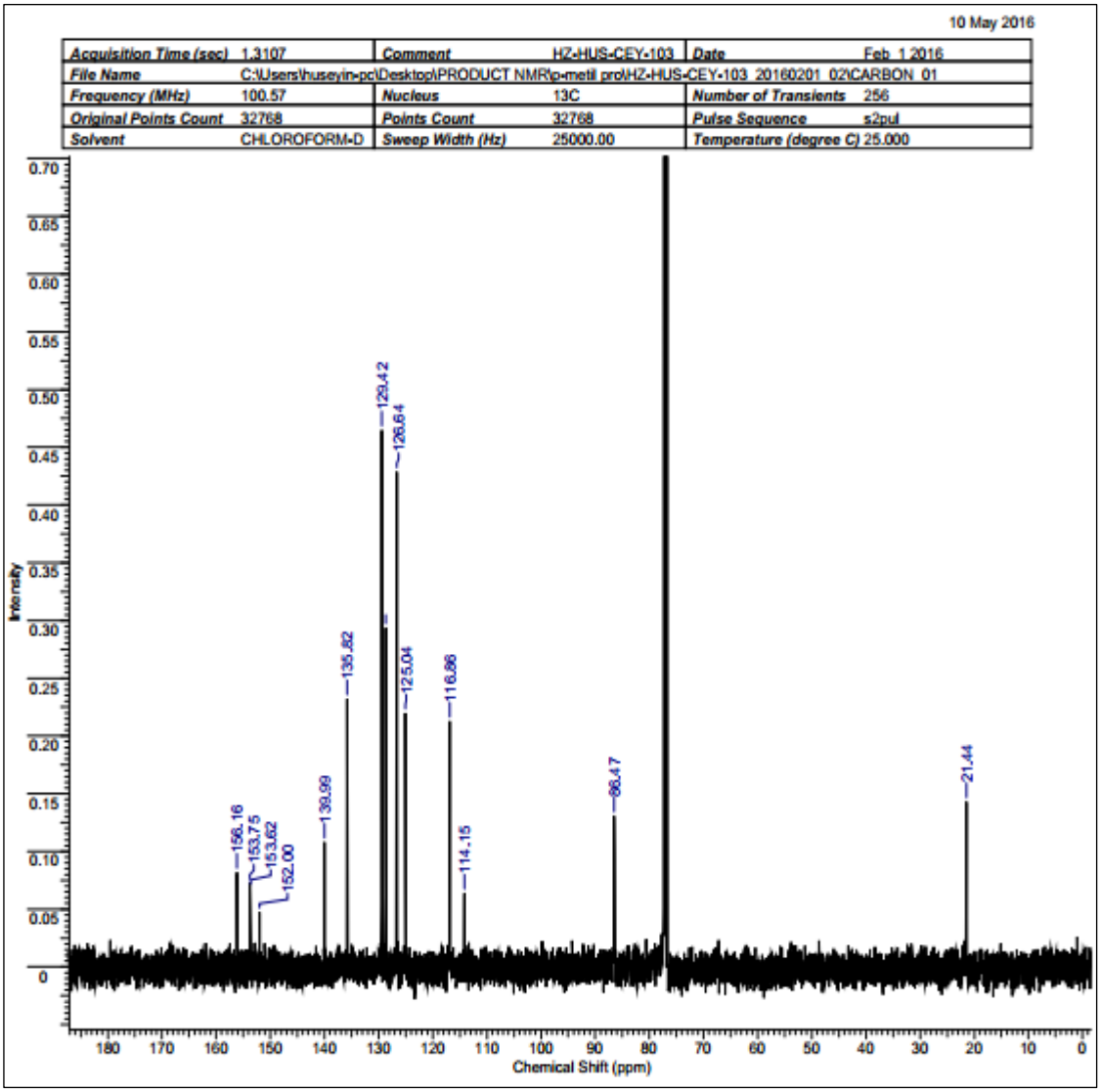

Figure A.58. ^{13}C-NMR of 3-(p-tolyl)pyrazolo[1,2-a]indazole-1,9-dione

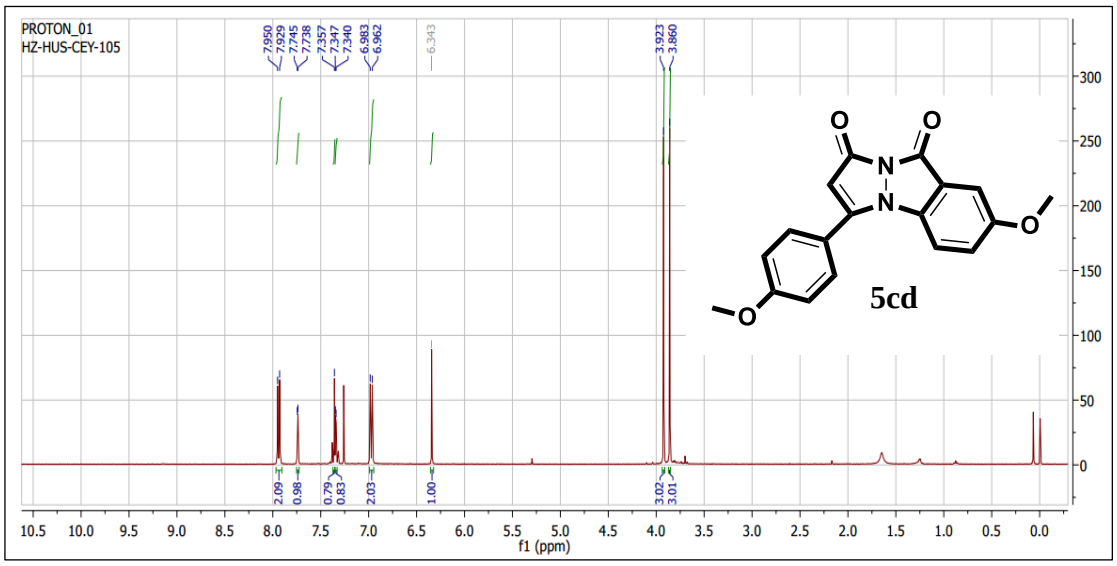

Figure A.59. [1]H-NMR of 7-methoxy-3-(4-methoxyphenyl)pyrazolo[1,2-a]indazole-1,9-dione

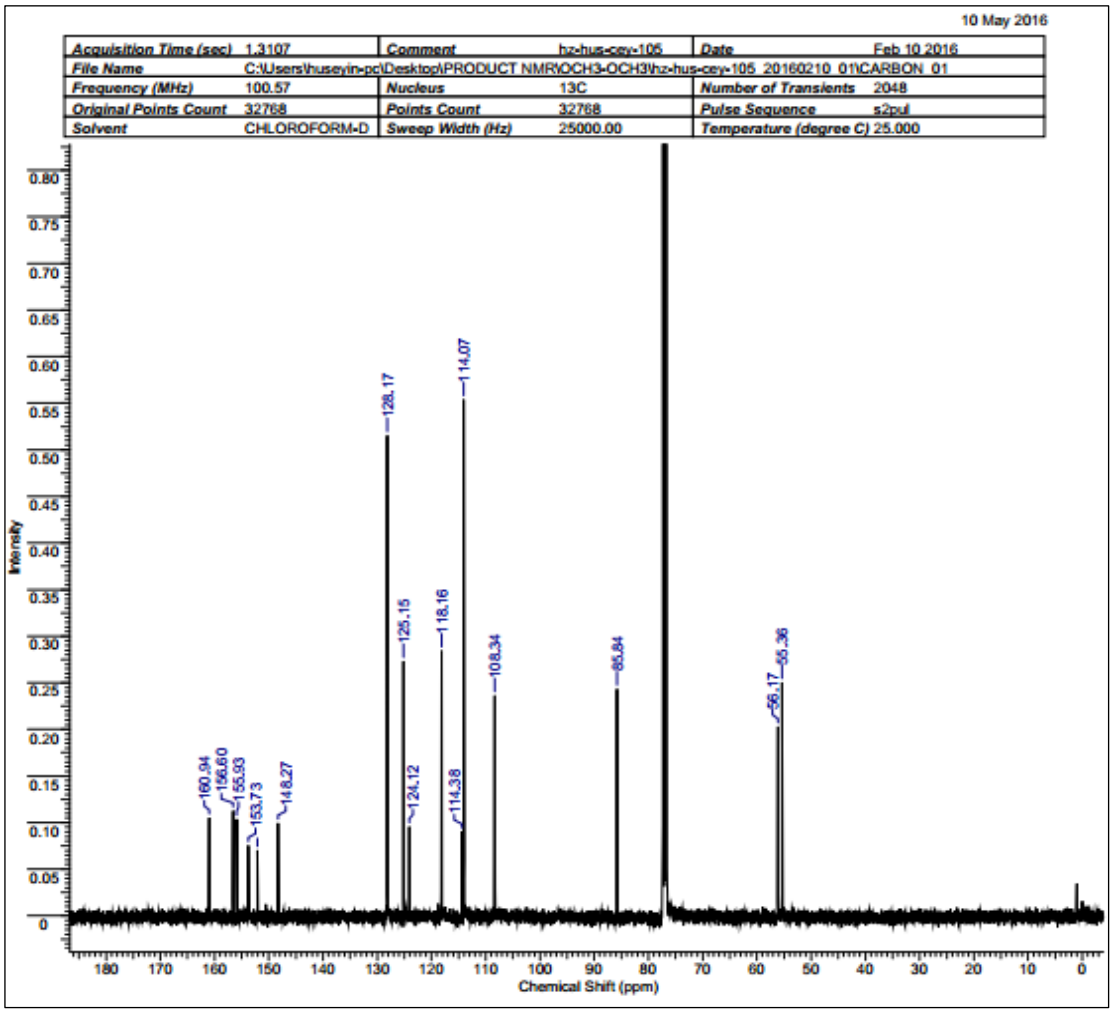

Figure A.60. [13]C-NMR of 7-methoxy-3-(4-methoxyphenyl)pyrazolo[1,2-a]indazole-1,9-dione

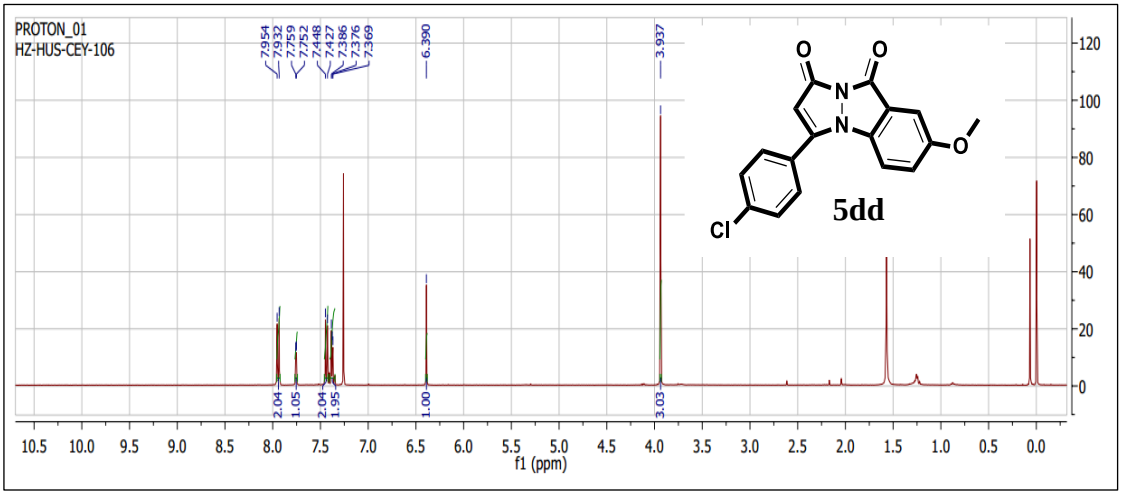

Figure A.61. [1]H-NMR of 3-(4-chlorophenyl)-7-methoxypyrazolo[1,2-a]indazole-1,9-dione

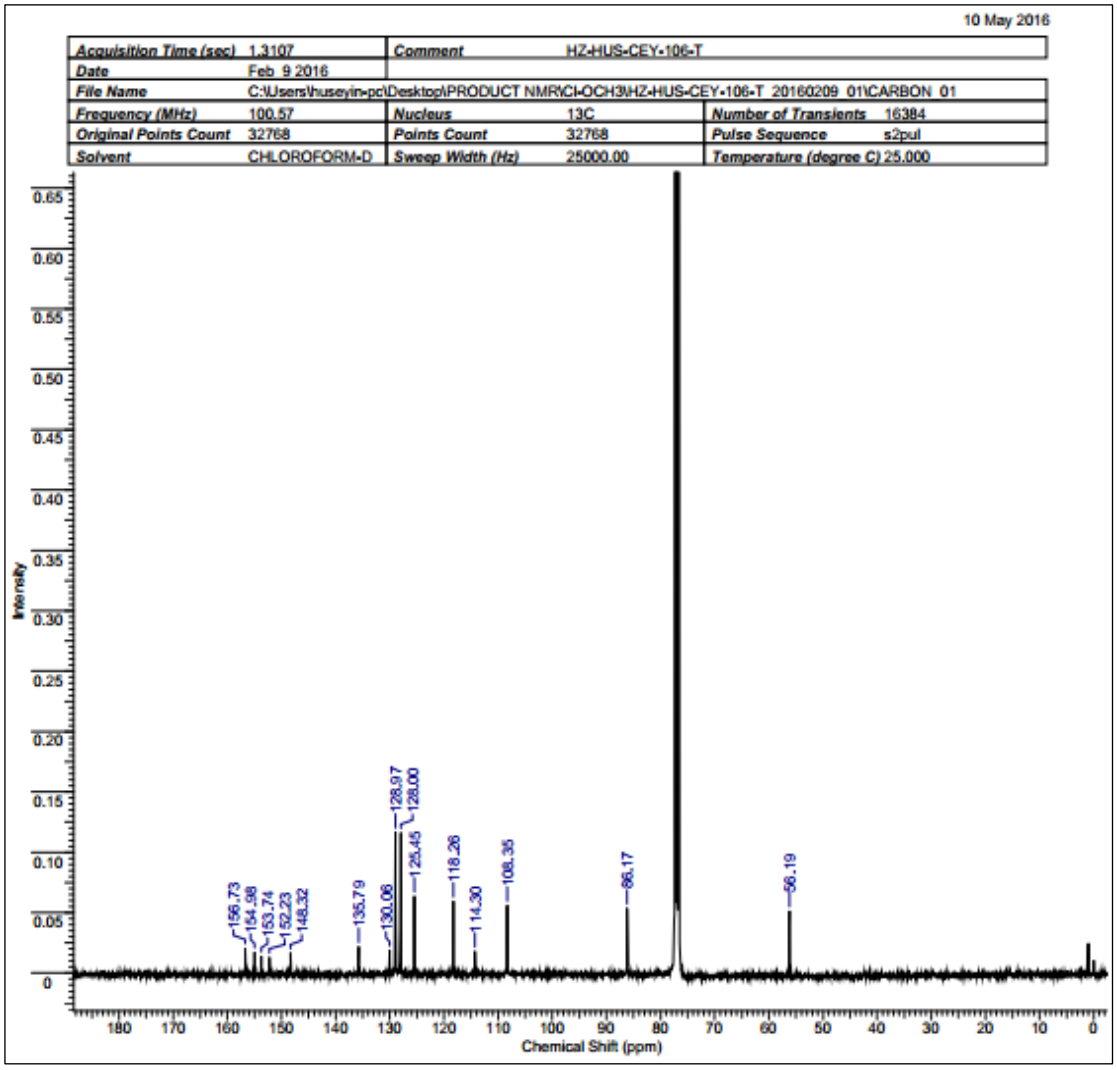

Figure A.62. [13]C-NMR of 3-(4-chlorophenyl)-7-methoxypyrazolo[1,2-a]indazole-1,9-dione

APPENDIX B

IR SPECTRA OF PRODUCTS

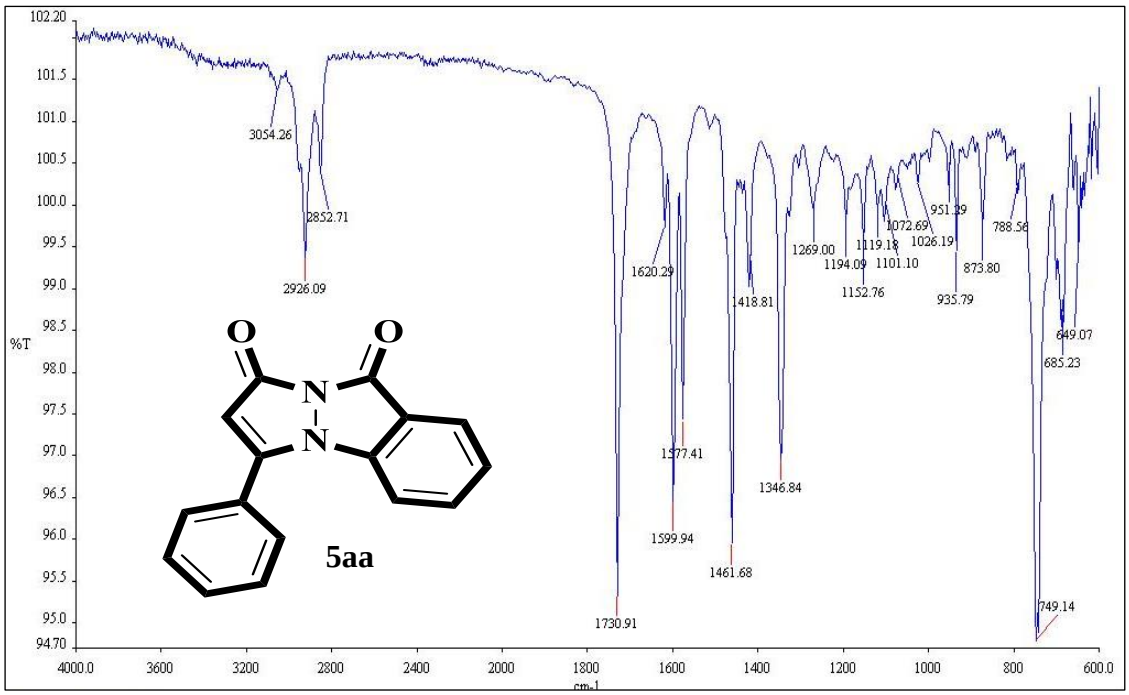

Figure B.1. IR Spectrum of 3-phenylpyrazolo[1,2-a]indazole-1,9-dione

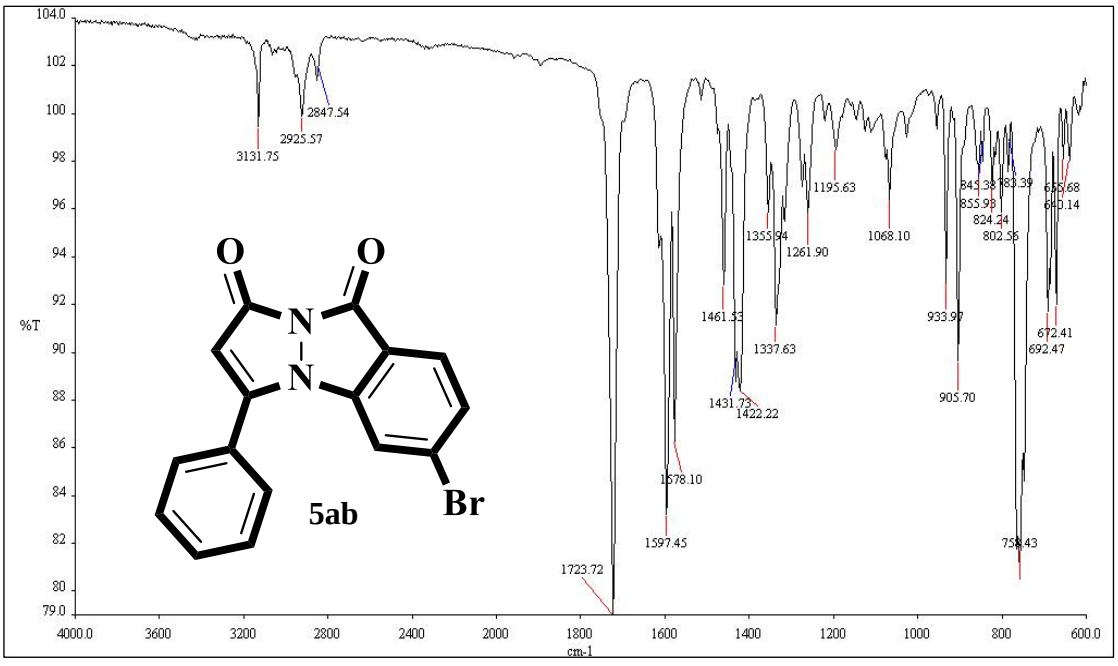

Figure B.2. IR Spectrum of 6-bromo-3-phenylpyrazolo[1,2-a]indazole-1,9-dione

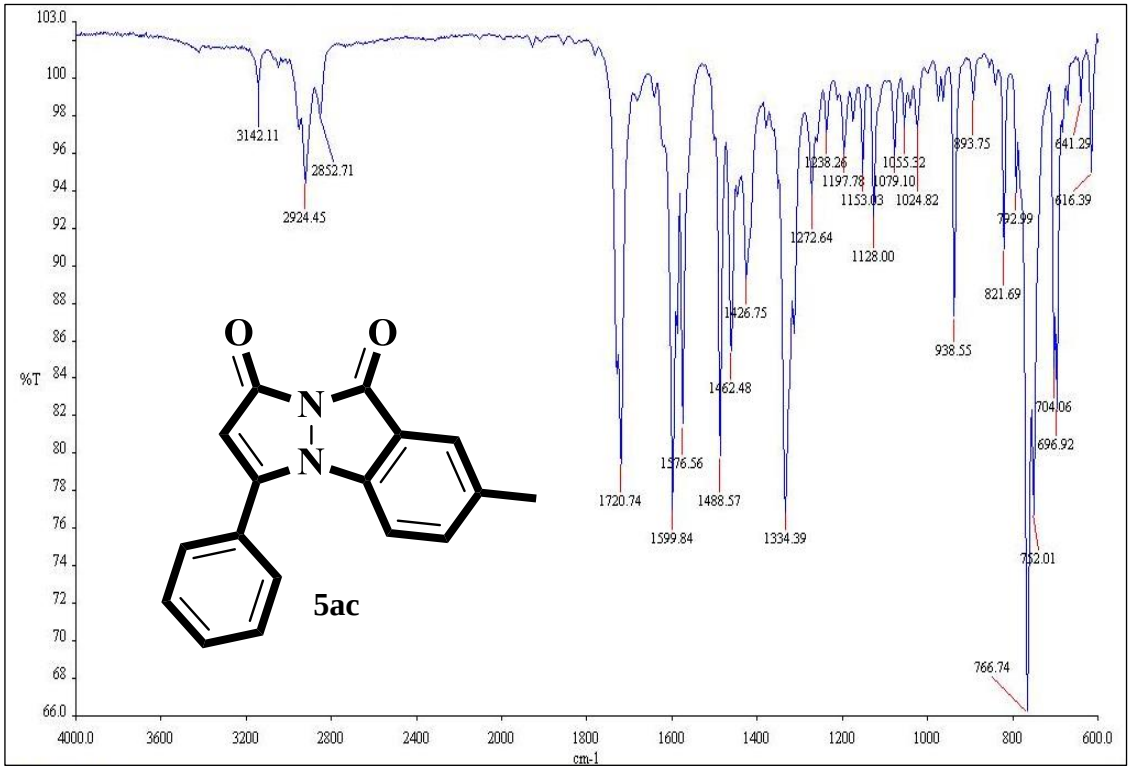

Figure B.3. IR Spectrum of 7-methyl-3-phenylpyrazolo[1,2-a]indazole-1,9-dione

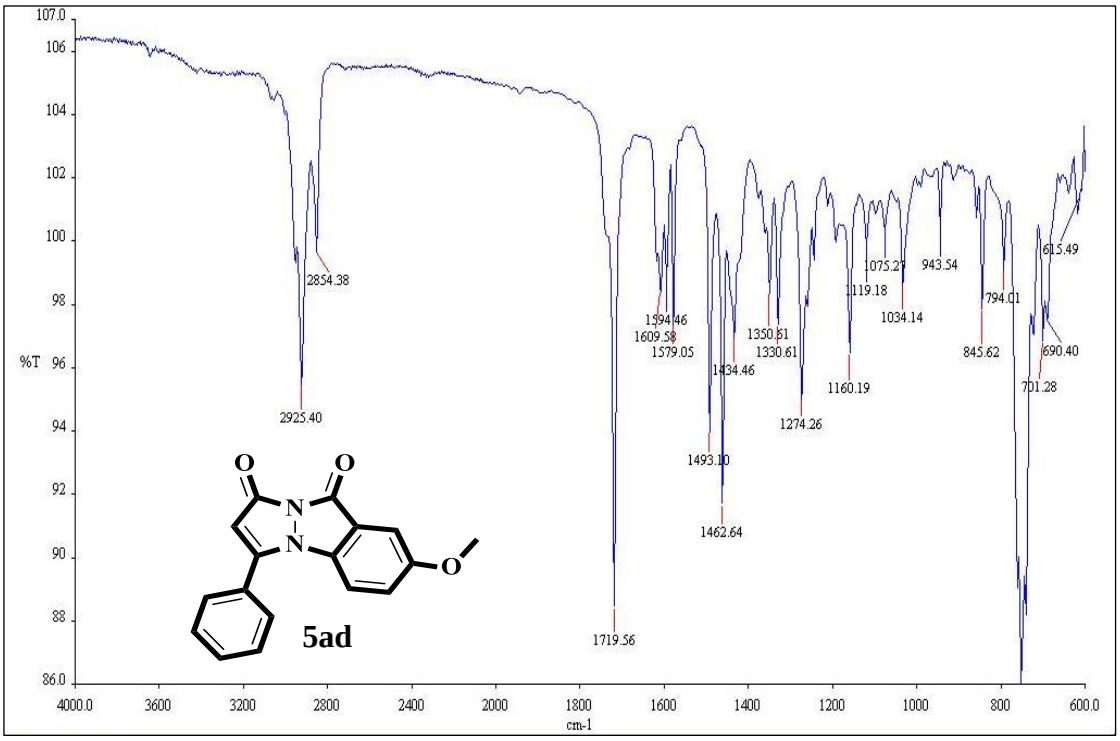

Figure B.4. IR Spectrum of 7-methoxy-3-phenylpyrazolo[1,2-a]indazole-1,9-dione

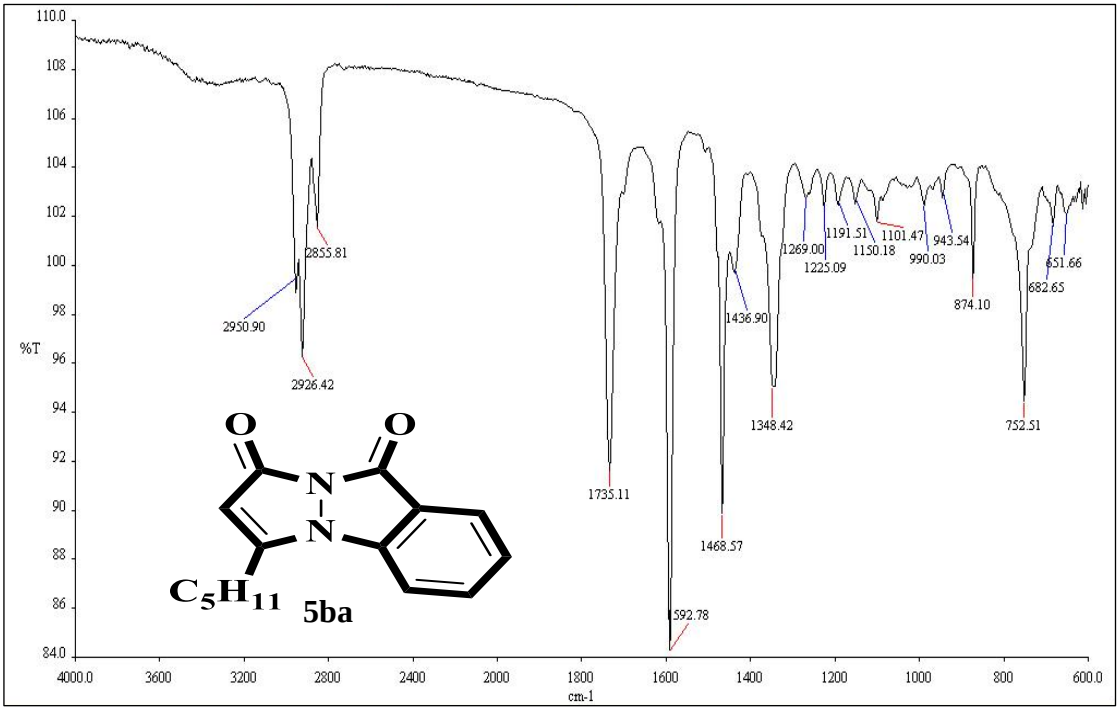

Figure B.5. IR Spectrum of 3-pentylpyrazolo[1,2-a]indazole-1,9-dione

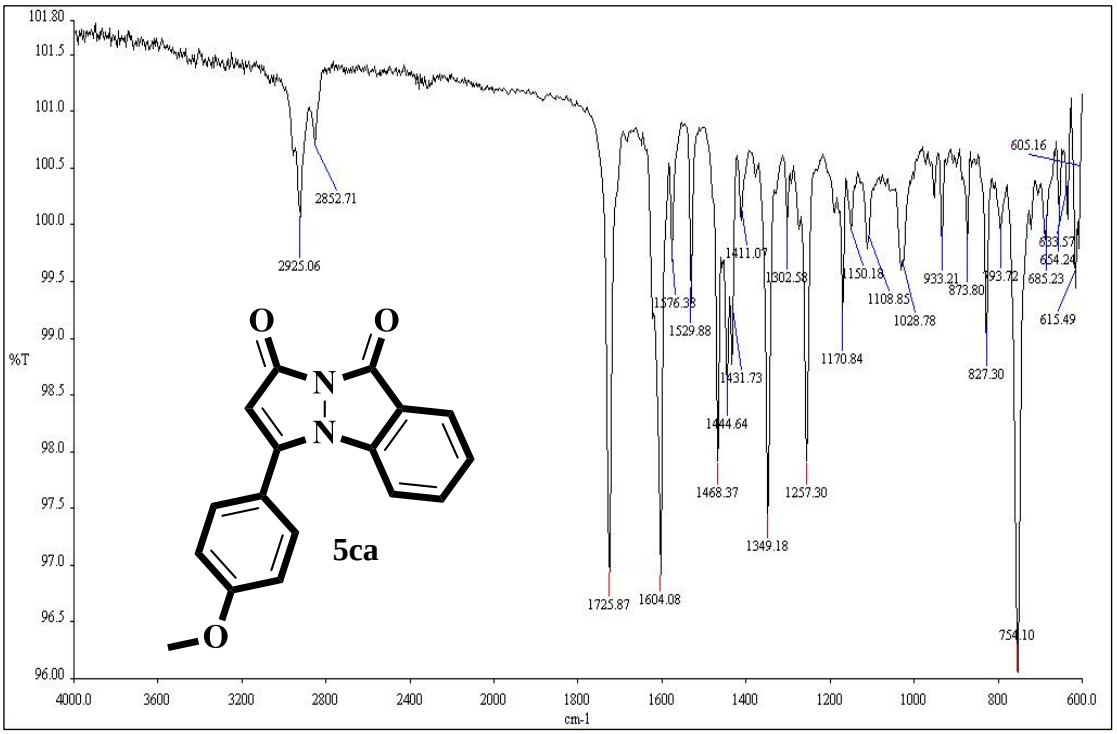

Figure B.6. IR Spectrum of 3-(4-methoxyphenyl)pyrazolo[1,2-a]indazole-1,9-dione

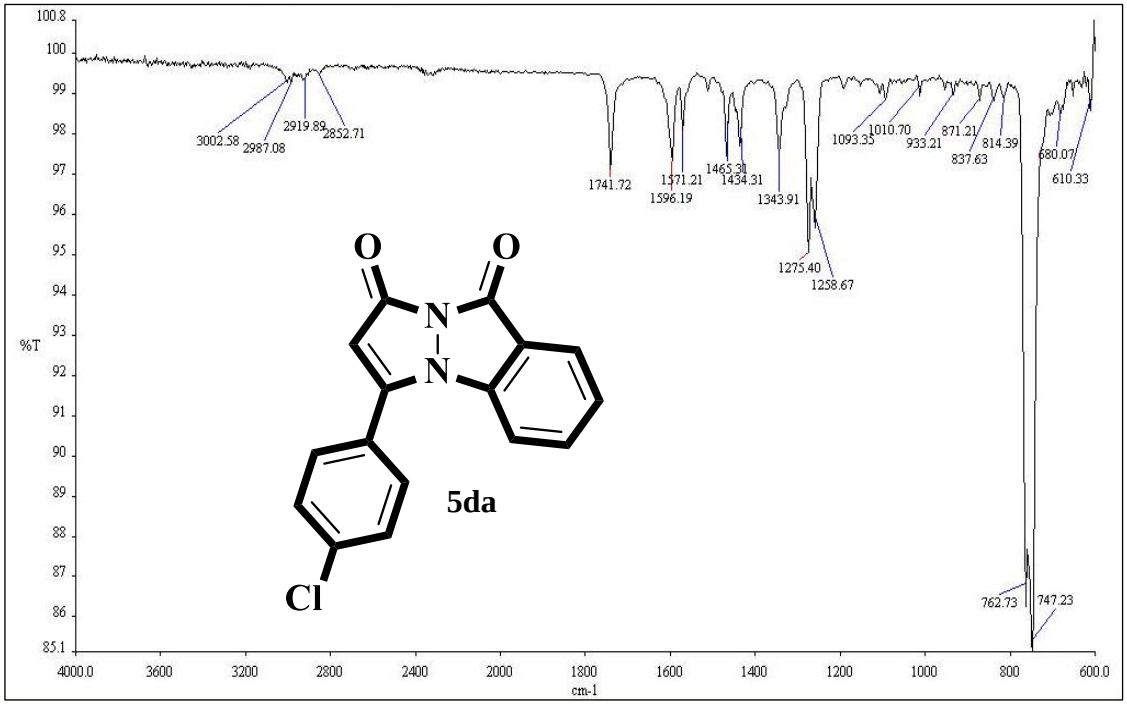

Figure B.7. IR Spectrum of 3-(4-chlorophenyl)pyrazolo[1,2-a]indazole-1,9-dione

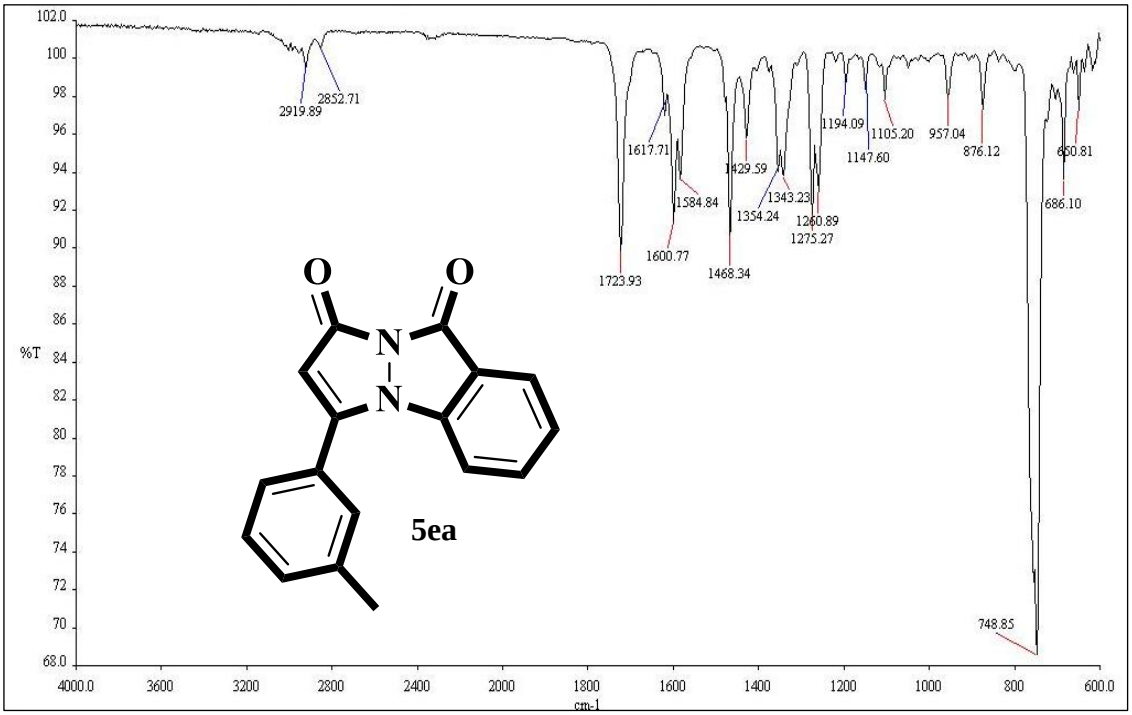

Figure B.8. IR Spectrum of 3-(m-tolyl)pyrazolo[1,2-a]indazole-1,9-dione

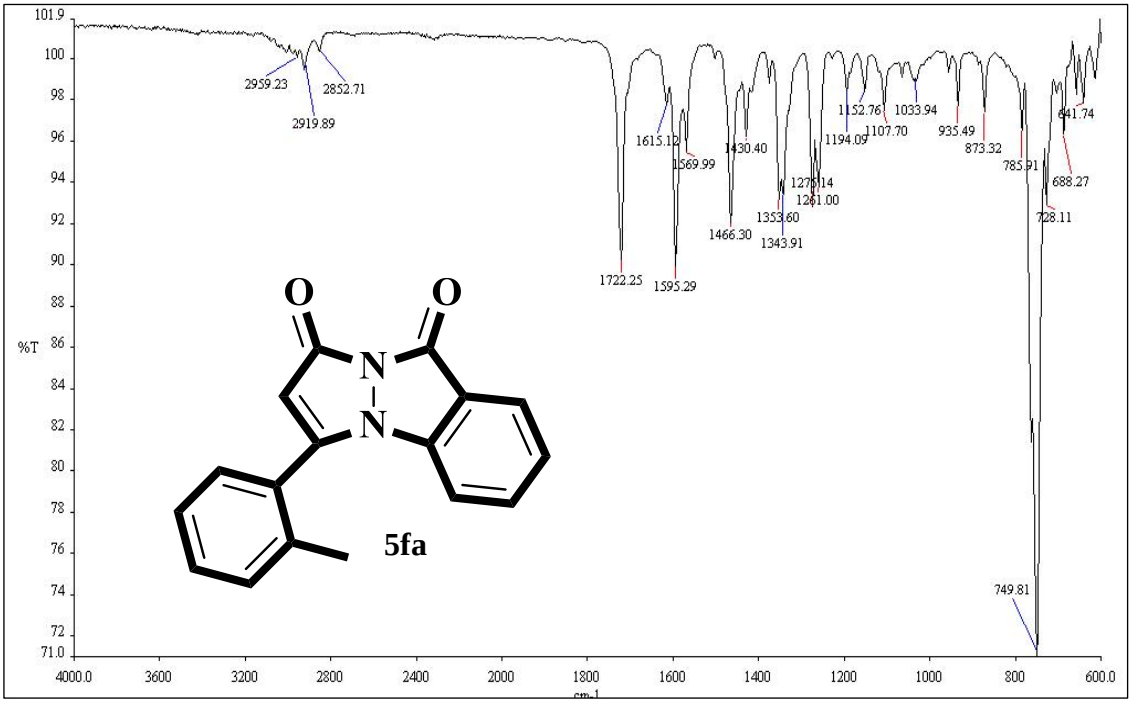

Figure B.9. IR Spectrum of 3-(o-tolyl)pyrazolo[1,2-a]indazole-1,9-dione

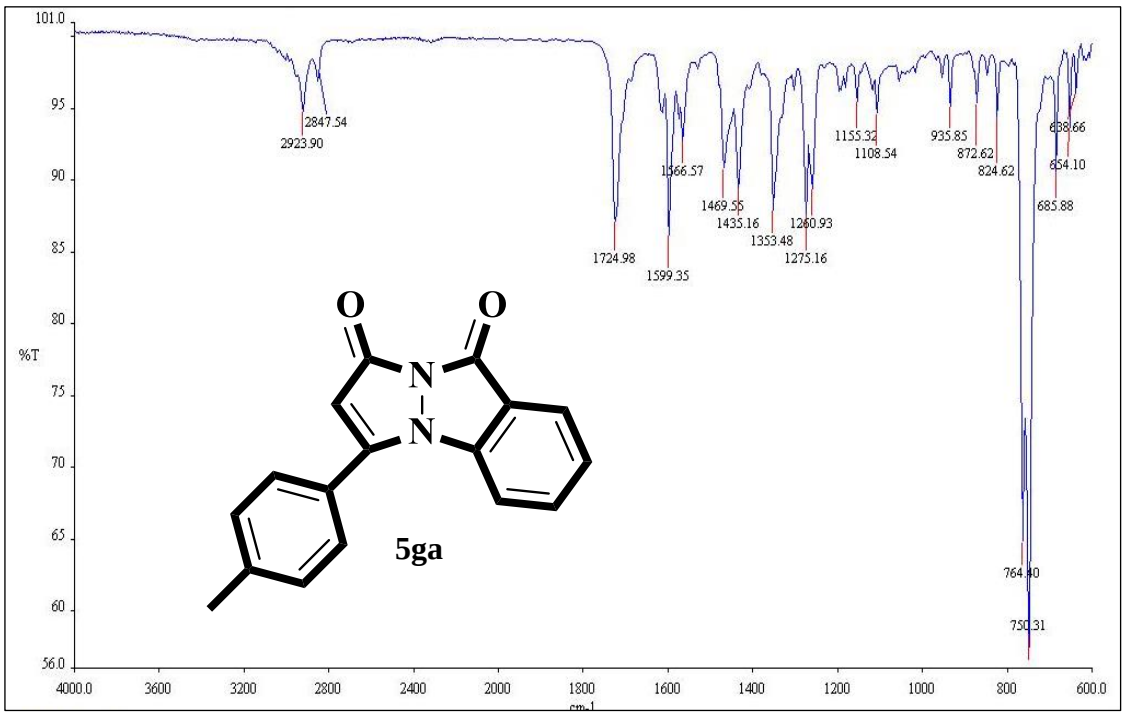

Figure B.10. IR Spectrum of 3-(p-tolyl)pyrazolo[1,2-a]indazole-1,9-dione

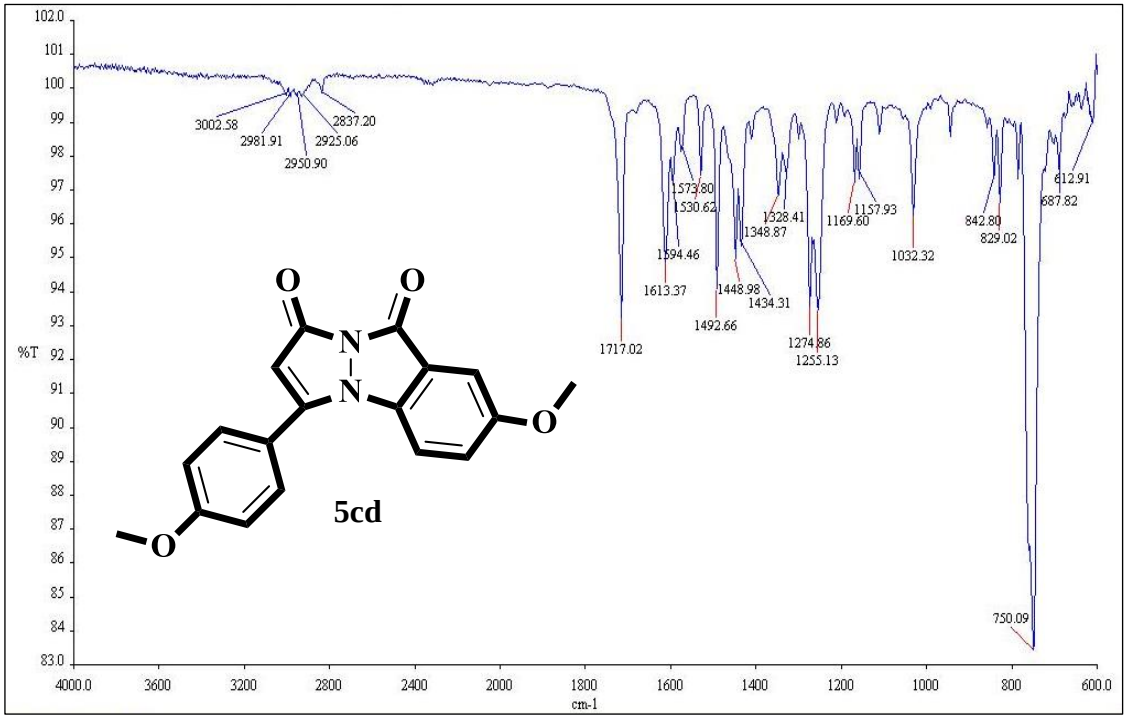

Figure B.11. IR Spectrum of 7-methoxy-3-(4-methoxyphenyl)pyrazolo[1,2-a]indazole-1,9-dione

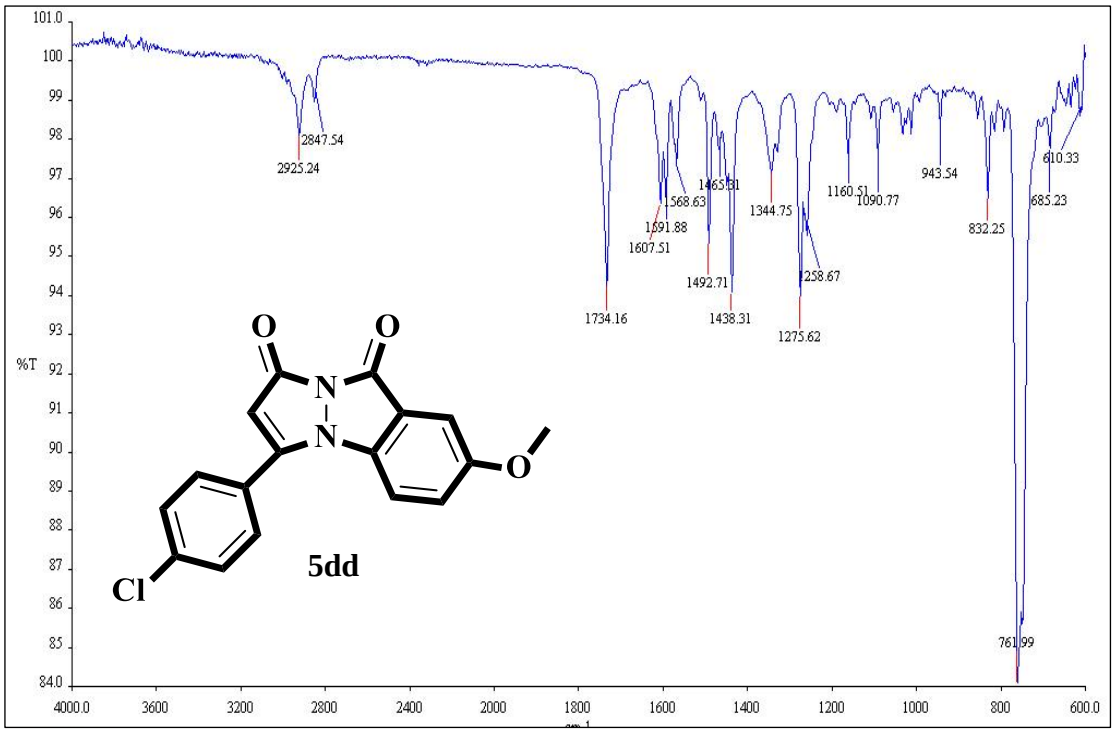

Figure B.12. IR Spectrum of 3-(4-chlorophenyl)-7-methoxypyrazolo[1,2-a]indazole-1,9-dione

APPENDIX C

FLUORESCENCE SPECTRA OF PRODUCTS

Figure C.1. Fluorescence spectra of 3-phenylpyrazolo[1,2-a]indazole-1,9-dione

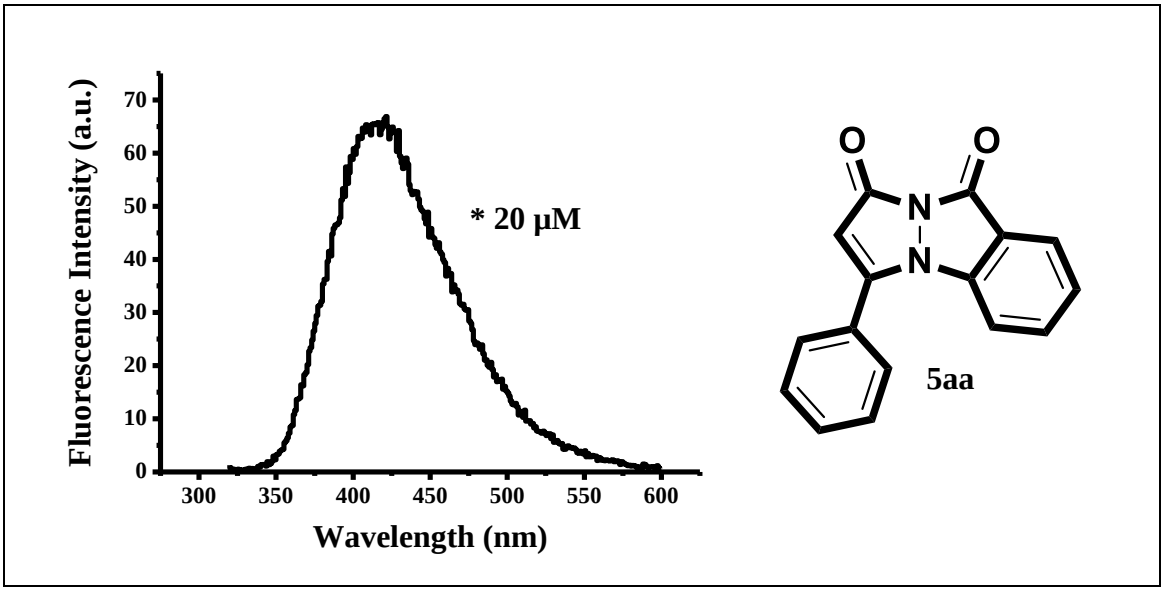

Figure C.2. Fluorescence spectra of 6-bromo-3-phenylpyrazolo[1,2-a]indazole-1,9-dione

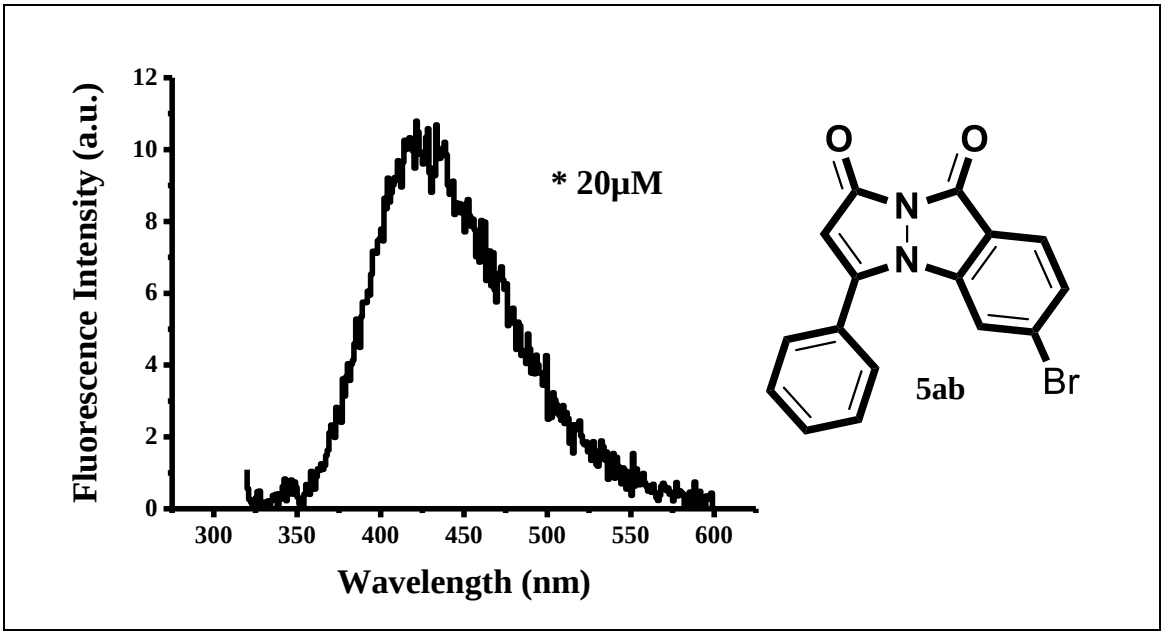

Figure C.3. Fluorescence spectra of 7-methyl-3-phenylpyrazolo[1,2-a]indazole-1,9-dione

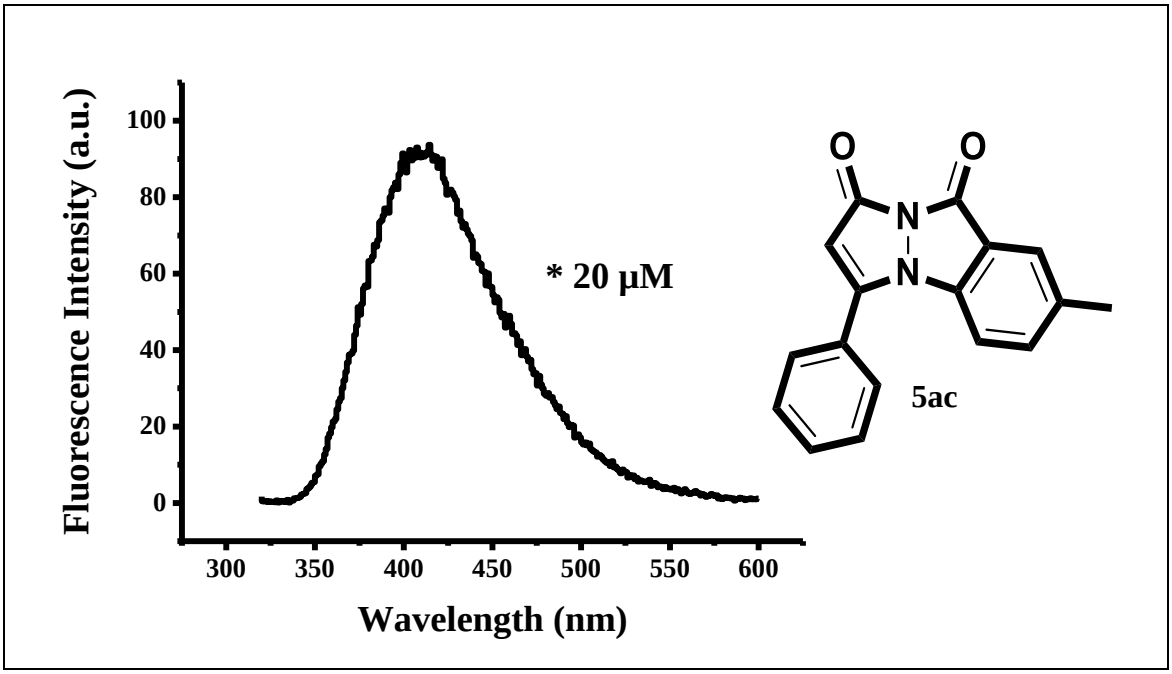

Figure C.4. Fluorescence spectra of 7-methoxy-3-phenylpyrazolo[1,2-a]indazole-1,9-dione

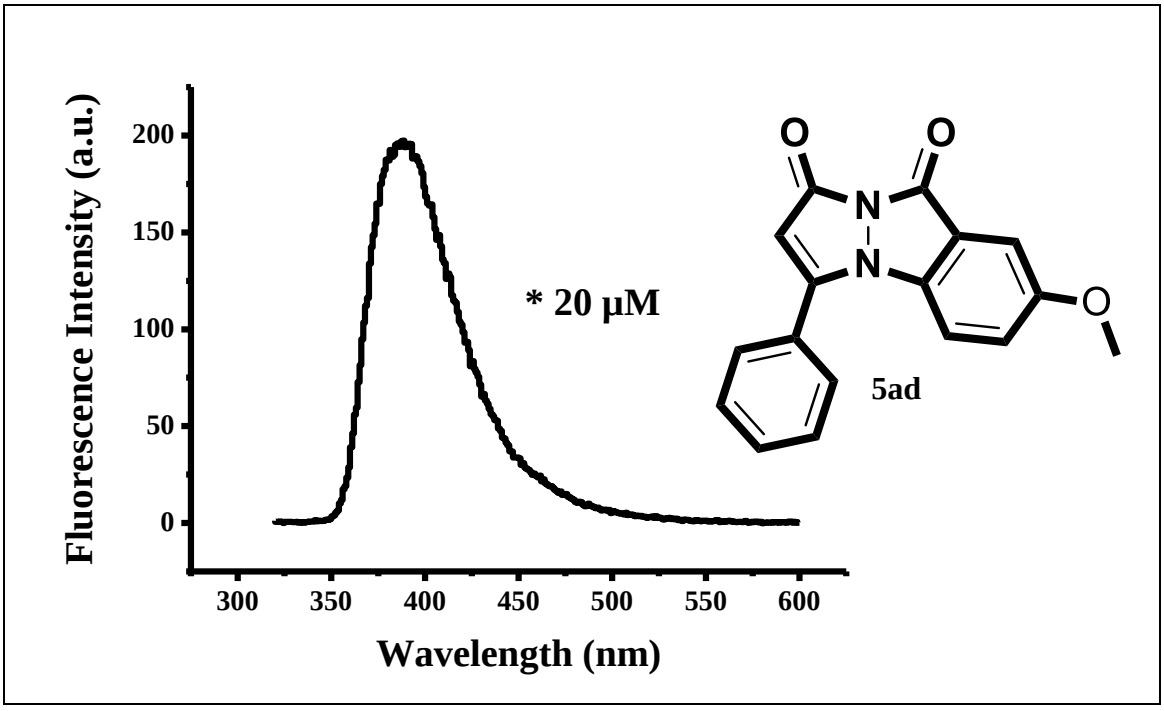

Figure C.5. Fluorescence spectra of 3-pentylpyrazolo[1,2-a]indazole-1,9-dione

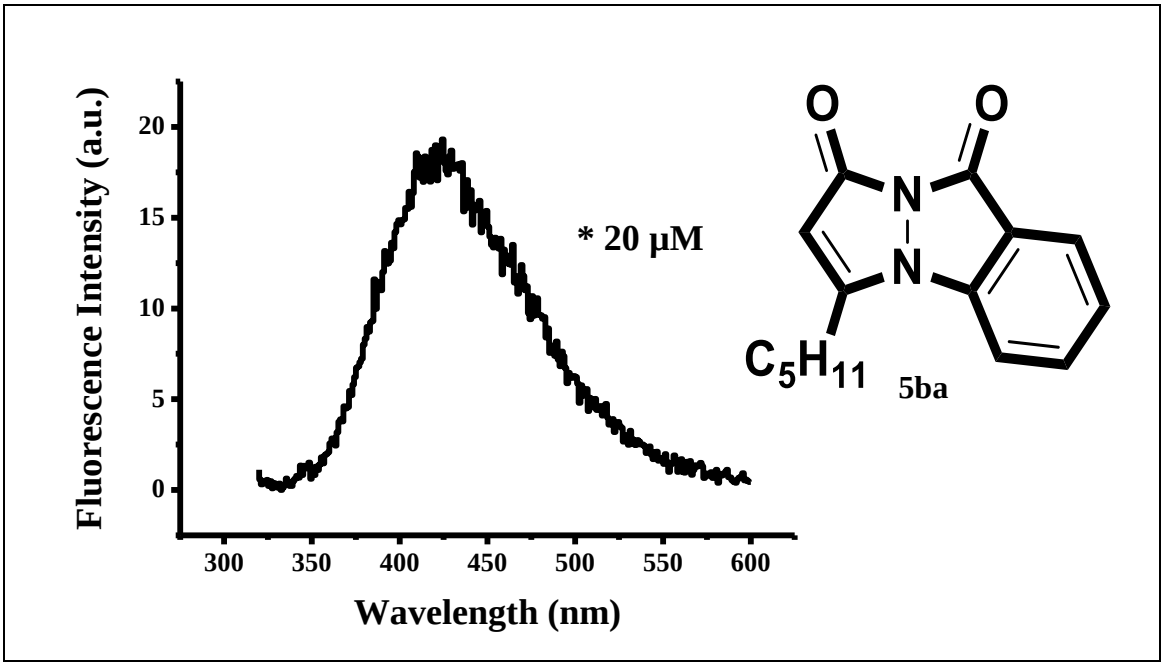

Figure C.6. Fluorescence spectra of 3-(4-methoxyphenyl)pyrazolo[1,2-a]indazole-1,9-dione

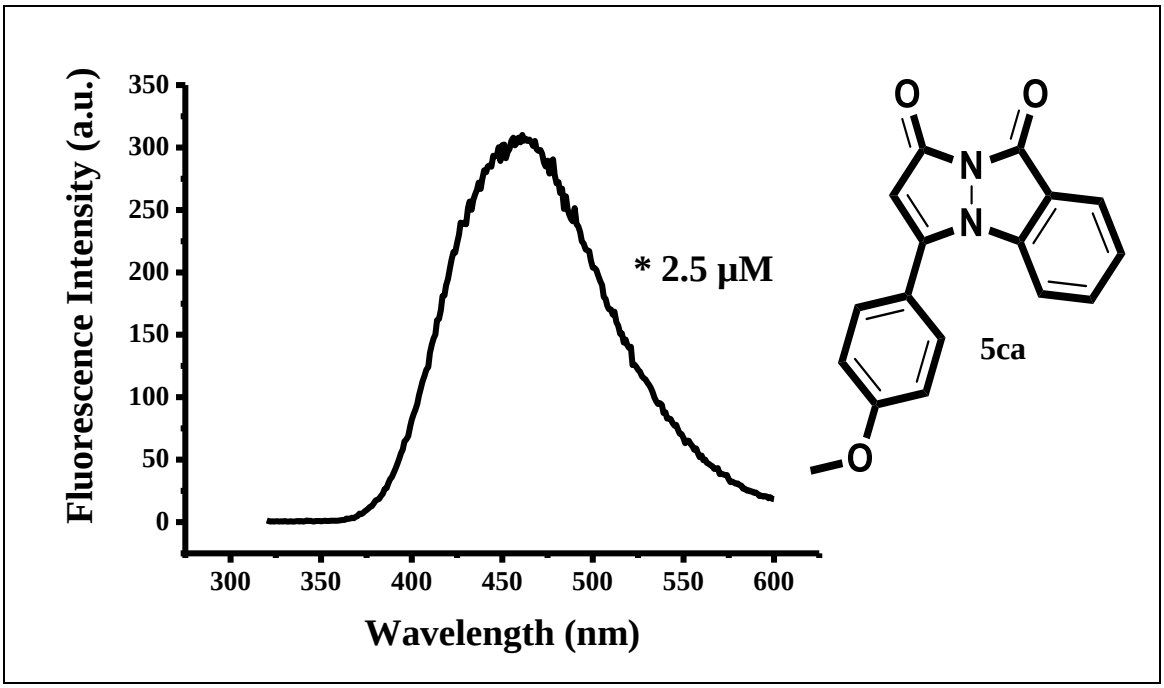

Figure C.7. Fluorescence spectra of 3-(4-chlorophenyl)pyrazolo[1,2-a]indazole-1,9-dione

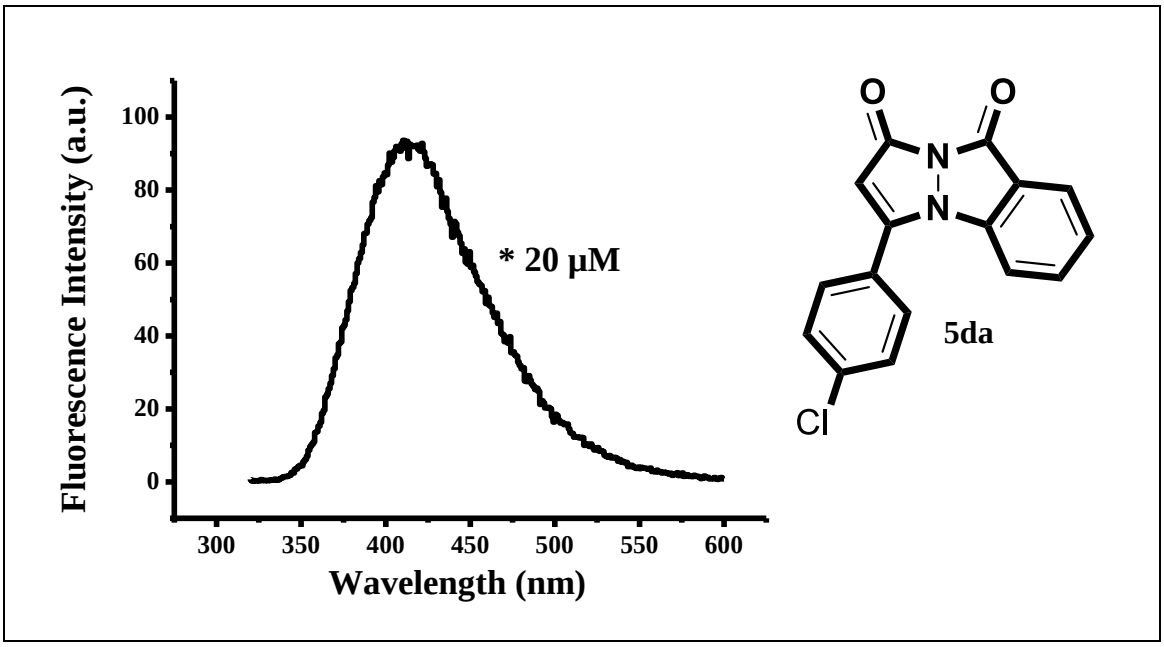

Figure C.8. Fluorescence spectra of 3-(m-tolyl)pyrazolo[1,2-a]indazole-1,9-dione

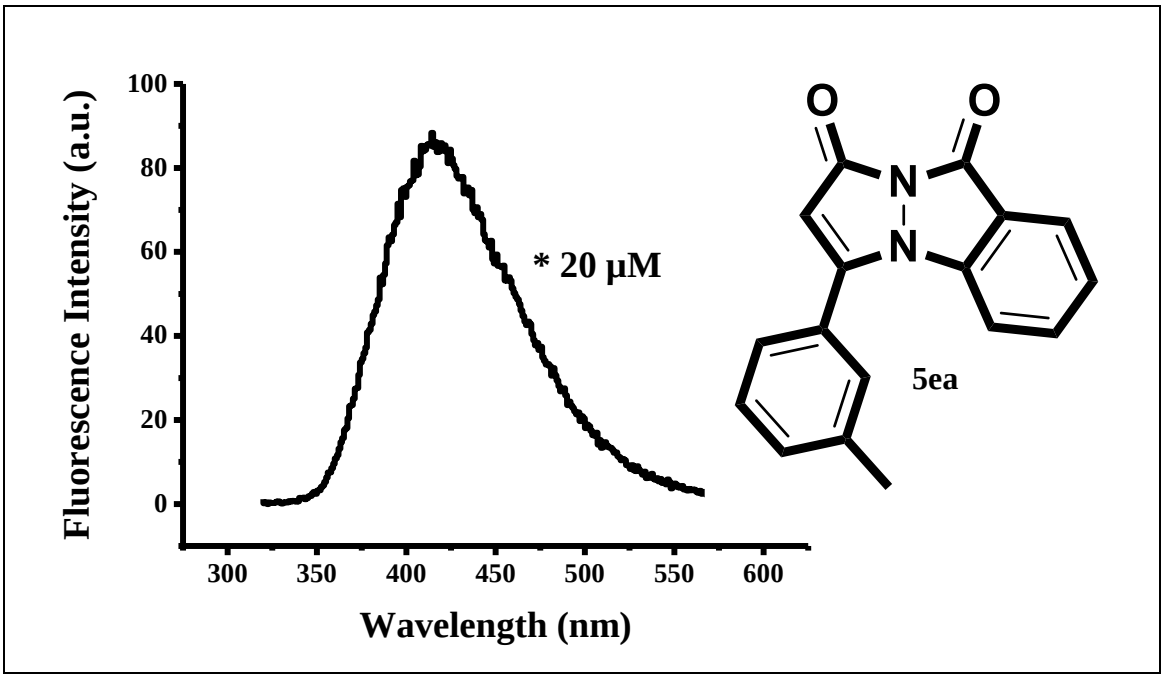

Figure C.9. Fluorescence spectra of 3-(o-tolyl)pyrazolo[1,2-a]indazole-1,9-dione

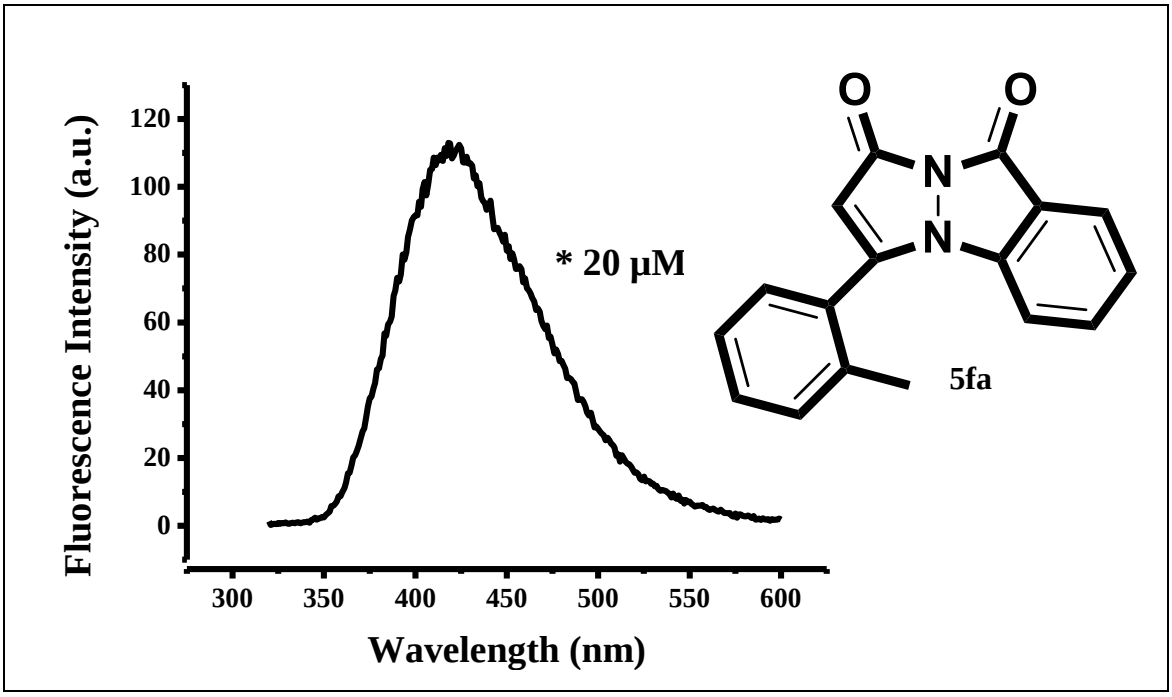

Figure C.10. Fluorescence spectra of 3-(p-tolyl)pyrazolo[1,2-a]indazole-1,9-dione

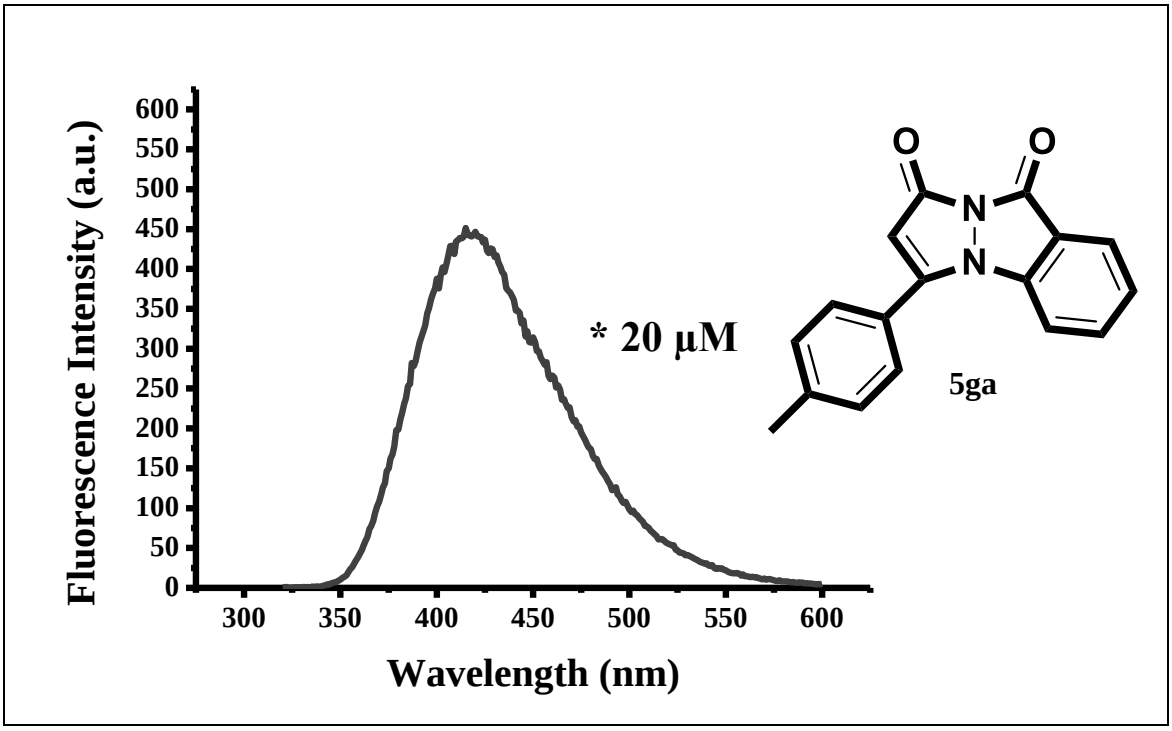

Figure C.11. Fluorescence spectra of 7-methoxy-3-(4-methoxyphenyl)pyrazolo[1,2-a]indazole-1,9-dione

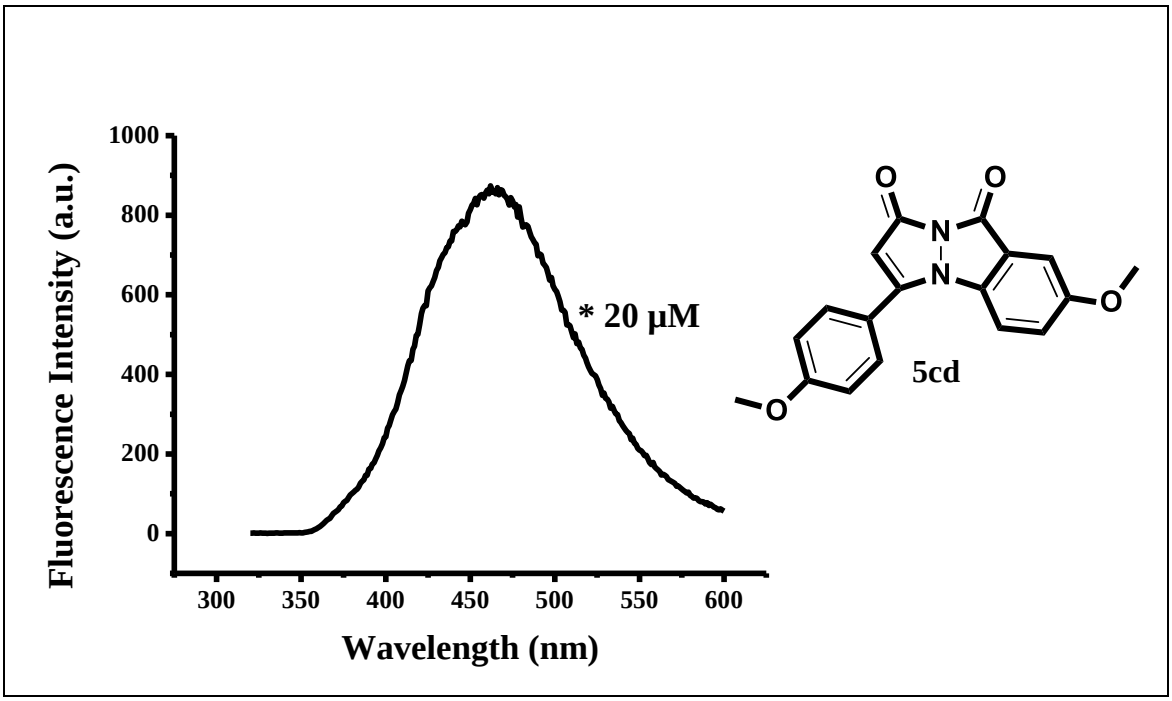

Figure C.12. Fluorescence spectra of 3-(4-chlorophenyl)-7-methoxypyrazolo[1,2-a]indazole-1,9-dione